

# Final report

## 1. Project details

<b>Project title</b>	2nd Generation Solar Direct-Drive Refrigerators
<b>File no.</b>	64017-0556
<b>Name of the funding scheme</b>	EUDP17-II
<b>Project managing company / institution</b>	Danish Technological Institute Project manager: Per Henrik Pedersen, +45 7220 2513, prp@teknologisk.dk
<b>CVR number</b> (central business register)	5697 6116
<b>Project partners</b>	Vestfrost Solutions, SECOP, DTU-MEK
<b>Submission date</b>	06 October 2021

## Content

<b>1. Project details .....</b>	<b>1</b>
<b>2. Summary .....</b>	<b>4</b>
2.1 English version .....	4
2.2 Danish version .....	5
<b>3. Project objectives .....</b>	<b>7</b>
3.1 Aim of the project .....	7
3.2 Work packages .....	9
3.3 Project participants and roles .....	11
<b>4. Project implementation .....</b>	<b>12</b>
<b>5. Project results .....</b>	<b>22</b>
5.1 Simulation program .....	22
5.1.1 Model 1: Dynamic cabinet model incl. ice bank .....	22
5.1.2 Model 2: Steady state compressor control .....	24
5.1.3 Model 3: Dynamic compressor control .....	28
5.2 Compressor and controller development .....	30
5.2.1 Development of the first prototype .....	32
5.2.2 Development of the second prototype .....	33
5.3 Design of new cabinet .....	37
5.3.1 Prolonging the hold-over time .....	37
5.3.2 Better temperature regulation .....	38
5.3.3 Humidity control .....	40
5.3.4 Remote monitoring .....	40
5.3.5 Robustness .....	44
5.3.6 New generation of the Solar direct drive vaccine cooler .....	44
5.4 Laboratory measurements .....	48
5.4.1 Temperature control experiments .....	48
5.4.2 Subcooling .....	49
5.4.3 Pull-down test .....	51
5.4.4 Humidity control .....	52
5.4.5 Energy harvesting .....	55
5.5 Dissemination .....	56
<b>6. Utilisation of project results .....</b>	<b>57</b>
6.1 Cabinet optimization .....	57
6.2 Steady state compressor control .....	58
6.3 Dynamic compressor control .....	63

6.4 Economic assessment.....	65
6.5 Summary of guidelines based on the simulation models .....	67
<b>7. Project conclusion and perspective .....</b>	<b>68</b>
<b>8. Appendices .....</b>	<b>70</b>
8.1 Appendix A: Temperature control experiments .....	71
8.2 Appendix B: Subcooling Experiments .....	84
8.3 Appendix C: Humidity Control .....	92
8.4 Appendix D: Energy harvesting .....	107
8.5 Appendix E: Paper: Direct Drive Solar Cooling .....	111
8.6 Appendix F: Paper: Comparison of compressor control strategies for solar DD refrigerators .....	120
8.7 Appendix G: Paper: Extending the autonomy time of an icelined solar powered vaccine cooler .....	129
8.8 Appendix H: Data sheet for the new compressor.....	138

## 2. Summary

### 2.1 English version

Two new Solar Direct Drive compressors have been developed and tested in this project.

The first one is based on the relatively new SECOP XV compressor platform. This was developed and tested with success. Because of a change of ownership and a change of strategy at SECOP, it was decided to stop the further development of this compressor because it is based on a household compressor platform. The new strategy for SECOP is to focus on compressors for professional appliances.

A new compressor platform has been developed for all DC compressors, including compressors for the automotive sector and for the Solar Direct Drive sector. The name is the "Nano-Compressor". The SECOP BD-Nano50K Direct Drive compressor is more efficient as it has bigger cooling capacity compared to the existing BD35K DD compressor.

For freezing applications ( $T_{\text{evap}} = -25 \text{ }^{\circ}\text{C}$ ), the cooling capacity has increased from 36W to 50.8W (+41 %), and the energy efficiency (COP) has increased from 0.87 to 1.19 (+36.8 %).

For refrigerator applications ( $T_{\text{evap}} = -10 \text{ }^{\circ}\text{C}$ ), the cooling capacity has increased from 83.8W to 109.1W (+30.2 %), and the energy efficiency (COP) has increased from 1.39 to 1.66 (+19.4 %).

SECOP plans to start the production of the new compressor in November 2021. Later on, a new version of the compressor controller will be set into production. This will include the new AEO control strategy developed in this project.

The price for the new compressor is not yet known.

At Vestfrost Solution, a new vaccine cooler cabinet with longer hold-over time has been developed and tested. An enlarged ice storage prolongs the hold-over time to 89h 32 min, tested according to the latest WHO-PQS protocols.

A more precise temperature regulation has been developed and tested. This consists of a more sophisticated control and a small electrical heater. In addition, a new freeze protection has been developed and tested.

The new cabinets will be more robust since the control sensors are coated and the wires are protected against humidity and influence from rodents. The increased robustness supplied by the new remote monitoring device (EMS) is expected to reduce the need for service and to prolong the lifetime of the coolers. Vestfrost plans to increase the guaranty period from 2 to 3 years for the new coolers.

Vestfrost has developed and tested a new remote monitoring device: "EMS". It has the size of an Iphone, and it is connected to GSM mobile phone net. It includes a GPS that makes it possible for the administrative authority to see where the unit is placed. The EMS sends periodical reports to the authority, and it sends an alarm, if something gets wrong. Energy Harvesting will be possible using the new EMS device. Two USB slots (5V) are built in.

The new cabinet with the new temperature control and the EMS remote monitoring device has been in field test in Africa with good results.

The new cooler has been tested at Danish Technological Institute and approved according to the WHO specifications.

The cost of the new cabinet is expected to be slightly higher compared to the existing Solar DD vaccine cabinets due to increased costs for the remote monitoring device (EMS) and a larger ice bank. It is however expected that the new cooler will be very competitive according to the better temperature regulation, the prolonged hold-over time and the remote monitoring possibility.

## 2.2 Danish version

To nye Solar Direct Drive-kompressor er udviklet og testet i dette projekt.

Den første er baseret på den relativt nye SECOP XV-kompressorplatform. Denne blev udviklet og testet med succes. På grund af nye ejere og strategændring hos SECOP blev det besluttet at stoppe den videre udvikling af denne kompressor, fordi den er baseret på en husholdnings-kompressorplatform. Den nye strategi for SECOP er at fokusere på kompressor til professionelle apparater.

En ny kompressorplatform er udviklet til alle SECOP's jævnstrømskompressor, inklusive kompressor til bilindustrien og til Solar Direct Drive-sektoren. Navnet er "Nano-kompressor". SECOP har udviklet BD-Nano50K Direct Drive-kompressoren, som er mere effektiv, og den har en større kølekapacitet sammenlignet med den eksisterende BD35K DD-kompressor.

For fryseanvendelser (Tevap = -25 ° C) er kølekapaciteten steget fra 36W til 50,8W (+ 41 %), og energieffektiviteten (COP) er steget fra 0,87 til 1,19 (+ 36,8 %).

For køleskabsanvendelse (Tevap = -10 ° C) er kølekapaciteten steget fra 83,8W til 109,1W (+ 30,2 %), og energieffektiviteten (COP) er steget fra 1,39 til 1,66 (+ 19,4 %).

SECOP planlægger at starte produktionen af den nye kompressor (BD Nano 50K) i november 2021. Senere vil en ny version af kompressorstyringen blive sat i produktion. Dette inkluderer den nye AEO-kontrolstrategi, der er udviklet i dette projekt.

Prisen for den nye kompressor er endnu ikke kendt.

Hos Vestfrost Solution er der udviklet og testet en ny vaccinekøler med længere "hold-over time". Et større islager forlænger "hold-over time" til 89 timer og 32 minutter, testet i henhold til de nyeste WHO-PQS-protokoller.

En mere præcis temperaturregulering er blevet udviklet og testet. Dette består af en sofistikeret styring, et lille elektrisk varmelegeme og en bedre placering af temperaturfølere. Derudover er der udviklet, testet og implementeret en ny frostsikring.

De nye vaccinekølere vil være mere robuste, da styringsfølerne er beskyttede (covered), og ledningerne er beskyttet mod fugt og gnavere. En ny fjernovervågningsenhed (EMS) forventes at reducere behovet for service og forlænge kølernes levetid. Vestfrost planlægger at øge garantiperioden fra 2 til 3 år for de nye kølere.

Den nye fjernovervågningsenhed (EMS), som Vestfrost har udviklet, har størrelse som en Iphone, og den er forbundet til GSM-mobiltelefonnettet. Den inkluderer en GPS, der gør det muligt for den administrative enhed at se, hvor køleren er placeret. EMS sender periodiske rapporter til den administrative enhed, og den sender en alarm, hvis noget går galt. "Energy harvesting" (f.eks. til opladning af en mobiltelefon eller lignende) vil være mulig ved hjælp af den nye EMS-enhed. To USB-stik (5V) er indbygget.

Det nye kabinet med den nye temperaturregulering og EMS-fjernovervågningsenhed har været i field test i Afrika med gode resultater.

Den nye køler er testet på Teknologisk Institut og godkendt i henhold til WHO-specifikationerne.

Omkostningerne ved det nye kabinet forventes at være lidt højere sammenlignet med de eksisterende Solar DD-vaccinekabinetter på grund af øgede omkostninger til fjernovervågningsenheden (EMS) og en større is-bank. Det forventes imidlertid, at den nye køler vil være meget konkurrencedygtig på grund af bedre temperaturregulering, den lange "hold-over time" og fjernovervågningsenheden.

### 3. Project objectives

It is a fact that vaccine coolers running directly on photovoltaic (PV) solar power without a battery has become the fastest growing health sector technology. It is also known as solar-direct-drive (SDD) cooling.

The main reason for this success is that batteries for refrigerator energy storage are no longer recommended by WHO, who states that batteries are historically the most vulnerable component and the most expensive part that needs regular replacement. Removing them has the potential to increase the long-term success of solar vaccine refrigeration. A simple battery failure can cost thousands of dollars in spoiled vaccines.

It is technically challenging to start a compressor directly on a PV panel and to keep the internal temperature stable, but this was achieved in a previous project supported by the Danish Energy Agency (EFP) with the same partners as in this project. Both SECOP and Vestfrost Solutions have had commercial success with their solar powered products due to this pioneer project where ice was used for energy storage. However, the technology used in photovoltaic (PV) direct-powered coolers with ice storage is now almost 20 years old, and the time seems right to think about upgrading the technology and developing new concepts in order to stay in front with this technology. The compressor design used in almost all WHO-approved DD vaccine coolers is also 20 years old. There are no - or very few - alternatives to this small solar direct drive compressor from SECOP (former Danfoss Compressors), and it is thus limited which size and type of refrigerators that can be developed with this technology.

Vestfrost Solutions is still one of the major suppliers of solar direct drive (SDD) cabinets, but other companies are constantly increasing the competitive pressure, and a reaction is therefore required to consolidate Danish SDD industry.

In this project, the next generation of Solar Direct Drive coolers and compressors for this application has been developed and tested.

The project activities have been a blend of theoretical work, simulation models, development of hardware, and laboratory experiments. An improved PV simulation power supply system for laboratory measurements on SDD refrigerators has been introduced to verify the compressor's response to fast fluctuations in solar irradiance level.

The project has been coordinated with international stakeholders, including WHO and UNICEF, to ensure that the new product is in line with the needs and wishes of the most important users. This was done at a meeting organized by WHO at the UN City in Copenhagen 26th June 2019 where the project was presented. This has continued by bilateral contacts between the project partners and the WHO technical groups.

#### 3.1 Aim of the project

The overall aim of the project is to develop and test the next generation of direct solar-powered coolers for storing vaccines and other temperature sensitive products such as fish and meat in areas without power supply.

The next generation of solar DD technology will use the energy from the PV panels more efficiently, enabling the use of smaller panels with less transport and installation costs. The product will be cheaper to produce and will be even more competitive than current models when compared to alternatives, including gas-powered absorption and refrigerators powered by gasoline-powered generators. The temperature distribution will be better than the current generation of vaccine refrigerators, which means that there will be better security against vaccine freezing.

Moreover, the new generation includes an optional monitoring system that is able to provide warnings (via SMS) when preset temperature limits are exceeded or another malfunction is detected. Service can thus be carried out before WHO accepted temperature limits have been exceeded. This can reduce spoiling of expensive vaccines.

Refrigerators for food and beverages will typically need bigger compressors than vaccine coolers, because the food and drinks need to be cooled down after loading. The project will therefore look at possible ways to find compressor solutions with increased cooling capacity compared to the models found today.

The project has the following specification targets for the new compressor:

- More than 20 % increased cooling capacity (suitable for cabinets up to about 200 l)
- Higher cooling efficiency (more than 20 %)
- Wider dynamic range 1:3 (Now it is 1:1.75)
- For natural refrigerant R600a or R290
- Voltage adapted to most common PV module market (72 cells)
- Improved power electronics for MPP tracking and soft start.

The project has the following specification targets for the new vaccine cooler:

- Better protection against dust and water intrusion
- Anti-freeze protection
- Built-in monitoring and warning system for fault detection
- Improved efficiency and energy harvesting
- Longer autonomy time
- Reduction of humidity and improved condensate drainage
- Safety (No exposure to electrical connections)
- Robustness
- Reduced need for service, which is often difficult and expensive in remote areas. (ultimately 20 years without any specialist service needed)
- Lower system cost, target price <2000\$.

These improvements will help Secop and Vestfrost Solutions expand the business and the international market share on solar DD coolers.

With new and advanced compressor controls, it will be necessary to verify the function with a solar module simulator, which will be acquired or constructed under the project. DTI is accredited for the so-called PQS test of WHO approved appliances and will strengthen its position through this project activity.



## 3.2 Work packages

The project development work is concentrated into 7 work packages:

### ***WP1: Documentation of existing SDD products and listing of relevant improvements***

- Market request and potential for new features and improvements
- Review of competitors and their products
- Identify SECOP compressor platform(s) suitable for the new product
- Identify cabinet types suitable for the new product.

Milestone 1: Internal report. The report will contain a catalogue of current SDD products and recommended platforms for compressor and cabinet development.

Responsible: DTI (With SECOP+VFS).

### ***WP2: Compressor and controller development***

- Current SDD control strategy and experience
- Potential improvements and their impact on energy efficiency and cost
- Sketch design of improved controller/energy management system
- Manufacture new compressor/controller prototype.

Milestone: Prototype compressor/controller developed.

Commercial milestone: Datasheet public for the new compressor.

Responsible: SECOP (With DTI).

### ***WP3: Thermal design of cabinet***

- Improved insulation
- Evaporator and condenser optimization
- Thermal storage and thermostat design
- Integration of electronic alarm/monitoring system.

Milestone: New cabinet ready for test.

Commercial milestone: Datasheet public for the new SDD model.

Responsible: Vestfrost Solutions (With DTI and DTU).

### ***WP4: Laboratory measurements***

- Improve measurement procedure by introducing a PV simulator
- Operation of prototypes in climate chamber
- Identify and report possible improvements
- Operation and measurements on improved prototype.

Milestone: Measurement report.

Responsible: DTI (With VFS and SECOP).

**WP5 Development of simulation model**

- Modelling of power supply
- Modelling of control system
- Modelling of thermal storage and heat transfer
- Validation of simulation software.

Milestone: Scientific publication.

Responsible: DTU MEK and DTI (with all partners).

**WP6: Design optimization and guidelines development**

- Parameter study and conclusions
- Economic assessment and case studies
- Development of guidelines for potential manufacturers.

Milestone: Guideline developed.

Responsible: DTU MEK (With all partners).

**WP7: Project management, international cooperation, and exchange of information**

- Administration
- Arrange meetings with UNICEF and CHAI
- Write an article about the public parts of the project
- Exchange information with the current SolarChill project
- Final reporting.

Milestone: Final report.

Responsible: DTI (With all partners).

### 3.3 Project participants and roles

The project partners are Vestfrost Solutions, SECOP, DTU MEK and DTI (project manager).

***Danish Technological Institute (DTI):***

DTI is placed in Taastrup, just outside Copenhagen, Denmark.

Refrigeration specialist Per Henrik Pedersen and solar energy specialist Ivan Katic have been involved in the project.

***Vestfrost Solutions (VFS or Vestfrost):***

Vestfrost is placed in Esbjerg, Denmark.

Innovation manager Claus Cording, refrigeration specialist Per Nygaard Hansen, and construction specialist Kenneth Nielsen have been involved.

***SECOP:***

SECOP is placed in Flensburg, Germany.

Application engineering manager Hendrik Möller has been project manager, and many others, including application engineer John Svane Christensen (who retired during the project), have been involved.

***DTU-MEK (DTU):***

DTU (the Danish Technical University) is placed in Lyngby, just outside Copenhagen, Denmark.

Associate professor and PhD Wiebke Markussen and Postdoc Jonas Jensen have been working on this project. A MSc study was involved in the project, conducted by the student Christoffer Reinhold Busk.

## 4. Project implementation

The story of solar direct drive vaccine refrigerators dates to before year 2000 where DTI conducted the first experiments with a 12 V DC Danfoss compressor. The primitive setup proved that it was possible to store sufficient energy in ice instead of in a battery, thus creating a very robust and simple cooling device for developing countries where battery lifetime is often very short in practice and replacement can be difficult and expensive. This prototype relied on a large capacitor to provide the high start current needed by the compressor.

In 2002, Danfoss Compressors marketed the first dedicated solar PV compressor with integrated soft start circuit, so that any equipment manufacturer could connect it directly to a standard PV panel. The result was that a few manufacturers took up this idea and became shortlisted in WHO's certification scheme for solar direct drive vaccine refrigerators. Vestfrost and shortly later Dometic were the first movers in this market.

Until that time, off grid vaccine cooling had only been possible with DC refrigerators driven by PV systems including a lead acid battery or by absorption refrigerators driven by gas or kerosene.

The development of SDD vaccine refrigerators was very much encouraged by WHO when the first field test results proved that the technology was extremely reliable compared to all other alternatives. The only drawback was the initial cost and an oversized PV panel to compensate for the relatively short runtime during day hours. Since then, the cost of PV has decreased dramatically so this factor is now less important (PV costs less than 1 USD/W).

Until today, the SDD technology has only been used in the health sector due to its very high demand for reliability and less focus on cost. Besides this market, there is a well-established market for solar+battery refrigerators in the commercial and household sectors. There is also a growing market for large-scale solar refrigerated containers and cold stores. At present, this sector cannot make use of the SDD technology because there are only a few SDD compressors available and their cooling capacity is far too low. However, such cold stores could already now benefit from a combination of a small battery and a large ice bank, using known technology.

Haier has recently developed a walk-in SDD cold store based on six compressors in cascade operation.

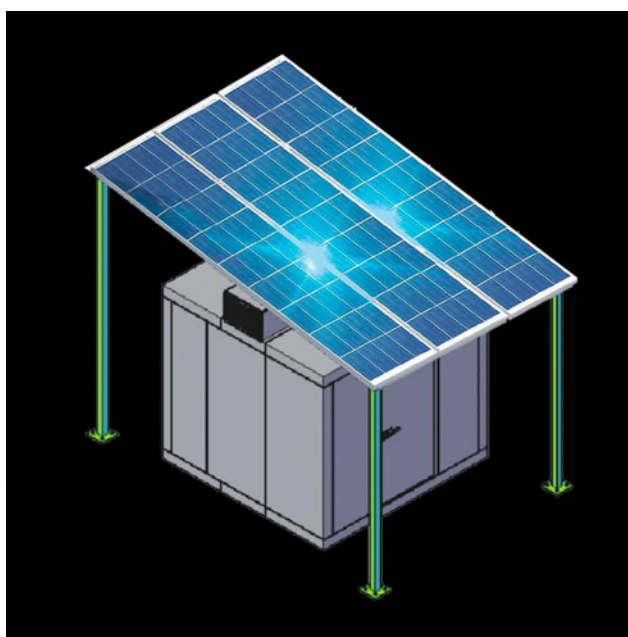


Figure 1: The Haier SDD Walk-in cold room found at the internet.

[Haier Biomedical, the world's only complete cold chain provider \(haiermedical.com\)](https://www.youtube.com/watch?v=e2CyWemG9hk)  
<https://www.youtube.com/watch?v=e2CyWemG9hk>  
[210fdbd2ce6361569948f9855d20f8fc.pdf \(aliyuncs.com\)](https://www.youtube.com/watch?v=e2CyWemG9hk)

Though it was launched in 2020, it is not found as a standard product at Haier's homepage so there might still be some issues to be solved.

### Electrical design

In principle, the electrical design of a SDD refrigerator or freezer is extremely simple if the compressor and PV panel voltages are compatible. A PV panel can only generate a certain current and voltage, so if these values do not exceed the input limits of the compressor, the panel(s) can be directly connected without any fuses or converters in the line. The current is directly proportional to the amount of solar radiation on the PV panel, so if the start current of the compressor is too high, it may never start or start too late when the sun is intense enough.

### Soft start devices

The main technical challenge when combining a DC compressor with a PV panel is that the compressor needs a high start current that the PV panel cannot deliver unless it is excessively large. This inrush current is typically 5-6 times higher than the nominal current. This is not a specific problem for PV systems only, but for all power sources with limited output current. Some manufacturers have therefore developed various electronic soft start devices for compressors used with such power sources, e.g. battery inverters on boats or in caravans.



Figure 2 Example of a soft starter for AC compressors.

There does not seem to exist any commercial DC compressor starters - except very large capacitors that are charged before a start attempt. The first prototype at DTI used such a capacitor with the size of a tin can. With the development of supercaps, the power and energy density of capacitors has increased a lot so this may be a practical method today.

When the start problem is solved, there is yet a technical challenge. Ideally, the operating voltage of the compressor should fit the maximum power point (MPP) voltage of the PV panel, i.e. the voltage where it generates most power. This requires a special electronic circuit, which is now standard in PV inverters, charge regulators and other PV loads (Maximum Power Point Tracker, MPPT). The MPP voltage changes with temperature and irradiance, but not dramatically. It is therefore also possible to define a typical fixed operating voltage that will work well under most conditions.

For a SDD refrigerator, the critical time of the year is when irradiance is low and temperature is high, typically during the rainy season. It requires a simulation tool to define the ideal voltage for a given combination of refrigerator and PV panels (DTU has developed a model for this reported in chapter 3). High ambient temperature causes the optimum voltage to decrease by about 0.5 % per Kelvin. In a hot climate, it is not unusual to have 70 °C cell temperature instead of the 25 °C used in the standard PV module test. Voltage should therefore be reduced by  $(70-25) \cdot 0.5 = 23\%$  compared to the data sheet value. Furthermore, the voltage drops slightly with decreasing solar irradiance. The current increases proportionally with irradiance level, so the start current should match the module current at a reasonable irradiance level to ensure as long a daily runtime as possible.

**PV modules**

The cheapest standard PV modules (for on-grid applications) are usually made with 60 or 72 cells in series, which for 60 cells results in a nominal MPP voltage of about 32 Volt. Therefore, 25 V would be a reasonable choice taking the above arguments into consideration. The nominal power is typically 250-400 Wp (Watt Peak) with the cell size used today, but smaller modules are available for solar home systems and special applications. It is likely that increasing cell size in the future will result in higher current of standard PV modules, but there will always be a market for (smaller) off grid PV panels in 12 V or 24 V battery systems, should the standard modules grow too large compared to the cooling demand of the SDD appliance. Thin film PV modules do not come in standard voltage or dimensions and do often have more than 60 V MPP voltage, which is over the limit for WHO SDD refrigerators according to PQS specifications. It should be mentioned that there are thin film types with better high temperature performance than the usual crystalline types and that they are more tolerant to partial shading.

**PV module: Generic, Poly 250 Wp 60 cells**

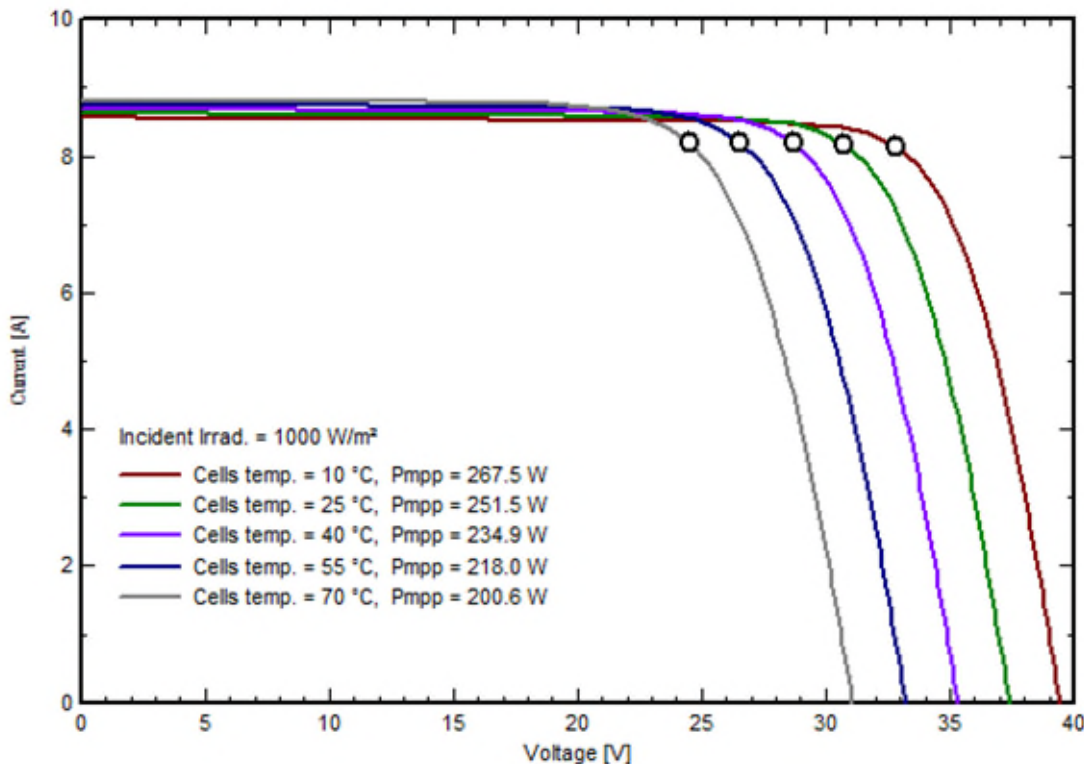


Figure 3 Typical characteristics for a crystalline silicon PV module. For this module, 25 V is a suitable operating voltage at elevated cell temperature.

**Compressor and cooling capacity estimate**

All WHO approved solar direct drive refrigerators/freezers models are using a DC compressor. A very popular type is SECOP BD35K\_Direct Current Compressor for Solar Applications with a voltage range of 10 - 45V DC. In fact, this compressor type is completely dominating the market for SDD vaccine refrigerators, where

almost all WHO approved products are using it (with R600a (isobutane) as refrigerant). An important exception is Sundanzer (using R134a, which is an HFC-refrigerant).

The specialty of the BD35K compressor in SDD version is that it uses a so-called adaptive energy optimizer (AEO) to control the operating voltage. It is a very primitive kind of regulator working after the trial and error principle:

1. The compressor attempts to start up at lowest possible speed (less current draw).
2. If start is successful, speed is slowly ramped up, and power is increasing.
3. If a cloud blocks the sun, the voltage collapses, and the compressor stops completely.
4. The procedure is repeated after some minutes pause.

Though this sounds very simple, it works in practice because a few good and sunny days can charge the ice storage so it can keep the temperature stable for some days without sun. However, on days with drifting clouds, the system is not the best because there are too many compressor outages and restart attempts. All SDD refrigerators must therefore use oversized PV panels or a more advanced thermal design leading to a higher system cost than necessary.

Alternative solutions to the common system configuration could be:

- Linear compressor with inherently low start current, which could be interesting in connection with a simple inverter circuit (LG uses this in some AC appliances).
- Standard AC compressor with a soft start device and a PV inverter.
- Standard DC compressor with external DC/DC converter to match a variable PV voltage.

It is possible that there are other not commonly known solutions.

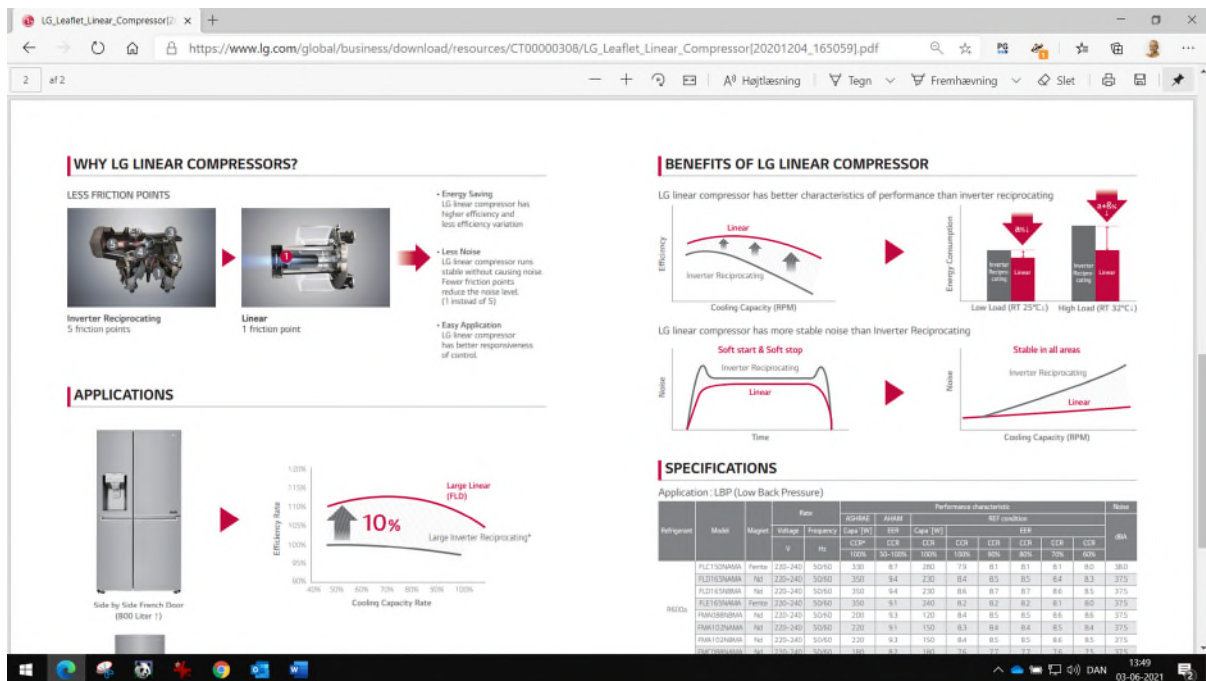


Figure 4 Data for linear compressor from LG: LG\_Leaflet\_Linear\_Compressor[20201204\_165059].pdf

The most important compressor data for BD35K are given here:

Capacity (EN 12900 Household/GECOMAF)						12V DC, static cooling						watt
rpm \ °C	-30	-25	-23.3	-20	-15	-10	-5	0	5	7.2	10	15
2,000	13.2	21.0	23.8	29.7	39.6	51.0	64.0	79.1	96.3	105	116	
2,500	16.8	25.5	28.8	35.6	47.5	61.3	77.5	96.2	118	128		
3,000	20.7	30.5	34.3	42.3	56.3	72.9	92.4	115				
3,500	24.9	36.0	40.2	49.3	65.1	83.8	106					

Capacity (ASHRAE LBP)						12V DC, static cooling						watt
rpm \ °C	-30	-25	-23.3	-20	-15	-10	-5	0	5	7.2	10	15
2,000	16.0	25.5	29.0	36.1	48.2	62.1	78.0	96.4	118	128	142	
2,500	20.4	31.0	35.0	43.4	57.8	74.7	94.4	117	144	157		
3,000	25.2	37.1	41.7	51.4	68.5	88.7	113	140				
3,500	30.3	43.8	49.0	59.9	79.2	102	129					

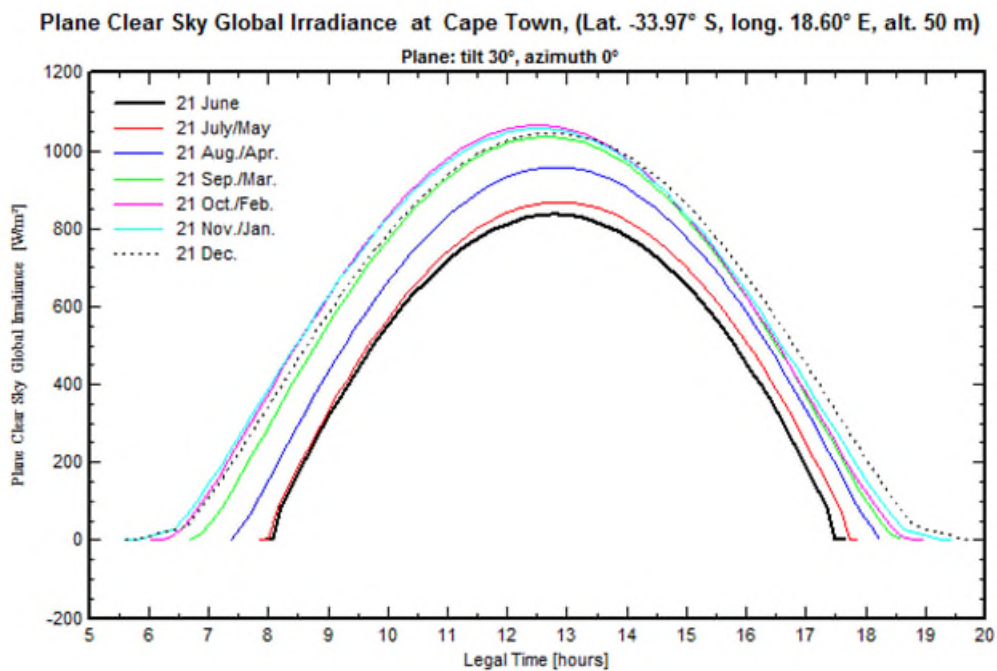
  

Power consumption						12V DC, static cooling						watt
rpm \ °C	-30	-25	-23.3	-20	-15	-10	-5	0	5	7.2	10	15
2,000	18.5	22.5	23.9	26.4	30.3	34.2	38.0	41.8	45.7	47.4	49.6	
2,500	23.8	28.5	30.0	32.9	37.2	41.5	45.8	50.2	54.9	57.1		
3,000	29.5	35.9	38.0	41.8	47.4	52.9	58.6	64.6				
3,500	35.1	42.7	45.2	49.7	56.4	63.0	69.7					

Figure 5 Data for Secop BD35K. Dynamic range for the cooling capacity at -5degC evaporator temperature is 106/64 = 1.65.

The power consumption of up to 69.7 W can be fulfilled by a single standard module of 250 W<sub>p</sub>, i.e. full compressor power is reached at about ¼ of the nominal PV output (250W<sub>p</sub> is the nominal output power @ 1 sun = 1000 W/m<sup>2</sup> and ¼ of this is 63 W).

Typical clear sky daily irradiance curves will look like:





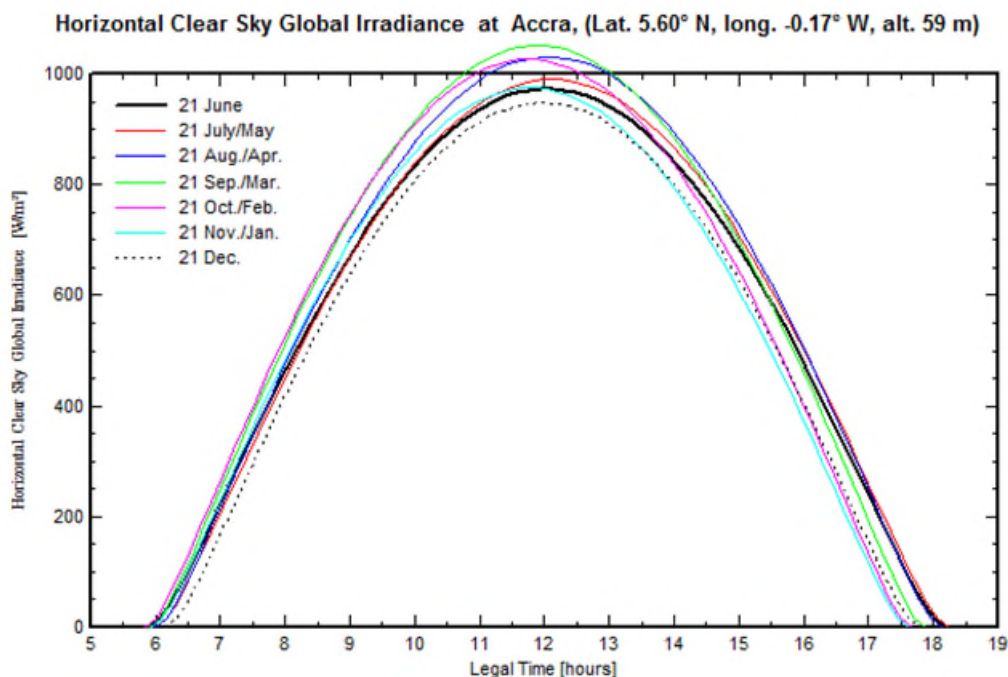


Figure 6 Solar irradiance curves for a clear day from PVsyst simulation software.

For Cape Town, there is significant seasonal variation. For Accra this is not the case due to its location near the equator.

If we assume a typical runtime of 6 hours per day at full capacity for BD35K, it is possible to produce  $6 \times 69.7 = 0.4$  kWh thermal energy. This corresponds to the cooling of 17 kg of water from 25 to 5 °C. If the heat influx to the cabinet is estimated to 0.2 kWh/24 h, then the actual cooling capacity is only 8.5 kg of water in this example. In the startup phase where the ice storage is being frozen, the ice accumulation is about 2 kg per 24 h runtime when net cooling capacity is 0.2 kWh/24 h.

The electricity consumption of SDD refrigerators (measured in the PQS stable running test) is 0.24 – 1.2 kWh/24 h. The cooling capacity is not measured by the test, but according to the compressor specifications it would typically be 1.5-2 times higher than the electric input power. It is evident that excellent insulation is important if not all power should go for balancing losses.

### Cabinet design options

Most manufacturers of SDD appliances use a chest type cabinet, and some of them include vacuum insulation panels for improved hold-over time. The thermal storage capacity is either established in the form of ice-packs, special icelining or a complete water/ice tank surrounding the storage volume. Useful volume is generally less than 100 l for vaccine refrigerators. Household and commercial models need to be larger and will mostly not use expensive vacuum panels. The energy consumption will thus be much higher, not at least due to higher input rate of warm food and drinks. The system designers must take this into account, and it may be necessary to develop SDD compressors with higher capacity or use compressors in parallel.

On the other hand, temperature stability and hold-over time is not so critical for commercial and household refrigerators, since the alternative is often no refrigeration at all.

Upright cabinets with a door are used by some manufacturers, especially vaccine refrigerators based on the SureChill® principle where a water/ice tank surrounds the storage compartment. The ice is formed at the top of the tank, and the cold water flows to the bottom by natural convection. While this ensures a very stable temperature around 4 °C, the door opening causes a certain exchange of air, and therefore energy consumption can be higher than for the chest type.

If freezing is required, it is possible to construct SDD cabinets for freezing only or for combined cooling and freezing where the latter is more complicated to build and control (See PQS listed models later in this chapter). Freezing of icepacks is also feasible by simple thermostat adjustment of many refrigerators. Freezing to very low temperatures (as required for some types of covid19 vaccine) is not possible with current models.

Since heat transfer between the storage compartment and the thermal storage relies on passive means, there is a risk that temperatures deviate from the desired 2-8 °C range. For example, a cold icebank combined with low ambient temperature may cause freezing in the storage compartment. Some manufacturers are therefore using fans or electric heaters in an attempt to avoid temperature excursions.

### Use of excess power

It is evident that on clear days, a solar direct drive refrigerator can only use a fraction of the potential power production from the PV panel(s) and some stakeholders have therefore suggested to add a circuit for diversion of excess power to secondary loads. There is currently a single WHO approved product on the market from Dulas Ltd. The control system automatically senses when excess energy is available and turns the Solar Socket on. Should the sunshine reduce, the Solar Socket output is correspondingly reduced or turned off, always ensuring that the cooling system has priority over the available power.



Call us: +44 1654 705055 [Client login](#)

[Products](#) [Solutions](#) [Why Dulas Solar](#) [News](#) [Contact](#) [Downloads](#)

## Integrated Solar Harvesting with the Solar Socket

### A simple add-on with extraordinary potential

Dulas' new Solar Socket turns your SDD refrigerator into an energy source for a wide range of devices and equipment. Utilising surplus energy generated by the refrigerator, the Solar Socket makes the most of the photovoltaic system whilst remaining 100% safe and stable for vaccines. Our intelligent control system continuously varies the amount of energy available to the socket whilst prioritising vaccine storage at all times. The Solar Socket has two USB ports and one 12v cigarette lighter socket for multipurpose use.



### Options

This simple but effective product will empower any facility to offer so much more to their patients. Medical equipment, lamps and fans are now widely supplied with USB plugs and can be powered directly from the refrigerator. The Solar Socket is also ideal for charging a mobile phone which in turn can become a hand-held blood pressure or pulse monitor, a bank, a patient medication scheduler or quite simply, a lifeline to call out for help.



Figure 7 Solar Socket from Dulas Ltd. It is not clear from the homepage how much power can be extracted this way.

The organization PATH has carried out a practical study of various power control strategies and published it at [http://www.path.org/publications/files/DT\\_ehc\\_full\\_doc\\_rpt.pdf](http://www.path.org/publications/files/DT_ehc_full_doc_rpt.pdf) WHO has set up a test and approval procedure to ensure that similar devices do not compromise basic refrigeration service.

In the commercial and household sectors, it would be extra relevant to use excess power to charge a battery that can run lights, TV, fans etc. since users would otherwise have to buy a parallel stand-alone PV system.

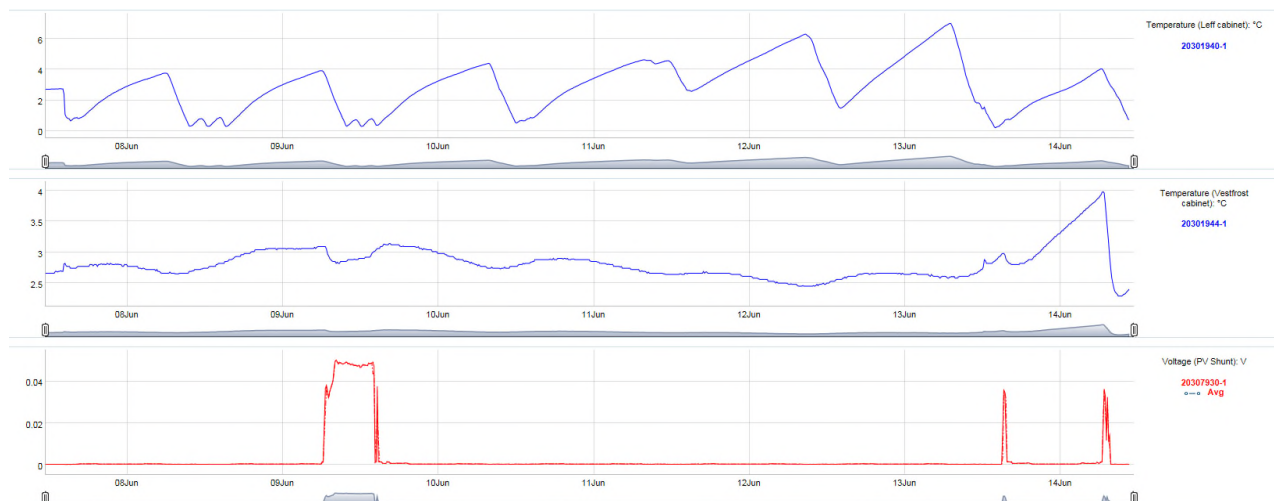


Figure 8 Measured temperature profile for two SDD cabinets running at DTI. The upper curve is for a chest cabinet with normal insulation, the lower uses vacuum insulation. Shunt voltage indicates when the compressor is running at the unit with vacuum isolation (using a 180 W panel).

**Experience from the field**

Several projects and organizations have collected field experience from SDD units in health clinics and some of the observations are:

- Vaccine packages are sometimes becoming wet by condensation of water vapour in humid climates. Especially for upright models where the air is exchanged by gravity when the door is opened. A good drain system is important.
- Occasional freezing near the surface of the cabinet, especially some models with an icelining.
- In deep chest models, it can be difficult to keep an overview of the stock.
- In models with integrated ice pack freezing, it is important not to overload the system with warm ice packs.

WHO PQS Listed SDD appliances as per 03-06-2021:

003/092	Solar Direct Drive Refrigerator and Freezer	Vestfrost Solutions	VLS 056 RF SDD
E003/048	Solar Direct Drive Combined Refrigerator/Freezer	Dulas Ltd	VC150SDD
E003/057	Solar Direct Drive Combined Refrigerator/Freezer	Qingdao Haier Bio-medical Co., Ltd	HTCD-160
E003/020	Solar direct drive refrigerator	SunDanzer Refrigeration Inc.	BFRV55
E003/030	Solar direct drive refrigerator	B Medical Systems Sarl	TCW 3000 SDD
E003/037	Solar direct drive refrigerator	Zero Appliances (Pty) Ltd	ZLF 100 DC (SureChill ®)
E003/106	Solar direct drive refrigerator	Vestfrost Solutions	VLS 054A SDD Green line
E003/049	Solar Direct Drive Refrigerator	Godrej & Boyce MFG. Co. Ltd.	GVR 50DC SDD
E003/050	Solar Direct Drive Refrigerator	Godrej & Boyce MFG. Co. Ltd.	GVR 100 DC (SureChill®)
E003/052	Solar direct drive refrigerator	Zero Appliances (Pty) Ltd	ZLF 150 DC (SureChill ®)

E003/107	Solar direct drive refrigerator	Vestfrost Solutions	VLS 094A SDD Greenline
E003/108	Solar direct drive refrigerator	Vestfrost Solutions	VLS 154A SDD Greenline
E003/055	Solar direct drive refrigerator	Zero Appliances (Pty) Ltd	ZLF 30DC SDD (SureChill ®)
E003/040	Solar Direct Drive Refrigerator	Dulas Ltd	VC200SDD
E003/068	Solar Direct Drive refrigerator	B Medical Systems Sarl	TCW 40R SDD
E003/069	Solar direct drive refrigerator	Vestfrost Solutions	VLS 024 SDD
E003/067	Solar direct drive refrigerator	B Medical Systems Sarl	TCW 15R SDD
E003/075	Solar direct drive refrigerator	Qingdao Haier Bio-medical Co., Ltd	HTC 40 SDD
E003/076	Solar direct drive refrigerator	Qingdao Haier Bio-medical Co., Ltd	HTC 110 SDD
E003/078	Solar Direct Drive refrigerator	Dulas Ltd	VC50SDD
E003/084	Solar Direct Drive refrigerator	Dulas Ltd	VC60SDD-1
E003/085	Solar Direct Drive Refrigerator	Dulas Ltd	VC30SDD
E003/090	Solar Direct Drive Refrigerator	B Medical Systems Sarl	Ultra 16 SDD
E003/093	Solar Direct Drive Refrigerator	B Medical Systems Sarl	TCW 4000 SDD
E003/098	Solar Direct Drive Refrigerator	Qingdao Aucma Global Medical Co.,Ltd.	CFD-50 SDD
E003/102	Solar Direct Drive Refrigerator	Qingdao Haier Bio-medical Co., Ltd	HTC-112
E003/105	Solar Direct Drive Refrigerator	Godrej & Boyce MFG. Co. Ltd.	GVR 25 Lite DC
E003/116	Solar Direct Drive Refrigerator	Qingdao Haier Bio-medical Co., Ltd	HTC-120
E003/117	Solar Direct Drive Refrigerator	Qingdao Haier Bio-medical Co., Ltd	HTC-240
E003/118	Solar Direct Drive Refrigerator	Qingdao Aucma Global Medical Co.,Ltd.	ARKTEK YBC-10 SDD
E003/119	Solar Direct Drive Refrigerator	Vestfrost Solutions	VLS076SDD
E003/077	Solar Direct Drive Refrigerator and Freezer	B Medical Systems Sarl	TCW15 SDD
E003/091	Solar Direct Drive Refrigerator and Freezer	Vestfrost Solutions	VLS 026 RF SDD
E003/095	Solar Direct Drive Refrigerator and Freezer	Godrej & Boyce MFG. Co. Ltd.	GVR 55 FF DC
E003/039	Solar direct drive refrigerator BFRV15 SDD	SunDanzer Refrigeration Inc.	BFRV 15
E003/045	Solar direct drive refrigerator TCW3043SDD	B Medical Systems Sarl	TCW 3043 SDD

E003/035	Solar direct drive refrigerator/freezer	B Medical Systems Sarl	TCW 2000 SDD
E003/074	Solar direct drive refrigerator/freezer	Qingdao Haier Biomedical Co., Ltd	HTCD 90 SDD
E003/042	Solar direct drive refrigerator/freezer TCW 40 SDD	B Medical Systems Sarl	TCW 40 SDD
E003/043	Solar direct drive refrigerator/freezer TCW2043SDD	B Medical Systems Sarl	TCW 2043 SDD
E003/058	Solar Direct Drive vaccine refrigerator	Dulas Ltd	Dulas VC110SDD
E003/059	Solar Direct Drive vaccine refrigerator	Dulas Ltd	VC88SDD
E003/073	Solar Direct Drive Waterpacks Freezer	B Medical Systems Sarl	TFW 40 SDD
E003/086	Solar Direct Drive Waterpacks Freezer	Qingdao Haier Biomedical Co., Ltd	HTD-40
E003/099	Solar Direct Drive Waterpacks Freezer	Vestfrost Solutions	VFS 048 SDD

More details for the units can be seen at the WHO PQS list:

[https://apps.who.int/immunization\\_standards/vaccine\\_quality/pqs\\_catalogue/categorypage.aspx?id\\_cat=17](https://apps.who.int/immunization_standards/vaccine_quality/pqs_catalogue/categorypage.aspx?id_cat=17)

## Project implementation

The project implementation followed the planned schedule until October 2019.

At a project meeting in October 2019, SECOP announced that they had to stop the development of the new compressor based on the XV platform. This surprising announcement also stopped the tests at Vestfrost, since the situation (and the future) for the prototype compressor became unclear.

SECOP had been owned by Nidec since August 2017. Nidec also bought another global compressor manufacturer, Embraco, in July 2019. This created some turbulence because some cabinet manufacturer feared that this would influence the market for compressors for small commercial appliances. They feared a lack of competition for compressors in this market segment.

The EU Commission agreed on this and decided that Nidec had to sell SECOP. This happened in September 2019, and SECOP was bought by a German financial company. The new owners decided to change the focus for SECOP to only manufacture and market compressors for professional appliances.

Since the XV platform is mostly focused on the household appliance market, the development based on this platform was stopped.

SECOP announced that the developed technology would be moved to another platform, and that this would take some time to change and to develop.

Based on this, the project partners asked EUDP for permission to postpone the finalization of the project, and this was approved. The new finalization date became 30 June 2021.

After this, the project was conducted as planned.

## 5. Project results

### 5.1 Simulation program

Numerical modelling and simulation is a strong tool for investigating possible system improvements before entering the lab and thereby being able to target time needed for laboratory experiments to the most promising solutions. In this project, three different validated numerical models were developed. Each of these models had a different purpose and focus area:

#### *Model 1: Dynamic cabinet model incl. ice bank*

This model was developed with the objective of investigating optimal cabinet and ice storage dimensions and insulation thicknesses in order to increase the autonomy time of the vaccine cooler, while keeping the temperatures inside the vaccine cooler at acceptable levels.

#### *Model 2: Steady state compressor control*

This model was built for investigating the interaction between the PV panel and the compressor for different compressor control strategies. The compressor control strategy was investigated using a steady state model, which was used to make a first assessment of the possible control strategies: Adaptive Energy Optimization (AEO), Constant Voltage (CVC) and Peak Power Tracker (PPT). The steady state analysis was based on the performance over a simple clear sky solar irradiance profile.

#### *Model 3: Dynamic compressor control*

The purpose of this model was to both investigate the detailed settings of the PID controllers in the compressor control and to assess the performance under more challenging solar profiles with e.g. intermittent cloud covers.

The investigation of the cabinet design (Model 1) and the steady state assessment of the compressor control (Model 2) have both been presented at the International Congress of Refrigeration in Montreal 2019 and have been published in the associated proceedings (Appendix F and Appendix G). Model 1 was based on a Master's Thesis work carried out by Christoffer Reinhold Busk. The Master Thesis is available from <https://findit.dtu.dk/en/catalog/2436371797>. This chapter contains excerpts from these reports and papers.

#### 5.1.1 Model 1: Dynamic cabinet model incl. ice bank

Figure (left) shows a sketch of the considered vaccine cooler layout. The sketch is a cut through the middle of the vaccine cooler, and it should be noted that the ice storage surrounds the four side walls of the vaccine compartment. Furthermore, the evaporator is a spiral-shaped pipe, wrapped around the ice storage. The condenser is also a long pipe, but placed on one side of the unit, similarly to a household refrigerator. The ice storage itself is placed in the top part of the side wall and separated from the vaccine chamber by the frame with a thin layer of insulation between the frame material and the ice storage. All walls are insulated with PU foam as well as a vacuum insulation panel on the outside of the insulation. The vaccine cooler also contains a lid, which is insulated by PU foam.

For the modelling, the condenser and evaporator tubes were disregarded since the refrigeration system is idle during autonomy time. The vaccine cooler was divided into eight control volumes as seen in Figure (right). The arrows indicate how a given control volume interacts with the neighboring control volumes.

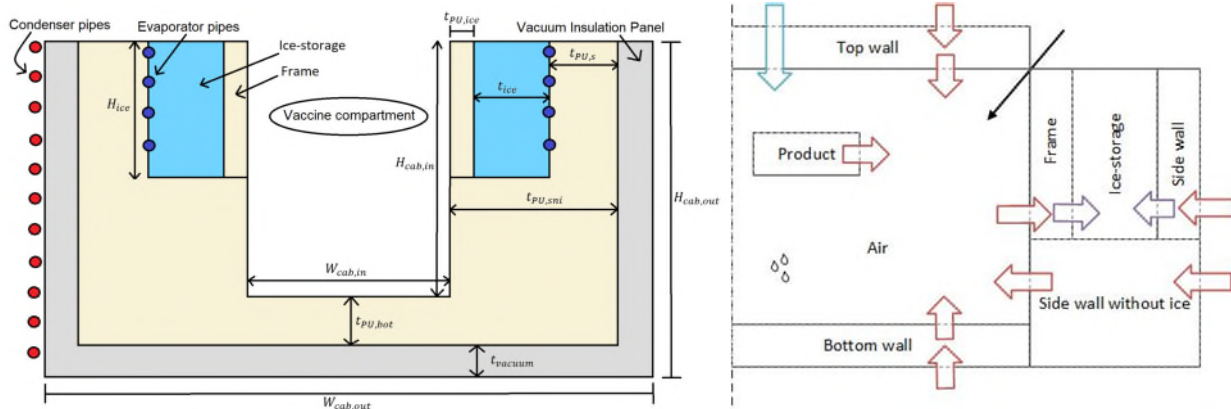


Figure 9 (Left) Sketch of the vaccine cooler cabinet with ice storage. (Right) Sketch of the modelled control volumes and their interactions.

Red arrows indicate heat transfer by convection, calculated by multiplying a convective heat transfer coefficient with the heat transferring area and the temperature difference between the surface and the ambient or cabinet inside air temperature. The two purple arrows indicate heat transfer by conduction. The blue arrow indicates heat transfer through thermal bridges. This was modelled by fixing a UA-value for the thermal bridges and multiplying this with the temperature difference between the ambient air and the air inside the vaccine compartment. Air infiltration, indicated by the solid black arrow in Figure , was taken into account in the energy balance of the air control volume as well as possible condensation of moist air.

Dynamic mass and energy balances were formulated for all control volumes. For the air, product and ice storage control volumes, a lumped capacitance approach was chosen, while transient conduction through a composite wall was applied for the wall and frame insulation control volumes. The walls consisted of an outer layer of steel, a vacuum insulation panel, a layer of insulation material (PU-foam) and another layer of steel on the inside. The walls were discretized such that a calculation node was placed at each material interface, and additionally 10 nodes were placed inside the layer of PU foam. The frame consisted of an aluminum layer, a thin layer of insulation material, and another aluminum layer. Since the insulation material was only a thin layer, only three nodes were added in this layer. Furthermore, a contact resistance of  $500 \text{ Wm}^{-2}\text{K}^{-1}$  between the ice and the aluminum layer was defined.

The product consisted of a number of vials. Each vial was assumed to have a cylindrical shape. The density and heat capacity of the vials were assumed to be similar to liquid water.

The ice bank storage was able to interact with the frame and the side wall. The model was built such that both freezing and thawing of the ice could be simulated. Since the water is placed in a closed and stable container, some degree of subcooling of the liquid is experienced prior to freezing, and the water will be at a metastable state until it reaches the freezing point. For the simulations, the freezing point temperature was a user input. The properties of the subcooled water were considered similar to non-subcooled liquid water. When reaching the freezing point temperature, part of the ice will freeze rapidly, and the temperature will increase to  $0 \text{ }^\circ\text{C}$ .

As a first step, a calibration of the model was carried out. The parameters fixed in the calibration were:

- The UA-value representing the losses through thermal bridges in the cabinet.
- The convective heat transfer coefficient on the inside and outside of the cabinet.

It was assumed that the heat transfer coefficient on the outside of the cabinet was equal to the heat transfer coefficient on the inside of the cabinet, and also the heat transfer coefficient between the product and the air was assumed equal to the heat transfer coefficient between the inside wall and the air. For the calibration, the simulated results were compared to test results from autonomy time measurements of three different test setups using the considered vaccine cooler cabinet. Apart from the autonomy time, the steady state temperature was also used as a target parameter. The steady state temperature denotes the temperature of the air when the entire system is in a steady state condition during phase change in the ice storage.

One of the tests was carried out according to the WHO performance quality and safety (PQS) standard at hot zone conditions, i.e. an ambient temperature,  $T_{amb} = 43 \text{ }^\circ\text{C}$ . According to the test standard, 1/5 of the nominal cabinet volume should be filled with water packages, each package containing 0.4 kg of water, which corresponded to 4.4 kg for the considered cabinet. For the simulations, a single volume of water was assumed. The second test was carried out by Danish Technological Institute (DTI), at temperate zone conditions, i.e.  $T_{amb} = 32 \text{ }^\circ\text{C}$ . In this test, the hold-over time was measured instead of the autonomy time. This meant that the measurement was carried out until the vaccines reached a temperature of  $12 \text{ }^\circ\text{C}$  instead of  $8 \text{ }^\circ\text{C}$ , which was the case for the two other tests. The product inside the cooler cabinet was one test package Tylose gel of 0.5 kg. The last test was carried out at DTU. In this test, the ambient conditions were not controlled, and the average ambient temperature in the lab during measurements was  $22.1 \text{ }^\circ\text{C}$ . In this test, the cabinet was empty during measurements, and the time was stopped when the air inside the cabinet reached  $8 \text{ }^\circ\text{C}$ .

### 5.1.1.1 Model Calibration

By running the model with different combinations of the convective heat transfer coefficient and the overall heat transfer coefficient representing the thermal bridges, the best combination of parameter values was found using the values stated in Table 1.

Table 1: Values of calibrated parameters for the cabinet model

Convective heat transfer coefficient	$7.0 \text{ W m}^{-2} \text{ K}^{-1}$
UA-value of thermal bridges	$0.26 \text{ W K}^{-1}$

Using the baseline model including the values presented in Table 1 and input parameters for ambient conditions corresponding to the three different measurement environments, simulated autonomy times were found as seen in Table 2. The simulated autonomy times corresponded well with the measurements, showing discrepancies of less than 3 %. Apart from the autonomy time, the steady state temperatures are shown in Table 2 as well. As seen, the steady state temperature during simulations corresponded very well with the measured temperatures.

Table 2: Comparison of autonomy time and steady state temperature of the air for measurements and simulations with the calibrated model

	Measured h	Simulated h	Deviation h
WHO	72.4	74.5	2.1
DTI	111.3	111.6	0.3
DTU	156.4	154.3	2.7
	Measured $^\circ\text{C}$	Simulated $^\circ\text{C}$	Deviation $^\circ\text{C}$
WHO	5.8	5.8	0.0
DTI	4.3	4.2	0.1
DTU	3.0	2.9	0.1

The validated model was used to develop the guidelines presented in chapter 7.

### 5.1.2 Model 2: Steady state compressor control

In a configuration such as the one seen in Figure ,Figure it is the control of the compressor speed that will ensure optimal utilization of the available power from the PV panel. Here it is important to realize that the operation of a PV panel is characterized by the voltage - current curves seen in Figure . Here the solid black lines represent the voltage - current relation for a given solar irradiance.



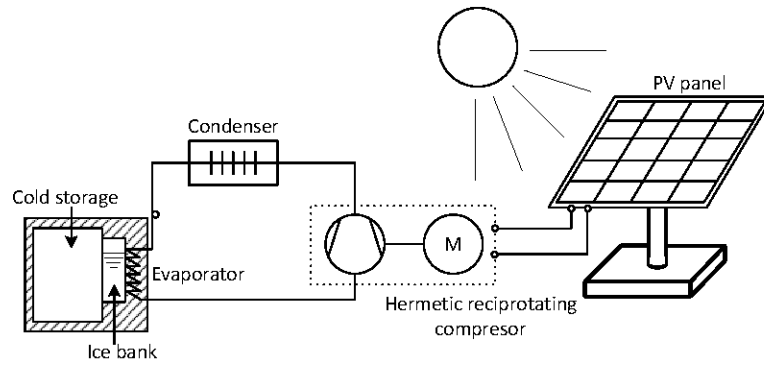


Figure 10 Principle sketch of the direct drive solar refrigeration system with ice bank storage.

Realizing that the power extracted from the PV panel is the product of the voltage and current results in the dashed blue lines. It may be seen that for each solar irradiance there is a peak power point and that this point occurs at approximately the same voltage. Furthermore, it is seen that the higher the solar irradiance, the higher the peak power.

If the system driven by the PV panel, in this case the compressor, tries to draw more power from the panel than the peak power at the given irradiance, the PV panel will experience what is called a collapse. A collapse results in no power being delivered and consequently that the system is turned off. If the compressor is run too fast there is thus a risk that it will collapse the PV panel and force a shutdown of the system. However, if the compressor is run too slow, the refrigeration system will not be utilizing as much of the available power.

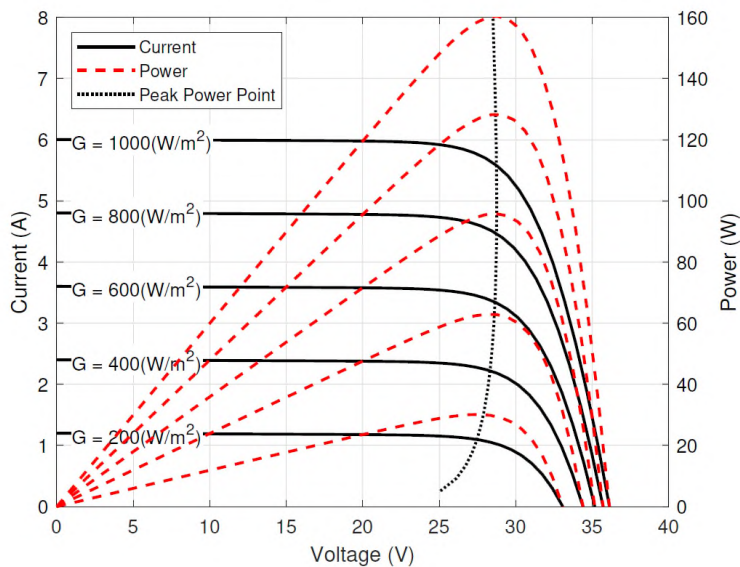


Figure 11 Principle sketch of the voltage – current operating characteristics of a PV panel.

Therefore, it is relevant to find compressor control strategies that can ensure that the system will operate as close to the peak power point as possible at the varying solar irradiance that the system will experience during a day or a year. A sketch of the applied daily solar profile may be seen in Figure . As seen here, the profile is sketched for peak irradiances from  $100 \text{ Wm}^{-2}$  to  $1000 \text{ Wm}^{-2}$ . These peak irradiance variations may resemble both seasonal variation but also cloud covers of different intensity. The work related to this model was limited to the smooth profiles seen in Figure and thus did not include intermittent cloud covers and the rapid transients involved in these. The different compressors and compressor control strategies were evaluated at the different range of solar profiles seen in Figure . This, as it was relevant to investigate both the

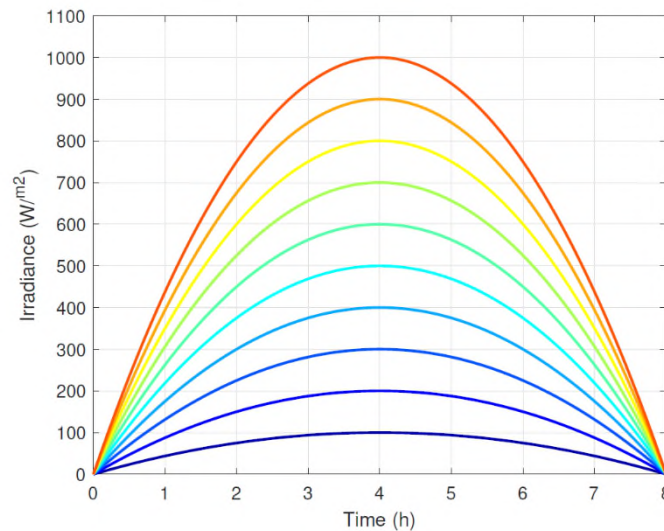


Figure 12 Sketch of the applied daily solar profiles.

minimum peak irradiance needed for the system to deliver a cooling load, but also the peak irradiance at which the available power from the solar panel cannot be fully utilized due to speed restriction of the compressor.

To perform this investigation, numerical models were developed for both the PV panel and the refrigeration system. Furthermore, the different control strategies were implemented in these models.

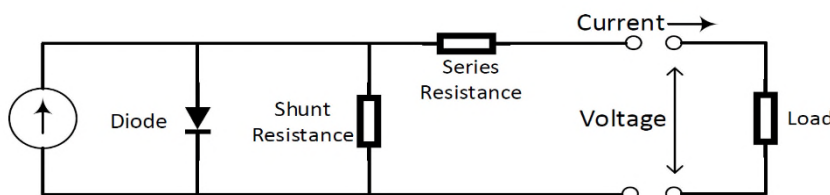


Figure 13 Circuit diagram of the one diode equivalent circuit used to model the PV panel.

The behavior of the PV panel was modelled using a "one diode" model. The one diode model uses an equivalent circuit, see Figure , to describe the operation of a single solar cell. Assuming all cells to operate identically, the one diode cell model can be used to model a complete PV panel.

The values for the shunt and series resistances as well as the diode quality factor were determined based on standard test conditions (STC) data for a given 60 cell PV panel. The STC data may be seen in Table 2 where the assumed cell operating temperature is also stated.

Table 2: Input data for the PV panel model of a single 60 cell array, operating conditions for the refrigeration system, and data for the investigated compressors

PV Panel			Refrigeration system			Compressor			
Number of cells	60	-	$T_{evap}$	-10	°C		BD35K	BDS5.0K	
Temp. coeff.	0.03	K <sup>-1</sup>	$T_{cond}$	50	°C	Disp. Vol.	3	5	cm <sup>3</sup>
STC Max Power	90	W	$\Delta T_{SH}$	10	K	Min. Speed	2000	1000	RPM
STC Max Voltage	32	V	$\Delta T_{sc}$	5	K	Max. Speed	3500	3000	RPM
STC Open Circuit Voltage	39.5	V							
STC Short Circuit Voltage	3	A							
Cell operating temp.	35	°C							

As seen in Table 2, Table 2 each PV panel has a STC max power output of 90 W. In order to supply sufficient power to the refrigeration systems, several PV panels in parallel were applied. The present work investigated the application of both 2 and 4 PV panels in parallel. These two solutions will in the following be referred to as the 180 W and 360 W PV panels, respectively, in reference to the resulting STC maximum power output of the total installation. It should be noted that the actual maximum power of the PV panels may be reduced as the assumed cell operating temperature of 35 °C was higher than the STC cell operating temperature.

The modelled refrigeration system may be seen in Figure 10 Principle sketch of the direct drive solar refrigeration system with ice bank storage. Assuming a constant ambient temperature in the room where the refrigeration system was located and that the ice bank storage was kept at a constant temperature of 0 °C, it was assumed that the evaporation and condensation temperatures as well as the level of superheating and sub-cooling would not change significantly during the operation of the system. Therefore, these values were assumed constant at the values stated in Table 2.

Two different compressors were investigated for the application in the refrigeration system. Both compressors are built for R600a. The first was the BD35K which is a DC compressor produced by SECOP, and the second compressor was a compressor called BDS5.0K - a potential new compressor produced by SECOP. The displacement volumes and speed ranges of the two compressors are stated in Table 2. As seen, the BD35K has a lower displacement volume compared to the BDS5.0K. Furthermore, the dynamic range of the BD35K is significantly lower than that of the BDS5.0K.

The operational characteristics of the two compressors, i.e. isentropic and volumetric efficiencies, were modelled using speed specific compressor polynomials supplied by the manufacturer. The polynomials were supplied at four values of compressor speed ranging from the minimum to the maximum speed. For operation at speeds in between the supplied polynomials, the efficiencies were interpolated between the values of the nearest polynomials.

Apart from the work derived from the application of the compressor polynomials, the initial start-up of the compressor requires additional power. This will in the following be referred to as the compressor start power. The compressor start power is associated with the initial positioning of the rotor. The start power for both compressors has been assumed to be 60 W. However, soft start procedures or the application of super capacitors may alleviate the need for the PV panel to supply the start power. Consequently, results were derived both with and without the 60 W compressor start power.

As the compressor in the suggested system was driven directly by the PV panel, the only manner by which sufficient utilization of the available power can be ensured was to impose a suitable compressor speed control strategy. In the present work, three different speed control strategies were investigated and compared based on their ability to utilize as much of the available power during a complete day as possible.

To quantify to which extent the compressors utilize the available power, a Utilization Factor was defined. The Utilization Factor was defined as the ratio of the integrated compressor work from sunrise to sundown over the integrated peak power over the same duration. The Utilization Factor thus indicates how well the compressor control strategy was at adapting the speed during the increasing and decreasing irradiance experienced during a day.

Apart from the Utilization Factor, the Accumulated Daily Cooling Load was also determined as the integrated cooling load delivered over the full day.

The first control strategy investigated was the PPT control. This control strategy requires the application of an external peak power tracker. The peak power tracker required the measurement of both solar irradiance and the cell operating temperature, which the peak power tracker then used to calculate the peak power point. This was then applied as a set point for the compressor speed regulation. Consequently, the PPT control ensured that when the compressor was on it ran at a speed at which the needed compressor power was equal to the PV panels peak power. However, the ability to run at the requested speed was limited by the minimum and maximum speeds of the compressors.

An alternative to the PPT control is CVC. As seen in Figure , the peak power points for increasing irradiance coincide at a close to constant voltage. Hence, it is possible to approximate the peak power point by measuring only the voltage over the PV panel. Supplying the speed control of the compressor with a set point for the PV panel voltage would thus allow the compressor to adjust the speed in order to attain a constant voltage and thus operate close to the peak power point. This control strategy alleviates the need for solar irradiance and cell temperature measurements and may thus be simpler to implement. The set point for the CVC was set to 22 V.

The final investigated control strategy was AEO. The AEO control strategy requires no additional measurements and was therefore implemented directly in the compressor. Therefore, it may be the most simple to implement. The principle of the AEO strategy was to continuously ramp up the compressor speed until the compressor would collapse the PV panel and shut the compressor off. The speed at which the collapse occurred was then stored in the controller. The compressor was then kept off for a short duration to allow pressure equalization between the condenser and evaporator in order to reduce the power consumption during start-up. It was assumed that three minutes would allow sufficient pressure equalization. After the short off period, the compressor was then turned on at a speed lower than the one at which the collapse occurred.

Two inputs are thus needed in order to run the AEO strategy: the compressor speed ramp-rate and the speed reduction when restarting the compressor. These were assumed to be constants during the operation of the system. The choice of these two constants both influences the utilization factor of the PV panel and the accumulated daily cooling load. It was found that a ramp rate of 2000 RPM h<sup>-1</sup> and a speed reduction of 400 RPM was a good trade-off for all investigated combinations of PV panel sizes and compressor types.

The results obtained from this simulation model and the guidelines developed based on these results are presented in chapter 7.

### 5.1.3 Model 3: Dynamic compressor control

For the dynamic investigation of the compressor control strategies, the same system configuration as seen in Figure was applied. However, the evaporator and condenser were described by dynamic control volumes. Furthermore, the geometry and refrigerant charge were chosen to represent the Vestfrost VLS054 solar direct drive refrigerator.

The compressor was modelled using compressor polynomials supplied by SECOP. The mass flow through the capillary was modelled based on an empirical correlation. The operation of the compressor and capillary tube were assumed to be reasonably approximated by a quasi-static approach. The inputs values to the dynamic model may be seen in Table 3. The results found based on this dynamic compressor control model are also presented in chapter 7.

Table 3: Inputs to the dynamic model of SDD refrigerator

Input	Value
<b>Condenser</b>	
Pipe length	5.6 m
Pipe diameter	4.76 mm
Fin length	8.1 mm
Fin diameter	1.2 mm
$\alpha_{\text{Air}}$	10 Wm <sup>-2</sup> K <sup>-1</sup>
$\alpha_{\text{Ref,gas}}$	200 Wm <sup>-2</sup> K <sup>-1</sup>
$\alpha_{\text{Ref,two-phase}}$	1000 Wm <sup>-2</sup> K <sup>-1</sup>
$\alpha_{\text{Ref,liq}}$	500 Wm <sup>-2</sup> K <sup>-1</sup>
<b>Evaporator</b>	
Pipe length	14 m
Pipe diameter	6.35 mm
$\alpha_{\text{Ice}}$	35 Wm <sup>-2</sup> K <sup>-1</sup>
$\alpha_{\text{Ref,gas}}$	200 Wm <sup>-2</sup> K <sup>-1</sup>
$\alpha_{\text{Ref,two-phase}}$	1000 Wm <sup>-2</sup> K <sup>-1</sup>
<b>Compressor</b>	
Type	XV5KX
$V_{\text{disp}}$	5.0 cm <sup>3</sup>
<b>Refrigerant</b>	
Type	R600a
Charge	0.05 kg

## 5.2 Compressor and controller development

SECOP (the former Danfoss Compressors) has manufactured DC compressors for mobile refrigeration since the 1977. The compressors are typical used in trucks (for the refrigerator in the driver's cabin) and for pleasure boats.

In the 1980s, the compressor was also used for the first PV powered refrigerators with battery energy storage. This type of refrigerators was used in areas without grid electricity. The compressor was also used in some vaccine coolers for developing countries. Many problems occurred using such coolers: Often the battery (and even the PV panels) was stolen for other usage. When this does not happen, the cooler worked fine for a couple of years until the battery breaks down because of deep discharging of the lead battery. Often this resulted in an end of life for the cooler, since no back-up battery was available, and no funding for buying a new battery in a remote shop was available. Therefore, the PV powered vaccine coolers got a rather bad reputation and LPG, or kerosene powered absorption coolers, continued to be standard in areas without grid connection.

In 2001/2002 this started to change. The need for environmentally friendly and affordable solar vaccine coolers and refrigerators was realized in 1998-2000 through separate discussions between the United Nations Environment Programme (UNEP), World Health Organization (WHO) and Greenpeace International (GPI).

At about the same time, Danish Technological Institute (DTI) independently began the development of a new solar refrigerator that bypassed the use of batteries (funded by the Danish Energy Agency). DTI worked together with Vestfrost and Danfoss Compressors.

UNEP, Greenpeace International and DTI met at a refrigeration conference for cooling food and drinks in Chicago, December 2000, and exchanged information about this issue. It was also agreed to continue the work and cooperate in what later became the SolarChill Partnership.

The first meeting of the SolarChill Project Partners was hosted by GTZ Proklima in Eschborn, Germany, on 5 May 2001. With an initial decision to proceed with the project, Greenpeace International provided the funds for the development of the first SolarChill prototypes. These were (later on) exhibited at the World Summit on Sustainable Development in the fall of 2002 in Johannesburg, South Africa. Danfoss Compressors and Vestfrost participated in the meeting in Frankfurt and ensured that they would continue to support the development work.

In connection to this, Danfoss Compressors developed the direct current hydrocarbon compressor BD35K.

It was important for the SolarChill partnership to use natural refrigerants, and Danfoss Compressors entered the project as industrial partner and developed the DC compressor for isobutane refrigerant (R600a). The displacement of the BD35K compressor is 3 cm<sup>3</sup>. Danfoss Compressors also developed a new integrated electronic control for the compressor, which ensures that the photovoltaic panels can be connected directly to the compressor without external control. The electronic control also ensures a "soft start" which is important when no battery is used.

The electronic control is equipped with an adaptive speed control (Adaptive Energy Optimizer – AEO). By using that control, the compressor will stepwise speed up from low speed to maximum speed in 12.5 RPM/min. If the photovoltaic panels cannot provide sufficient power, the compressor will stop, and after a short while it will try to start again. The compressor will try to start every minute, and once the power from the panels is sufficient, the compressor will start at lower speed. The first start in the morning is at app. 2500 RPM. After a compressor stop, the compressor will start up at the latest speed minus 400 RPM. The speed range is from 2000 to 3500 RPM.

The controller accepts a voltage between 10 and 45 V. The voltage from photovoltaic panels can vary and that is a good feature for solar powered refrigerators and freezers. Using normal electronic control, the start current would be much higher, requiring much bigger PV -panels or require the use of a capacitor to help start the compressor.

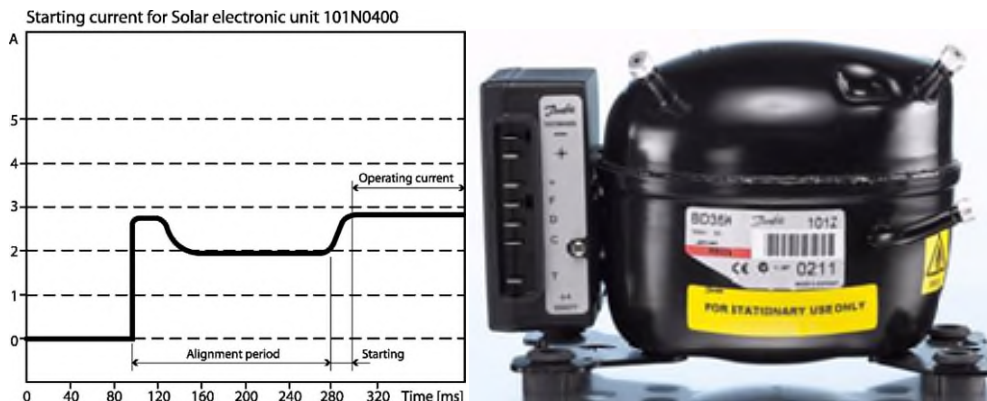


Figure 14 Starting current using the solar electronic control, 12 V, and a photo of the Danfoss BD35K Direct Current Compressor for the natural refrigerant R600a.

This compressor (and the Direct Current technology) has become a big success, and today dozens of different types of vaccine coolers using this technology are listed at the WHO PQS list (see chapter 2). They all (or almost all) use this compressor.

*This is one of the fastest growing technologies in the vaccine cold chain. The technology is more reliable than the battery powered solar systems as well as absorption technology previously used in immunization programs. In addition, the technology reduces vaccine wastage quite significantly previously caused by temperature excursion previously experienced with absorption systems. It is also worth mentioning the enormous impact of this technology in that it saves the atmosphere of the adverse effects of lead and the large quantity of CO<sub>2</sub> generated from burning fossil fuel for powering the absorption systems (Mr. Gregory W. Kiluva, Technical Specialist; Cold Chain, UNICEF Supply Division Copenhagen, 2016).*

The compressor platform used is the “BD” platform, and this has not changed since the 1990s. This is one of the reasons why SECOP decided to participate in the present EUDP project.

## 5.2.1 Development of the first prototype

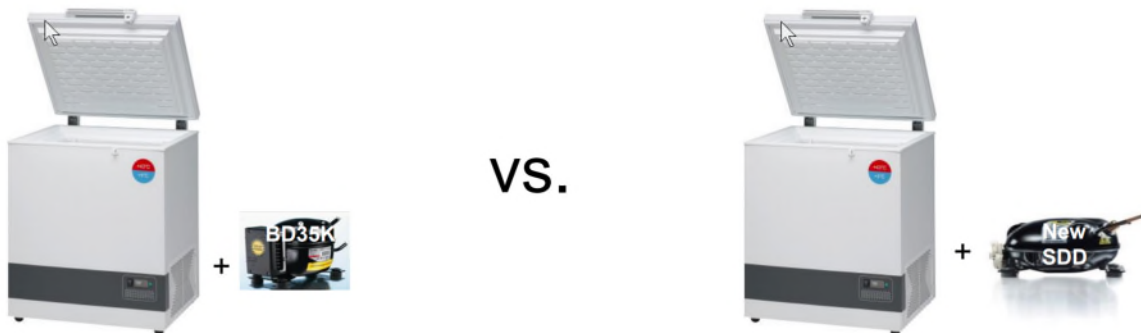
After the start-up of the project, SECOP decided to use the recent developed XV platform for the new Solar DD compressor, and a new electronic prototype was developed in 2018 - 2019.

The XV platform has shown good performance and efficiency for other purposes such as household refrigeration and wine coolers. Both DTU and DTI have been engaged in other projects with this compressor platform from SECOP, and the experiences are good.

The compressor prototype was installed in a Vestfrost vaccine cooler cabinet and tested in climate chamber at SECOP in Flensburg. The results for the first tests are shown in figure 15 and figure 16 below:

### **EUDP solar vaccine cooler project**

Test setup



- 1<sup>st</sup> Vestfrost VLS 054 SDD in original configuration
- 2<sup>nd</sup> Vestfrost VLS 054 SDD with new SDD compressor + electronic to be tested back to back according to WHO PQS E003, 3,5kWh/d curve

Figure 15: The test setup at SECOP for testing the first compressor prototype.

### **Compressor benchmark**

- Reduce Solar panels required (efficiency +20%, dynamic range +70%)
- Focus voltage to lower PV cost (60 / 72 cell)
- +20% cooling capacity (bigger cabinets)

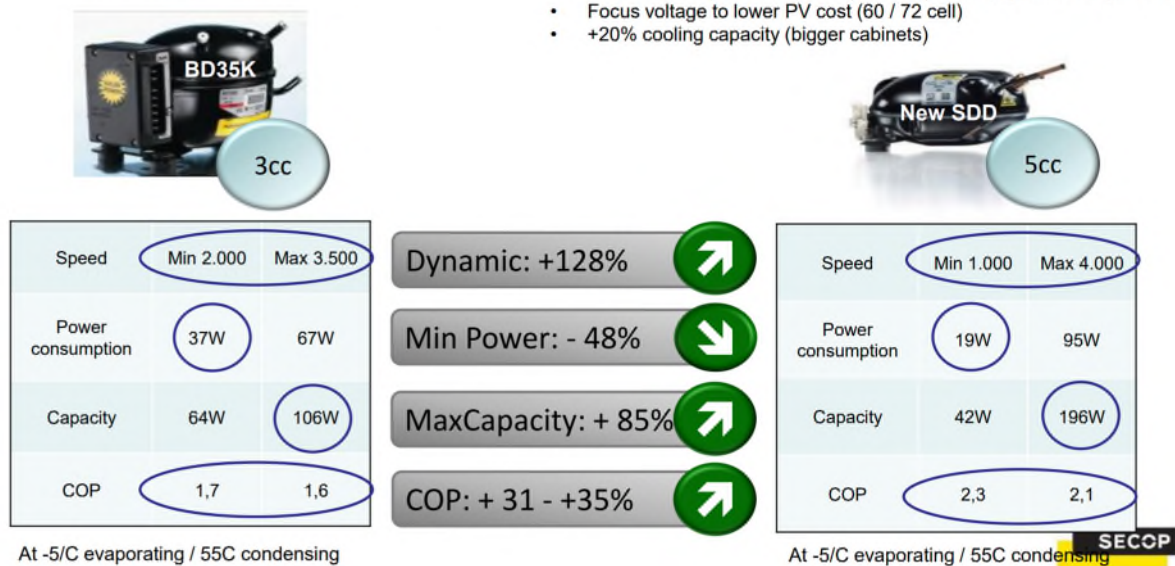


Figure 16: The main results from the test setup at SECOP.



In the figures above, the test setup and the main results from the tests in climate chamber are shown. SECOP first tested a Vestfrost vaccine cooler with the “old” compressor and then changed the compressor to the first prototype based on the XV platform.

The results were very good:

- The cooling capacity at maximum speed (at -5 C/+55C) was increased from 106W to 196 W (+85 %).
- The COP at maximum speed was changed from 1.6 to 2.1 (+31 %).
- The dynamic range was changed from 1.75 to 4.0 (+128 %).
- It was now possible to run the compressor at lowest speed with 19W power (before 37W).

Vestfrost received a prototype set (compressor and control unit) and started to conduct the first tests.

Danish Technological Institute received the cabinet and prototype compressor and the prototype control from SECOP and conducted a number of tests in the “Solar house” and in climate chamber (see chapter 5).

At the project meeting on 28 October 2019, SECOP announced that they had to stop the development of the new compressor based on the XV platform. This surprising announcement also stopped the tests at Vestfrost, since the situation (and the future) for the prototype compressor became unclear.

SECOP had been owned by Nidec since August 2017. Nidec also bought another global compressor manufacturer, Embraco, in July 2019. This created some turbulence because some cabinet manufacturer feared that this would influence the market for compressors for small commercial appliances. They feared a lack of competition for compressors in this market segment.

The EU Commission agreed on this and decided that Nidec had to sell SECOP. This happened in September 2019, and SECOP was bought by a German financial company. The new owners decided to change the focus for SECOP to only manufacture and market compressors for professional appliances.

Since the XV platform is mostly focused on the household appliance market, the development based on this platform was stopped.

SECOP announced that the developed technology would be moved to another platform, and that this would take some time to change and to develop.

Based on this, the project partners asked EUDP for permission to postpone the finalization of the project, and this was approved.

### 5.2.2 Development of the second prototype

At SECOP they discussed internally on which platform they should continue the development work. In the beginning focus was on the existing Delta platform used in household appliances. However, during the project, SECOP was acquired by a different owner, who decided to exit the household segment completely. Instead Secop developed a brand-new platform for the whole DC compressor program – the “Nano” platform. The aims of this platform are even higher energy efficiency, smaller size, less weight, and nevertheless a higher cooling capacity.

This work lasted a little more than a year and started with the basis compressor platform (compressor pot, motor, motor control, piping, and the mechanical part of the compressor). The first prototypes were made for the leisure and automotive market using R134a. In the spring of 2021, the first prototypes of the R600a variant were built and tested at SECOP as well. The R600a variant will be used for the vaccine refrigerators as well.



Figure 17: Images from the design phase of the Nano compressor.



Figure 18: Photo of the prototype BD Nano Compressor (photo by Hendrik Möller, SECOP).

The first prototypes of the BD-Nano 50 K compressor were tested at SECOP in the spring of 2021.

SECOP has developed a draft data sheet for the new compressor (see appendix H):

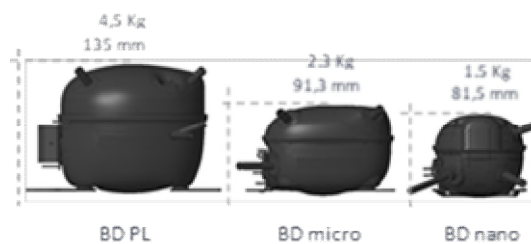


Figure 19 The Nano compressor is smaller and lighter compared to the BD compressor.

The new compressor is much lighter than the old compressor (1.35 kg compared to the old: 4.3 kg). The dimensions are also smaller: 89 mm high compared to the old: 137 mm. The displacement of the “old” compressor is 3.00 cm<sup>3</sup>, and for the new compressor it is 2.60 cm<sup>3</sup>.

The speed span for the old compressor is from 2000 to 3500 RPM (1:1.75), and the speed span for the new compressor is from 2300 to 4500 RPM (1:1.96).

Here are some other comparisons between the old and the new compressor:

**Freezer application:**

At the evaporation temperature of -25 °C and CECOMAF conditions (condensing temperature of +55 °C, ambient 32 °C and suction gas 32 °C):

Cooling capacity at maximum speed:

Old: 36 W

New: 50.8 W (additional 14.8 W, + 41.1 %)

Efficiency (COP) at maximum speed:

Old: 0.87

New: 1.19 (+36.8 %)

**Refrigerator application:**

At the evaporation temperature of -10 °C and CECOMAF conditions (condensing temperature of +55 °C, ambient 32 °C and suction gas 32 °C):

Cooling capacity at maximum speed:

Old: 83.8 W

New: 109.1 W (additional 25.3 W, + 30.2 %)

Efficiency (COP) at maximum speed:

Old: 1.39

New: 1.66 (+19.4 %)

Refrigerant is for both compressors the natural refrigerant R600a, which is the hydrocarbon isobutane.

The next steps for commercialization will be as planned in May 2021:

Production will start in November 2021.

A new control with much more features to fulfil future WHO requirements is in the planning phase and will be released at the end of 2022/mid 2023. This control will include improved AEO control and algorithms as developed by DTU as a part of this EUDP project (see chapter 3).

## 5.3 Design of new cabinet

Just after the start-up meeting in November 2017, the project team started to investigate how to fulfil the aims of the project in relation to the cabinet.

A technical meeting was conducted in December 2017 and here Vestfrost announced that they had decided to use the existing cabinet VLS 054 SDD as basis for the project. This cabinet is very popular and the most sold Solar Direct Drive cabinet.



Figure 20: Vestfrost VLS 054 SDD is the basis for the project.

Vestfrost Solutions supplied DTU and DTI with technical details and cabinets for the investigation.

### 5.3.1 Prolonging the hold-over time

The existing cabinet has an ice storage which ensures a hold-over time of 72 hours when there is no available solar power. The aim is to prolong this.

A MSc study at DTU was included in the project, and the student Christoffer Reinhold Busk did a great job along with the DTU team to develop solutions for obtaining the goal. A simulation program was developed and tuned to fit with real tests for the existing cabinet. Hereafter, some changes in the design were made, and the simulation program calculated the impact of the changes.

The recommended solution was presented at a technical meeting with Vestfrost at DTI in May 2018. This recommendation was to increase the size of the ice bank and to improve the insulation. It was recommended to increase the height of the ice bank from 200 mm to 350 mm.

Vestfrost built a first prototype cabinet with increased ice bank and tested it in climate chamber. The results were presented at a project meeting on 20 February 2019 in Flensburg, and they were promising: the hold-over time was measured to be 112.4 hours, and the temperature became a little too cold in the cabinet.

Vestfrost built and tested a second prototype with slightly better insulation between the ice bank and the vaccine storage chamber, and now the goal had been received: the hold-over time was 120 hours, and the temperature in the vaccine chamber was in the correct range (between +2 °C and +8 °C).

The ice bank was placed in the insulation foam and surrounds the upper part of the vaccine compartment. It was a welded aluminum container filled with water/ice. The evaporator was placed in contact with the ice bank.

### 5.3.2 Better temperature regulation

Vestfrost experienced some trouble in the field with some of the existing cabinets. This was discussed with WHO in the spring of 2019. Vestfrost found out that the trouble came from unintended loading of warm goods into the cabinet.

This caused some problems for Vestfrost, and 8 products were taken off the WHO PQS list in June 2019. As mentioned, Vestfrost identified the problem to be caused by the fact that unintended warm objects were inserted into the cabinet. The fact that the warm objects were placed upon the temperature sensor, positioned on the “step” (on the top of the compressor room), caused the cooling system to run for a long time, and the temperature in the cooler got too cold.

This issue was discussed at a project meeting at Vestfrost in October 2019.



Figure 21: Photo. The project meeting at Vestfrost on 28 October 2019. From left: Claus Cording, VFS, Hendrik Müller, SECOP, Ivan Katic, DTI, Jonas Kjær Jensen, DTU, Wiebke Brix Markussen, DTU, Per Nygaard Hansen, VFS, and Kenneth Nielsen, VFS. The photo was taken by Per Henrik Pedersen, DTI.

Vestfrost solved the problem by moving the sensor away from the original place and to the side wall, where the sensor measures the temperature of the (cold) wall near the ice bank. The 8 vaccine coolers were back on the WHO PQS list later in 2019.

Vestfrost also experienced other variations from normal temperature regulation in some extreme climate conditions. In some cold conditions the ice bank was not frozen during normal duty since the temperature control turned the compressor off before freezing the ice bank.

Efforts to solve this problem was done by both DTI and Vestfrost. DTI conducted a number of tests with additives in the ice bank in an effort to prevent subcooling of the water in the ice bank by initiating freezing at the freezing point (or at temperatures just below 0 °C). See Appendix B.

This effect was achieved by adding some droplets of a special alcohol: Hexanol. But by repeating the tests it was not convincing that the effect was repeated each time.

Therefore, both DTI and Vestfrost went for an alternative solution. The solution was to introduce a small heating element in the vaccine chamber.

The tests at DTI are shown in Appendix A.

The tests show that it is beneficial to add a small heating capacity by electrical resistance inside the vaccine chamber. This helps to keep the refrigeration system run for a longer period without compromising the temperature inside the vaccine chamber. This ensures that part of the ice bank freezes to ice to ensure the long hold-over time in case a period without sunshine appears.

Vestfrost implemented this system controlled by a temperature control that ensures that the heater only is on duty when there is a risk of low temperature in the vaccine compartment.

In addition to that, Vestfrost has also implemented an additional freezing protection by means of a thermostat that cuts off the refrigeration system in the occasion of danger of freezing the vaccine.

Vestfrost has conducted field test in Africa (Malawi) with units equipped with the new temperature control system and the new remote monitoring device ("EMS", see later on in this chapter). Vestfrost has experienced excellent performance of the units.

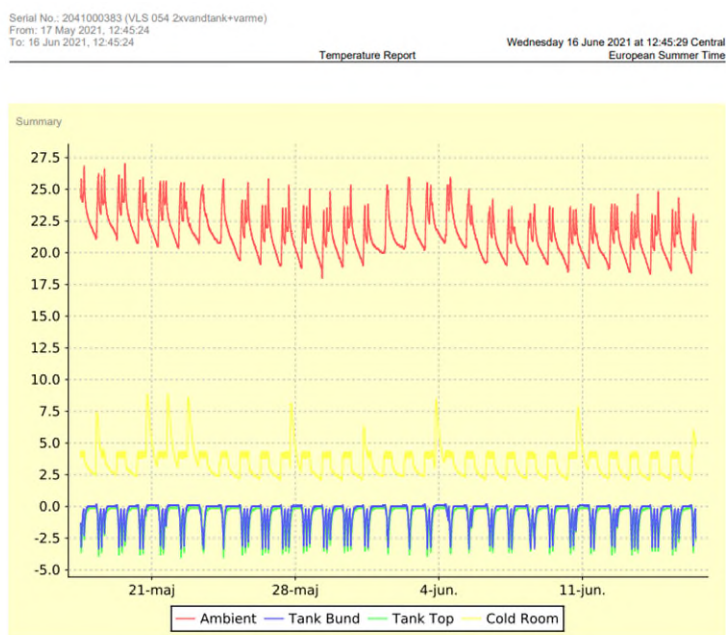


Figure 22: Temperature measurements for a Vestfrost vaccine cooler equipped with the new temperature control system. The unit is placed in Malawi, and the measurement period is one month. The temperature in the vaccine chamber is within the WHO specifications (Yellow curve). When the lid is open the temperature rises slightly for a short while. The data is sent to Vestfrost by the new remote monitoring device (EMS).

### 5.3.3 Humidity control

WHO has experienced some problems in the field with high humidity in some vaccine coolers. The problems occur most significantly in another type of cabinet with very stable temperatures (the “tank” models as described in Appendix E). Experiments took place at both Vestfrost Solutions and at DTI with passive and active dehumidification, and the results are shown in chapter 6 and in Appendix C.

A new active drain system, where condensate is let to a tray placed outside the vaccine chamber, has been developed. The condensate will evaporate in the tray using heat from the condenser in the refrigeration system. This technology is planned to be implemented in 2022.

### 5.3.4 Remote monitoring

Vestfrost has developed prototypes of the new EMS module for remote monitoring and control of the coolers. It has the size of an iPhone and looks very impressive.

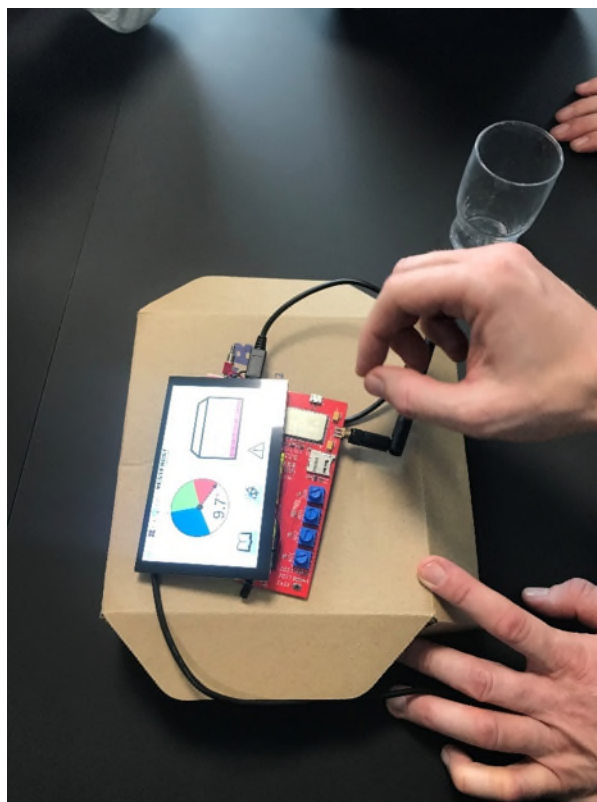


Figure 23: Photo. Prototype of the new remote monitoring EMS device, showed at the project meeting in October 2019 at Vestfrost.

A subcontractor has been involved in the development work. In 2021, Vestfrost has been conducting field tests with the new EMS remote monitoring device in different sizes in Africa, and the results are very promising.



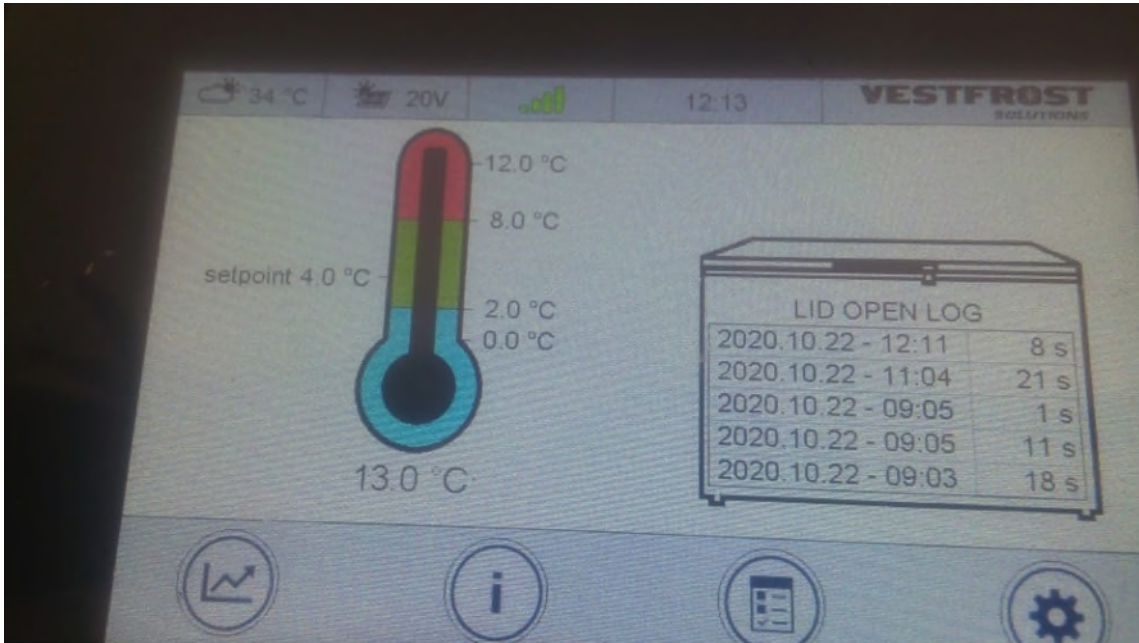


Figure 24: Detail from the screen of the EMS remote monitoring devise during a test.



Figure 25: The health care clinic where the test unit is placed.

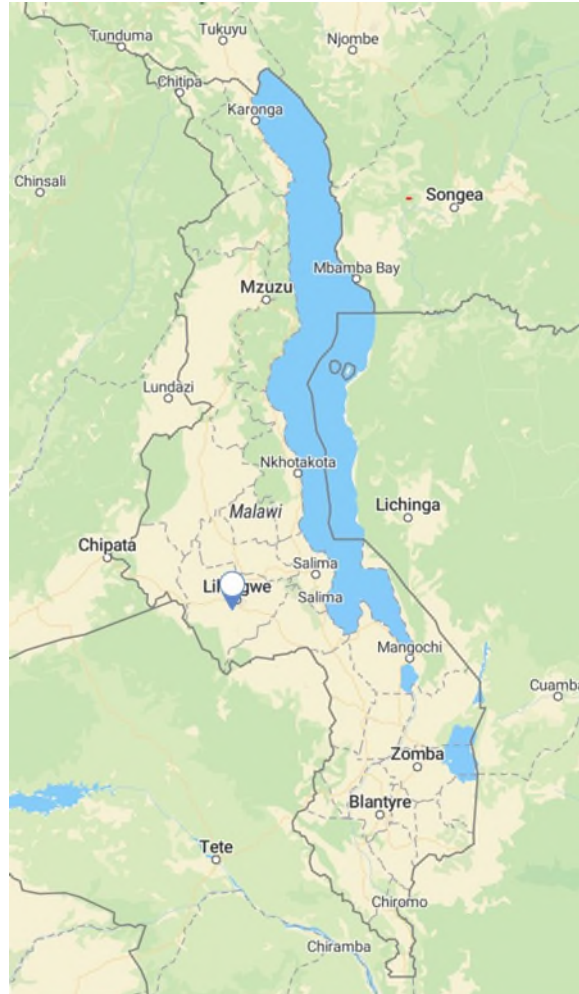


Figure 26. The EMS also includes a GPS. Then it is always possible to check where the cooler is located. Almost all of Africa is covered by GSM mobile phone net.



## Datasheet - VF EMS SYSTEM

### COLD CHAIN CATEGORY - RTMD/EMS SYSTEM

Electronic thermostat with build in datalogger, GPS and remote temperature data log via GSM. 5" touch display with access to actual temperature, datalog and diagnosis. Solar powered including datalog of voltage from PV cells.

#### SPECIFICATIONS

Display	5" touch screen
Temperature range	-25°C to +85°C
Accuracy	±0.5°C from -10°C to +85°C
Battery Backup	72 hours
Sim Card	Supplied with global sim card
Sim Card Optional	Can be supplied with local Sim Card
Voltage range	10-32VDC
IP rating	54
Type	Integrated in appliance

#### Sensor

Humidity	Yes
Compartment Air	Yes
Compartment surface	Yes
Ice bank	Yes
Ambient	Yes
Compressor	Yes
Freezer (if appliace)	Yes
Lid opening	Yes



#### Data Logger

Temperature data	60 days
Humidity data	60 days
Solar voltage	60 days
Compressor state	60 days
Lid Status	60 days
GPS coordinate	60 days

Figure 27: Data sheet for the new EMS remote monitoring devise.

The new EMS monitoring devise is also equipped with a USB slot (5V) that makes it possible to use excess power from the PV panels for e.g. charging a mobile phone (Energy Harvesting).

Vestfrost is planning to commercialize the EMS and will offer this system for customers in the fall of 2021.

### 5.3.5 Robustness

Vestfrost has changed the wiring system with the purpose of protecting the wires from damage from outside (e.g. from rodents). This has been done by introducing a new junction box that protects the wires (see figure 29 that shows the data sheet for the new cooler later on in this chapter). The junction box also ensures safety and no exposure to electrical connections.

Vestfrost has implemented coating of the sensors to make the control system more robust.

New feet for increasing the distance from the floor has been implemented.

The increased robustness supplied by the new remote monitoring device is expected to reduce the need for service and to prolong the lifetime of the coolers.

Vestfrost plans to increase the guarantee period from 2 to 3 years for the new coolers.

### 5.3.6 New generation of the Solar direct drive vaccine cooler

A new generation of the Vestfrost SDD vaccine cooler has been developed and equipped with the new technology developed and tested in the project. The new cooler has been tested at Danish Technological Institute and is approved according to the WHO PQS criteria.



Figure 28: The cover page of the test report from the refrigeration laboratory at DTI.

The test procedure for hold-over time has been changed during the project period. According to the new procedure, the hold-over time (“autonomy time”) has been measured to 89h 32min which is very good and significantly better than the first generation of SDD coolers. This figure cannot be compared directly with the 72 hours mentioned earlier.

Vestfrost plans to market the new cooler in the fall of 2021. In the following two pages the new data sheet for the new SDD vaccine cooler is shown:



# Datasheet - VLS 054A SDD

## COLD CHAIN CATEGORY - SOLAR DIRECT DRIVEN REFRIGERATOR

SPECIFICATIONS	
Vaccine storage capacity	55,5 L
Temperature range (43°C AMB)	+2° to +8°C
Hold-over time, hours	72,4
Refrigerant	R600a
Freeze protection, grade	A
Climate class	T
Min. solar radiation, kWh/m2/day	3,5

WHO SPECIFICATIONS	
Test procedure	E003/RF05-VP4
Performance specification	E003/RF05.4
PQS code	E003/106

Features	
Storage baskets	1
Temperature control	Automatic
Lock + keys	Yes
Junction box	Yes
Adjustable legs	Yes
Drainage for condensation water	Yes
Solar Panels	Bundled
Temperature monitoring	Fridgetag 2E
Remote temperature monitoring	Optional
Remote temperature adjustment	Optional
Remote Equipmetn monitoring	Optional



Construction	
Outer Dimensions, HxWxD (mm)	905x720x600
Gross volume, L	108
Gross Weight, KG	85
Net Weight, kg	65
Material Inner Cabinet	Pre-painted alluminium
Material Outer Cabinet	Painted galvanized Steel
Insulation Thickness, mm	100

Shipping details	
Packaging	Export grade wooden crate
Qty. per 20' / 40' container	44 / 92
Qty. per truck (EU standard)	106

## INDUSTRIAL GRADE LOCKS

Our equipment comes with a industrial grade locking mechanisms ensuring a tight lock.

## EMS module (Optional)

Our newly developed EMS module offers the user the ability to remotely monitor the the equipment via GSM network. Additionally it will also enable the user to remotely change the settings of the equipment.

## Junction box

The junction box located on the backside of the equipment offers technicians easy access to all electronic components. In addition, the junction box safeguards vital electrical components such as controllers, data logger components, stabilizer electronics (ILR's) etc.

## Anti-freeze

Due to the built in heating wires controlled by an safety thermostat, the equipment is able to maintain stable +2° to +8°C even in ambient temperatures below zero

## Plug & Play solar kit

Each unit is supplied with a 2 x 180W solar panels , which comes with an industrial grade alluminium mounting kit. The kit enables the panels to easily be roof mounted, and allows the panels to be positioned in the optimal angle towards the sun.



Figure 29: Draft data sheet for the new Vestfrost SDD vaccine cooler. Vestfrost plans to market the new cooler in the fall of 2021.

## 5.4 Laboratory measurements

Several test series were conducted at DTI in the “Solar house” and in climate chamber with the purpose of improving the function of the Solar Direct Drive principle.

### 5.4.1 Temperature control experiments

DTI has tested a vaccine cooler from Vestfrost in the project “Second generation vaccine cooler”. The unit has a special compressor control made by SECOP (“first prototype” in chapter 4) with 30-70 V input range from a PV simulator.

The purpose is to see how the new XV5K prototype compressor and the new prototype controller from SECOP perform when installed in a Vestfrost vaccine cooler. It was also to conduct experiments with temperature control, pull down test and humidity control. The efforts were analysed, and recommendations were made.

SDD appliances in field operation monitoring have sometimes shown a strongly fluctuating temperature pattern, probably when the ice bank is not frozen at all or is fully frozen. Full freezing could result in too low wall temperatures so that grade A freeze protection cannot be achieved.

If we can reproduce the observed behaviour in the laboratory, we could try to move the thermostat and do other modifications to see if it has any effect on temperature stability.

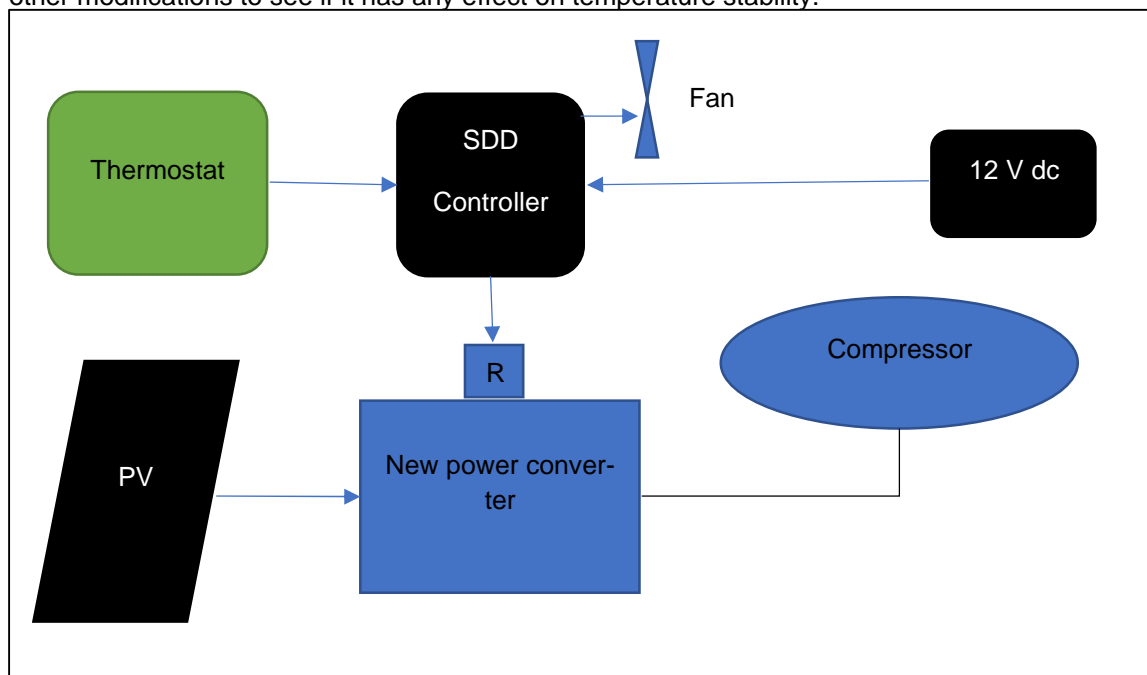


Figure 30 Diagram for the test setup.

The internal thermostat and display are powered by a 12 V dc supply which also powers the fan. The Secop special converter is active when the thermostat is on, i.e. the relay R is triggered.



**Test conditions:**

- The PV simulator is set up to simulate a single standard PV module with 72 cells and nominal power 150 Wp.
- Thermostat is initially set to 4 °C (factory setting).
- Running with WHO test cycle day/night.
- Laboratory temperature 15-20 °C.

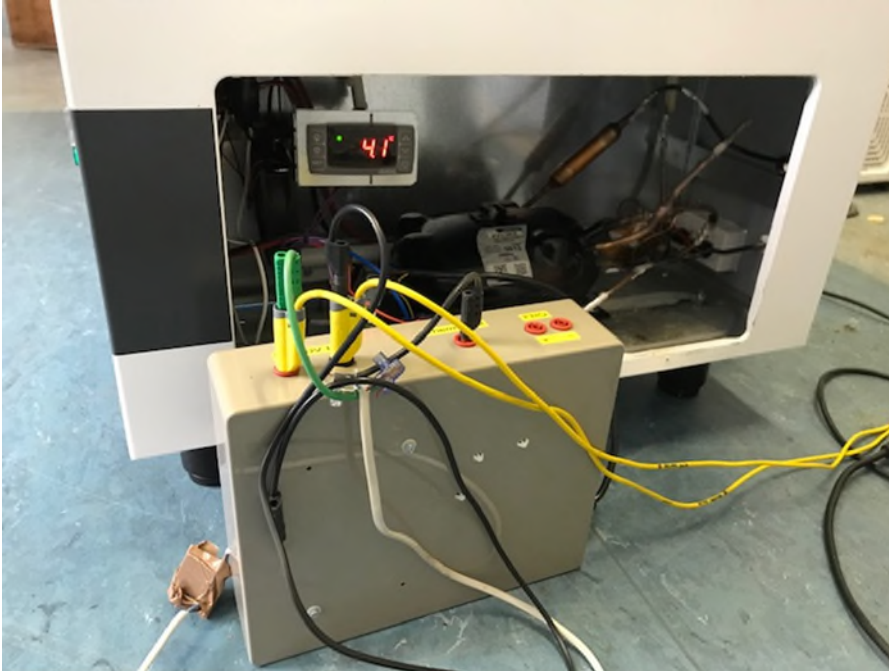
**Photo documentation and results:**

Photo 31: Compressor with external power supply.

In Appendix A, 12 different tests were conducted with the aim of analyzing ice formation, sensor placement, set points, insulation (between sensor and vaccine chamber) and load in the cabinet.

**The conclusion is:**

The many experiments and modifications have shown that there is no easy way to achieve the perfect temperature balance in a SDD appliance relying on ice as only means of energy storage. Compared to the original construction, the result is a significant improvement of the temperature stability by the following actions:

- 1) Re-positioning of the inner thermostat sensor so it becomes in closer contact with the ice storage.
- 2) Insulate the sensor surface (or move it to the inner side of the cladding).
- 3) Lower the thermostat setting to 1-1.5 °C which is just sufficient to initialize freezing.
- 4) Install a small heat load to counteract too low temperatures when ice is generated during daytime.

Especially the first and the last point (point 1 and 4) of placing the temperature sensor in close contact to the ice storage and installing a small heating element became essential for the rest of the work.

### 5.4.2 Subcooling

Laboratory and field experiments have shown that the current Vestfrost cabinet does not always freeze the ice storage, especially when the ambient temperature is low. This may be caused by the phenomenon subcooling. Subcooling of water is not desired in the case of ice formation for energy storage. This is because negative water temperatures trigger the thermostat to stop the cooling cycle before ice has been built up and

thus the state of charge of the energy storage remains very low – only sensible heat capacity of water is activated.

A literature survey has shown that there are different ways to accelerate the formation of ice but that some of the mechanisms are not fully understood. Methods mentioned in literature are:

- Mechanical impact
- Application of a DC electric field
- Application of a magnetic field
- Certain proteins (e.g. testosterone)
- Alcohols with long carbon chains (Pentanol and above)
- Small particles of solid matter.

### Experiments in the lab

Some of the ideas have been tested by DTI with the following results:

- 1) Two electrodes with a voltage difference of 12 V were submerged in the ice bank without any measurable effect on ice formation. The electrodes were switched on in parallel with the thermostat.
- 2) A freezer was set up for more controlled experiments and comparison of methods. First run was with the solid matters kaolin powder and saw dust. In both cases there was a positive effect compared to pure tap water, with sawdust as the best. The test used plastic cups with externally mounted sensors.
- 3) Next test compared the alcohols pentanol and hexanol with pure water and water with plastic foam granulate. About 10 drops of alcohol were used in each cup. The granulate performed best while the cups with pure water and with alcohol both exhibited subcooling.
- 4) The same test was repeated, but this time in small and closed plastic bags without free air surface. Only one drop of alcohol was used. In this case the bags with added alcohol had no subcooling, while pure water and water with granulate had.
- 5) Experiment no.3 was repeated with only one drop of alcohol per cup. This time the hexanol and the granulate worked best, while both water and pentanol exhibited some subcooling. Submerged sensors (incl. dust or other foreign object) for better accuracy may have influenced the results.

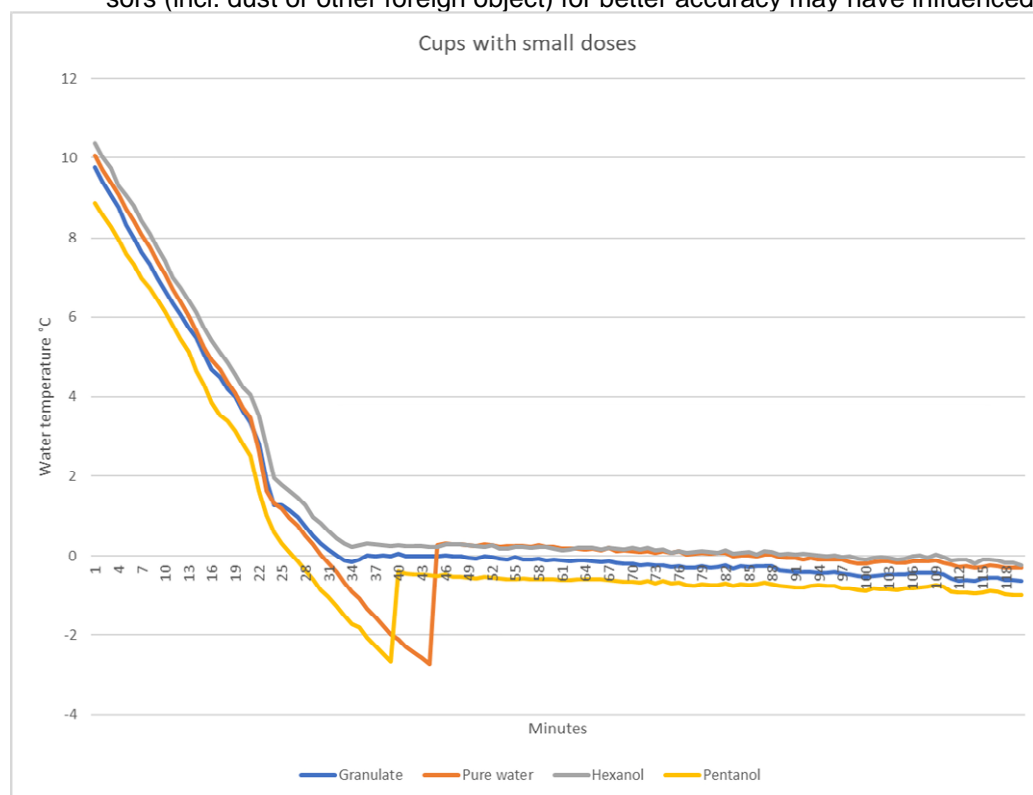


Figure 32 Effect of foam granulate and alcohols (1 drop) with an open surface to the air.

The above figure is one example of the tests done. In Appendix A, more details of the tests can be found.

There is a clear effect of floating granulate as ice nucleation agent on an open surface. This effect disappears when the granulate is submerged in the water. Both tested alcohols have a positive effect, but the optimum dose is not clear, and there seems to be some randomness in the results. It seems that very small doses have the best effect, maybe because larger amounts change the general surface tension in the open cups. It is suggested that the concentration should be specified as drops per surface area of the ice bank because these alcohols are not easily soluble in water and stay as droplets on top of the water. It is not clear if the alcohol will evaporate over time.

Literature study and tests have shown that the phenomenon of subcooling of water is difficult to fully understand but that additives may have a certain effect on the degree of subcooling.

### 5.4.3 Pull-down test

A “pull-down test” was conducted to investigate the cooling capacity of the prototype XV5K compressor.

In 2009 it was shown that the existing compressor (BD35K) in a Vestfrost vaccine cooler was able to cool 20 warm soft drink cans (330 ml) from +30 °C to +5 °C a day. (Test report from DTI: Report of tests of SolarChill B chest-type, 19th June 2009).

The warm cans were changed with a similar number of cold cans every day at “sunset”, which was supposed to be the most critical time of the day.

It was decided to conduct a similar test with the prototype XV5K compressor. The test was conducted in the Solar House at DTI in the beginning of June 2021, and the ambient temperature was about 20 - 22 °C.

A number of 50 warm soft drink cans (each 0.33 l) were changed with 50 cold cans every day at “sunset”. One test can (with water and a temperature sensor) was also changed every day and placed in the middle of the cabinet.



Figure 33: Pull-down test with 50 warm soft drink cans inserted per day. The test was conducted in the “solar house” at DTI in June 2021.

The result was that it is possible to cool 51 warm cans per day using the WHO power supply profile simulating a 150 W PV panel. They were cooled from about +21 °C to +5 °C.

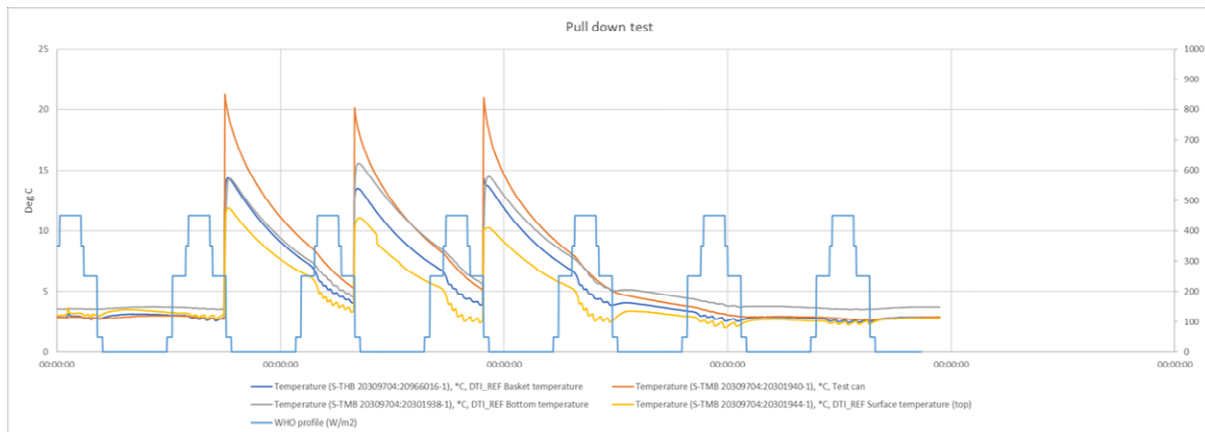


Figure 34 results of pull-down test of 51 soft drink cans inserted in the cooler every day at sunset.

#### 5.4.4 Humidity control

WHO wants to avoid the problems with high relative humidity in the future and has started to draft PQS criteria for the level of humidity inside the vaccine chamber. Therefore, it is relevant to investigate if it is possible and realistic to introduce humidity control inside the vaccine chamber.

It was decided to conduct tests at the solar house at DTI in an effort to control the humidity inside the vaccine chamber by using a small thermoelectric dehumidifier. The tests are reported in Appendix C.

Solar direct drive refrigerators have been in the market for more than two decades and have generally been proven as a reliable solution in areas without stable grid power supply. However, there is evidence from some health clinics that high internal levels of humidity can sometimes cause problems like mould growth and /or destruction of labels and vaccine packaging materials. WHO is constantly working to refine the qualification criteria and test methods for such refrigerators, lately with the draft protocol *WHO/PQS/E003/TPP05.1 Humidity Control for Vaccine Refrigerators*.

It was suggested to investigate dehumidifier technologies and compare results with the WHO draft requirements. The main findings of these investigations are reported in Appendix C.

#### Experiments with dehumidification of Vestfrost VLS 054 SDD

Vestfrost has delivered a VLS 054 SDD chest type vaccine refrigerator for the experiments. Apart from a special compressor, it is the same model as sold to the health care sector globally. It would be a market advantage if the refrigerator could pass the set criteria for dehumidification, so this was set up for a test in a laboratory at DTI.

Humidity can generally be removed from air if there is access to a surface with lower temperature than the dew point temperature. This can be done by using a part of the evaporator in the refrigeration system of the cabinet. When the humidity in the air condenses on the surface it can be let to a drain.

DTI has suggested that a simple way to implement humidity control would be by a small electric dehumidifier placed in the cabinet. Such devices are commercially available at low cost and are based on thermoelectric cooling. Such a dehumidifier was purchased to see if it could have two beneficial effects on the refrigerator's behaviour: Firstly, prevent high humidity which can cause condensation on surfaces, and secondly deliver some excess heat, which could force the compressor to run for a longer period and thus ensure that the ice

bank freezes during all operating conditions. In some cases under special circumstances, Vestfrost has experienced cut-off by the thermostat before the ice was frozen and this causes unwanted temperature excursions.

A dehumidifier was purchased and placed in the cabinet. It turns on and off in sync with the available solar power. Several tests were conducted, and the system worked fine.

### Test in climate chamber at 43 °C

The purpose of the test was to see how much water the dehumidifier would remove during normal operation in a hot and humid climate. The device was placed in the climate chamber and running for a week.



Figure 35: The thermoelectric dehumidifier placed inside the vaccine chamber. Drainage through bottom plug.

### Drying of a wet cardboard box

A water-soaked cardboard box was placed in the basket to measure how fast it would dry out.

Measurement results in Spring 2021:

- 8 March 14:30. Dry weight: 90.9 g. Soaked weight: 186.9 g
- 10 March 16:20. New weight: 144.9 g
- 12 March 13:00. New weight: 119.0 g
- 15 March 10:30. New weight: 94.9 g.

After almost complete drying, the internal air humidity level drops to a lower level.



Figure 36: Soaked cardboard box on the scale.

**Reference test run**

Following the run with active dehumidifier, a reference experiment was made with disconnected dehumidifier.

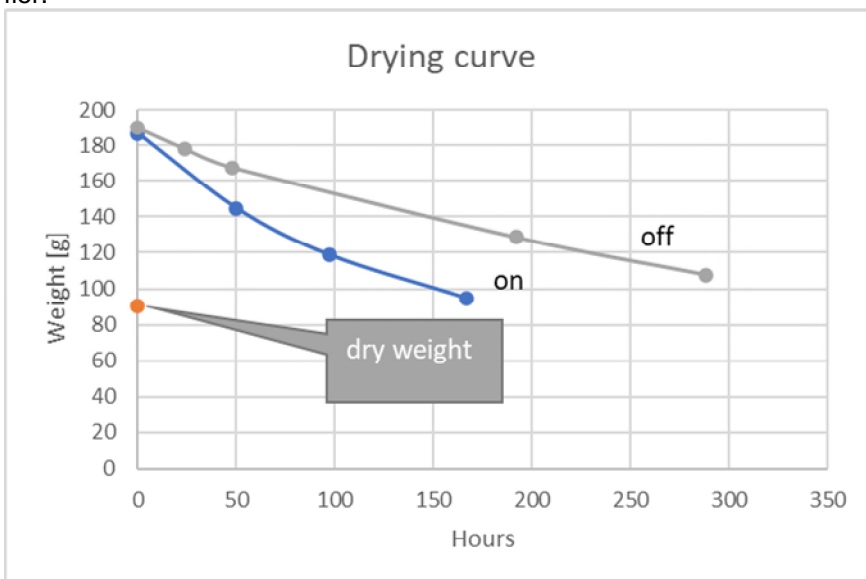


Figure 37 Drying time is almost halved when the dehumidifier is active. Furthermore, the relative humidity of the vaccine chamber is generally lower when the dehumidifier is active.

For more details, see Appendix C.

Vestfrost conducted similar tests by using a part of the evaporator in the compressor refrigeration system as dehumidifier and got some similar results.

### Conclusion

The Peltier principle has been demonstrated to work well as a solution for temperature and humidity control at the same time. Since the power can be regulated continuously, it is possible to find a voltage setting that suits a specific thermal balance. The dehumidification can be considered as a by-product. The water removal rate of the tested device is sufficient to keep content dry and to dry out wet packaging materials, but too low to pass the draft test criteria set by WHO. It is the project partners' impression that the humidity control draft requirements are far too strict and will be difficult to implement in a cost-effective way.

The proposed design and control strategy developed in this project will assure a stable temperature and dry surfaces in the tested appliance and can likely be implemented at low cost.

It has been demonstrated that an alternative test method using a soaked cardboard box as humidity load works well and can be documented by simple means. It is suggested to modify the WHO draft criteria for humidity control to a less strict and more realistic level, for example:

- RH less than 90 % after 72 hours with a humidity load of xx grams of water soaked in a cardboard or fabric surface of area YY cm<sup>2</sup>. This should be enough to assure condensation free interior surfaces which is the main problem to be avoided. More work is needed to find appropriate realistic levels.

The note in Appendix C has been sent to the WHO technical working group in June 2021.

### 5.4.5 Energy harvesting

A simple test was carried out in the laboratory at DTI with the purpose of observing how it would work if a SDD refrigerator was not only connected to a PV panel but also to a charge controller and a battery. The battery could provide electricity for light, phone charging etc. like in common solar home systems. The refrigerator should not be affected by the added components according to the WHO PQS test method for energy harvesting devices.

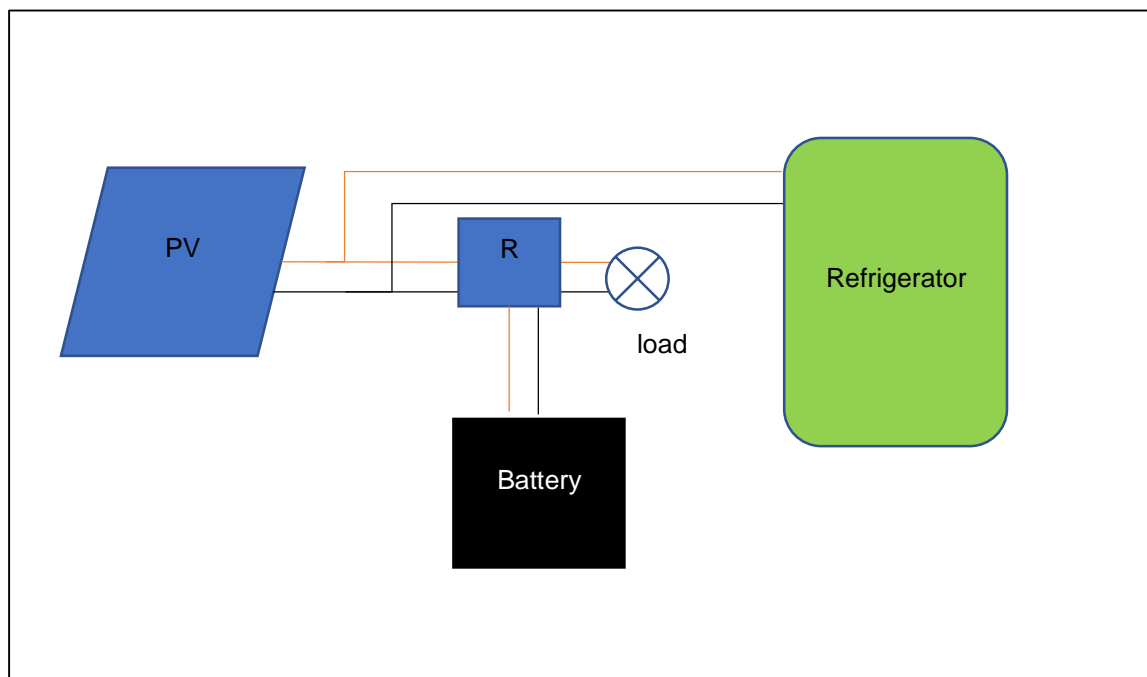


Figure 38 The test setup for energy harvesting.



Figure 39 Charge regulator and battery connected. The PV simulator is seen on top of the refrigerator cabinet.

The experiments in Appendix D show that with the right type of charge regulator, a SDD appliance can operate in parallel with a battery system without any technical problems. It has to be tested if there are challenges if other voltages than 12 V (Lead acid) are used.

## 5.5 Dissemination

The results obtained in the project have been disseminated at the 25th International Congress of Refrigeration, Montreal, August 2019.

Three papers were presented:

Per Henrik Pedersen, Danish Technological Institute presented the paper: DIRECT DRIVE SOLAR COOLERS. The paper is in Appendix E.

Jonas K. Jensen, DTU MEK presented the paper: Comparison of compressor control strategies for solar direct drive refrigerators. This paper is in Appendix F.

Wiebke B Markussen, DTU MEK presented the paper: Extending the autonomy time of an icelined solar powered vaccine cooler. This paper is in Appendix. G.

All three papers (and the presentations) were welcomed and created discussions at the conference.

At the "7th International Symposium on Advances in Refrigeration and Heat Pump Technology" (4 October 2021 at the Danish Association of Engineers), Ivan Katic presented "Second generation solar direct drive vaccine cooler, EUDP project on photovoltaic refrigeration" with the results from the project.



## 6. Utilisation of project results

This chapter presents the main results obtained from the simulation models, which are presented in chapter 5. Based on the simulation results, guidelines for the optimization of SDD vaccine coolers have been developed.

### 6.1 Cabinet optimization

In Figure 40 (left), the autonomy time and the steady state temperature of the air inside the cabinet are shown as a function of the ice bank height for two different ambient temperatures. The mass of ice was kept constant in this case, which meant that the ice bank thickness was decreasing with added height. As seen, the autonomy time decreases slightly with increasing height for both 32 °C and 43 °C ambient temperature. At the same time, the steady state temperature was found to decrease. By increasing the ice bank height also, the area between air and frame is increased, which results in an increased convective heat transfer from this surface, and the air temperature thus decreases. The lower air temperature inside the cabinet then results in larger heat losses through the outer walls which causes the decrease in autonomy time. At an ambient temperature of 32 °C, the steady state temperature of the air got below the lower limit of 2 °C when increasing the ice bank height by 18 cm. Figure 40 (right) shows the autonomy time and steady state temperature as a function of the ice bank mass. In this case the height of the ice bank was also increased while the thickness was kept constant. In this case, the autonomy time increases significantly with added mass of the ice. This trend was expected as added mass in the ice bank means a larger storage capacity. Adding 10 kg of ice to the storage of the reference model resulted in around 80 % increase in autonomy time for both ambient temperatures. The steady state temperatures show a similar decrease as for the case where height is increased with constant the ice bank mass, however, staying within the limits, above 2 °C.

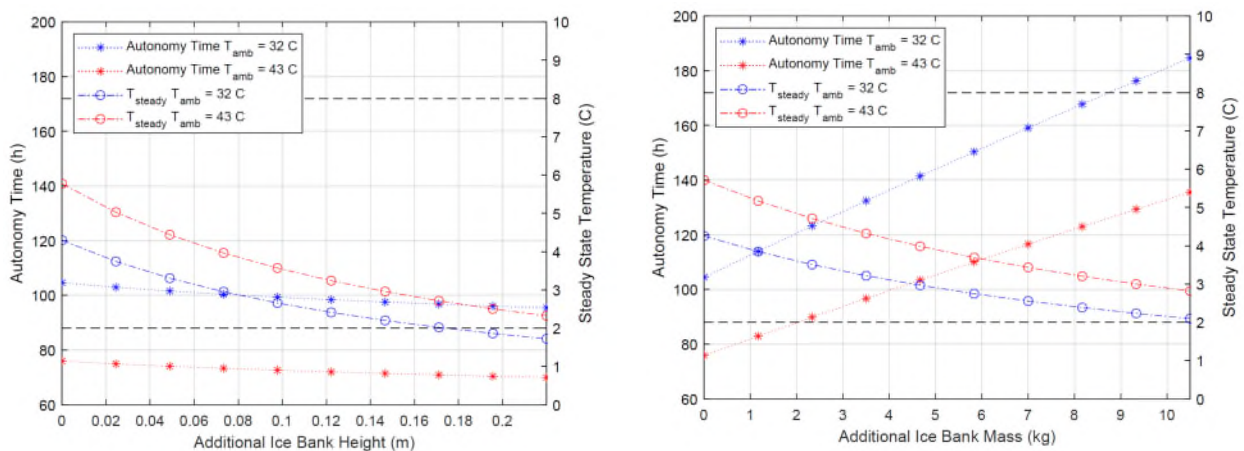


Figure 40 Autonomy time and steady state temperature as a function of additional ice bank height (left) and additional ice bank mass (right) compared to the baseline model.

Figure 41 (left) shows the autonomy time and steady state temperature as a function of added PU-insulation in all outer cabinet walls. As seen, the autonomy time increases slightly with increasing insulation thickness. Increasing the insulation thickness of the outer walls reduces the convective heat loss through the walls, which leads to the increase in autonomy time. Adding extra 5 cm to the insulation of the outer walls increases the autonomy time by 10 to 20 % depending on the ambient temperature. The steady state temperature is mainly governed by the insulation thickness between the ice storage and the cabinet, and is therefore only changing less than 1°C, when adding 5 cm to the insulation thickness of the outer walls.

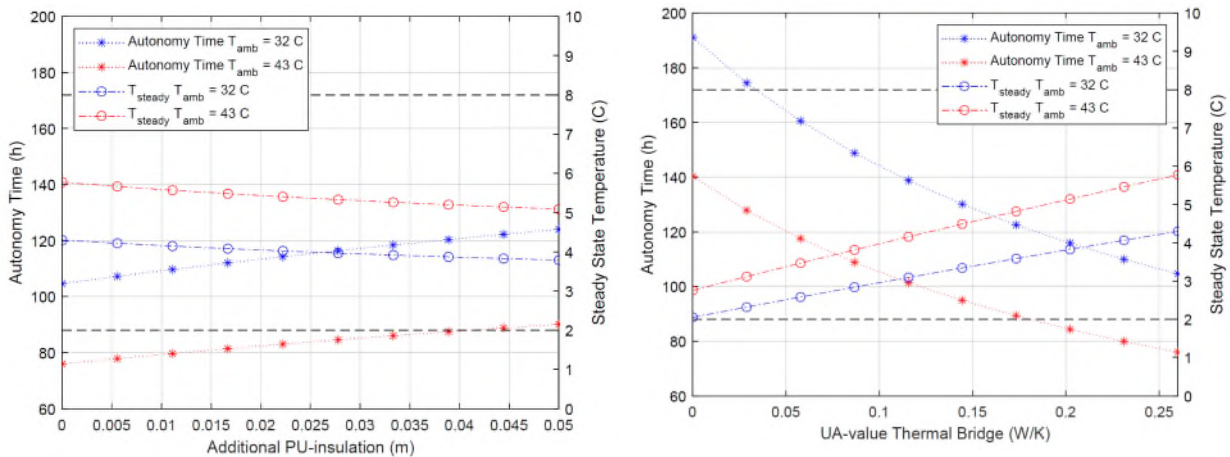


Figure 41 Autonomy time and steady state temperature as a function of additional ice bank height (left) and additional ice bank mass (right) compared to the baseline model.

In Figure 41 (right), the UA-value of the thermal bridges was varied between 0 WK<sup>-1</sup>, meaning no losses due to thermal bridges, and up to 0.26 WK<sup>-1</sup>, which was the value found from the calibration of the baseline model. For a cabinet without thermal bridges, autonomy times of 190 h and 140 h were obtained for ambient temperatures of 32 °C and 43 °C, respectively. Removing all thermal bridges thus has almost the same impact on the autonomy time as adding 10 kg of ice to the ice storage. Also, the steady state temperatures are significantly influenced by the thermal bridges. At an ambient temperature of 43 °C, the steady state temperature decreases from 5.8 °C to 2.9 °C when removing the thermal bridges, and at an ambient temperature of 32 °C, the steady state temperature decreases from 4.2 °C to 2.0 °C, which is at the limit of the acceptable air temperature inside the cabinet.

For the solar powered vaccine cooler, a longer autonomy time means a less vulnerable system in periods with low solar radiation. To extend the autonomy time, the results presented in Figure 40 and Figure 41 suggest that focus is put on increasing the mass of the ice storage and reducing the thermal bridges of the cabinet.

## 6.2 Steady state compressor control

Figure 42 shows the voltage - current curves for the 180 W (left) and 360 W (right) PV panels, respectively. Further, the voltage - current curves for the two compressors are presented under the operating conditions shown in Table 2 (Chapter 3) and their respective minimum and maximum compressor speeds. The compressor voltage - current curves are thus iso-power lines corresponding to the compressor power at minimum and maximum speeds. For a given solar irradiance the compressor must thus run between the intersections of the minimum and maximum compressor curve and the voltage - current curve at the given irradiance. If the curves do not intersect the compressor will collapse the PV panel at the minimum compressor speed and will thus not be able to run. If the PV panel voltage - current curve only intersects with the minimum speed compressor curve, the compressor will be able to run at the peak power point for that irradiance and will thus be able to utilize all the available power. If the PV panel voltage - current curve intersects with both the minimum and

maximum compressor speeds, the compressor will not be able to run at the peak power point and will thus not be able to utilize all the available power.

This figure gives an indication of how well the compressor can utilize the available power from the PV panel. It may be seen that the maximum speed curves for the two compressors occurred at more or less the same point. However, the BDS5.0K could run at a lower power, since the BDS5.0K had a lower minimum speed. The BDS5.0K would thus be able to run at lower levels of irradiance. Furthermore, it may be seen that for the 360 W PV panel both compressors would not be able to run at the peak power point at irradiances much higher

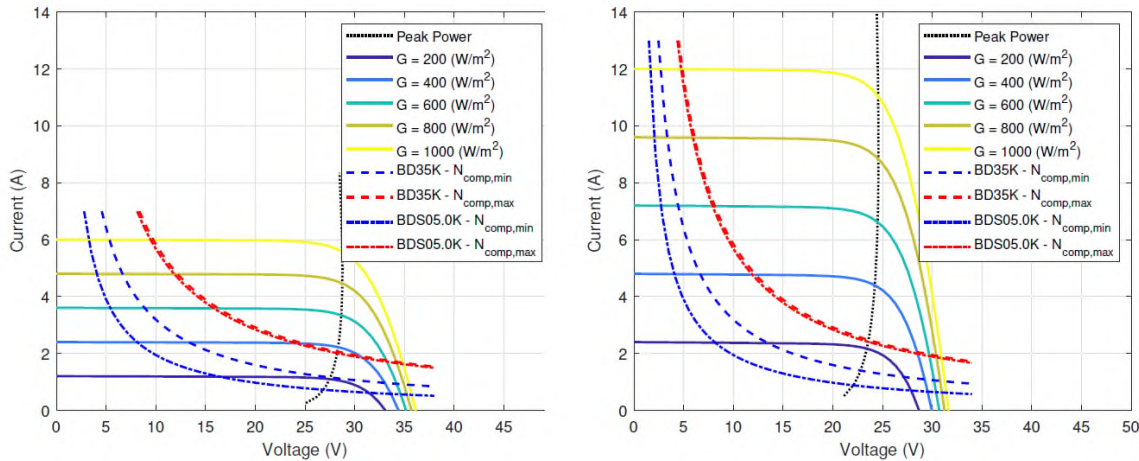


Figure 42 Current-voltage curves for the 180 W (left) and 360 W (right) PV panels, with the current – voltage curve for the two investigated compressors at their minimum and maximum speeds.

than  $200 \text{ Wm}^{-2}$ . For the 180 W this was possible up to  $400 \text{ Wm}^{-2}$ . However, the 180 W PV panel would require a higher irradiance before the compressor could run.

It should be noted that the compressor start power was not included in the curves shown in Figure 42. The need for compressor start power would shift the minimum speed curves upwards thus reducing the gap between the minimum and maximum curves.

Figure 43 shows an example of how the different control strategies perform under two different daily profiles, with  $200 \text{ Wm}^{-2}$  and  $800 \text{ Wm}^{-2}$  peak irradiances, respectively. This was exemplified with the BD35K compressor without the inclusion of compressor start power and the 360 W PV panel. Figure 43 presents both the available and utilized power and the compressor speed. As seen for both the low and the high peak irradiance profiles, the three different control strategies turned the compressors on and off at more or less the same time. It may further be seen that for the  $200 \text{ Wm}^{-2}$  profile both the PPT and CVC ran at their respective maximum values while the compressors were on. Further it should be noted that the difference between the PPT and CVC maximum power was insignificant. For the  $200 \text{ Wm}^{-2}$  profile the AEO control resulted in 13 on/off cycles. However, it may also be seen that the AEO actually kept the power consumption close to the power consumption of the PPT and CVC control. For the  $800 \text{ Wm}^{-2}$  profile, all three compressor control strategies ran the compressors at maximum speed after 1.8 hours of sunlight, the PPT and CVC already after 0.4 hours. The compressors then ran at maximum speed until approximately 0.5 hour before sunset. The PPT and CVC subsequently reduced their speeds to the minimum before turning off 0.25 hours before sunset. In the same duration, the AEO control ran 5 on/off cycles. It is clear that under the  $800 \text{ Wm}^{-2}$  peak irradiance profile none of the three control strategies would be able to utilize close the total available power.

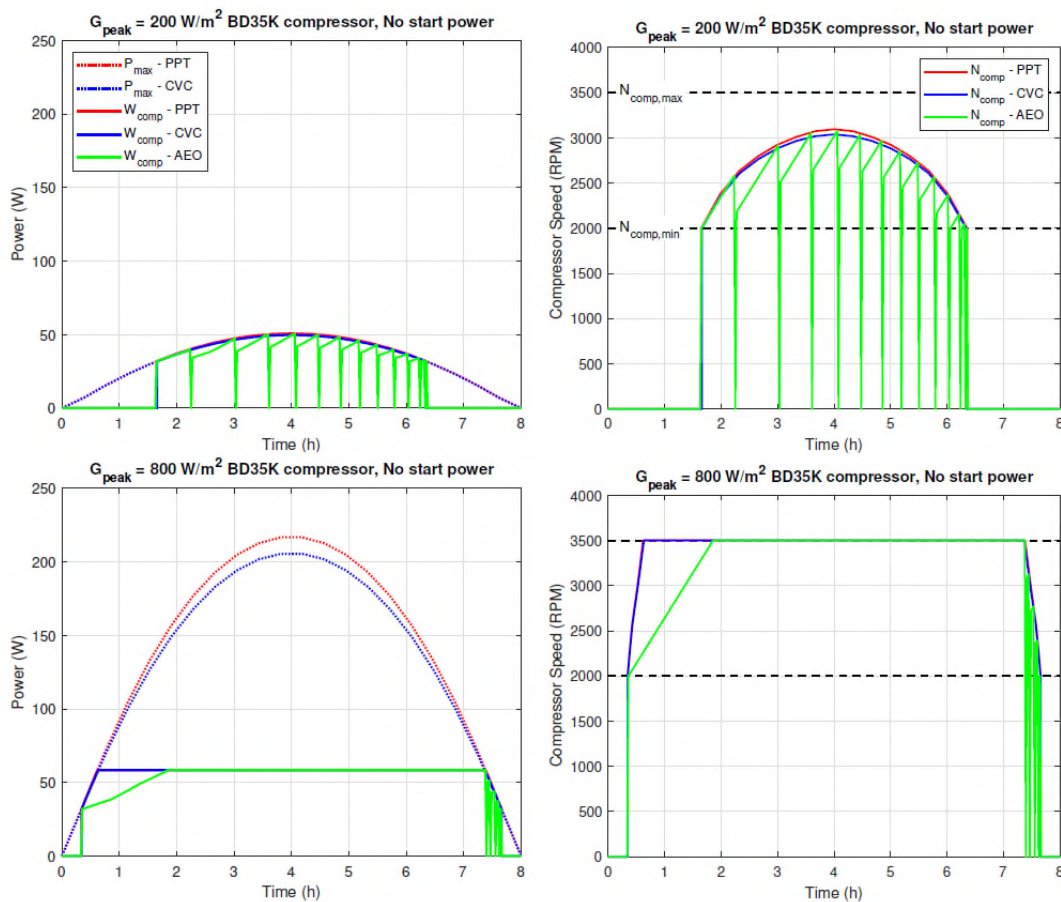


Figure 43 Compressor power and compressor speed for the PPT, CVC and AEO control strategies under two different irradiance profiles with 200 Wm<sup>-2</sup> and 800 Wm<sup>-2</sup> peak irradiances, respectively. Results are shown for the BD35K compressor without start power.

Figure 44 and Figure 45 show the utilization factor and the accumulated daily cooling load as a function of the daily peak irradiance. This was presented for both compressors under the three compressor control strategies. Furthermore, this was presented for four different system configurations: the 360 W PV panel and the 180 W PV panel, both with and without compressor start power.

As seen for the 360 W PV panel with 60 W of compressor start power, Figure 44 (a) and Figure 45 (a), the BDS5.0K compressor can deliver a cooling load as soon as the daily peak irradiance exceeds 300 Wm<sup>-2</sup>. It may further be seen that the CVC control will require a slightly higher peak irradiance to run. For the BD35K,

the daily peak irradiance must exceed  $350 \text{ Wm}^{-2}$  to deliver a cooling load for the PPT or AEO, while the CVC again required a higher peak irradiance of about  $360 \text{ Wm}^{-2}$ .

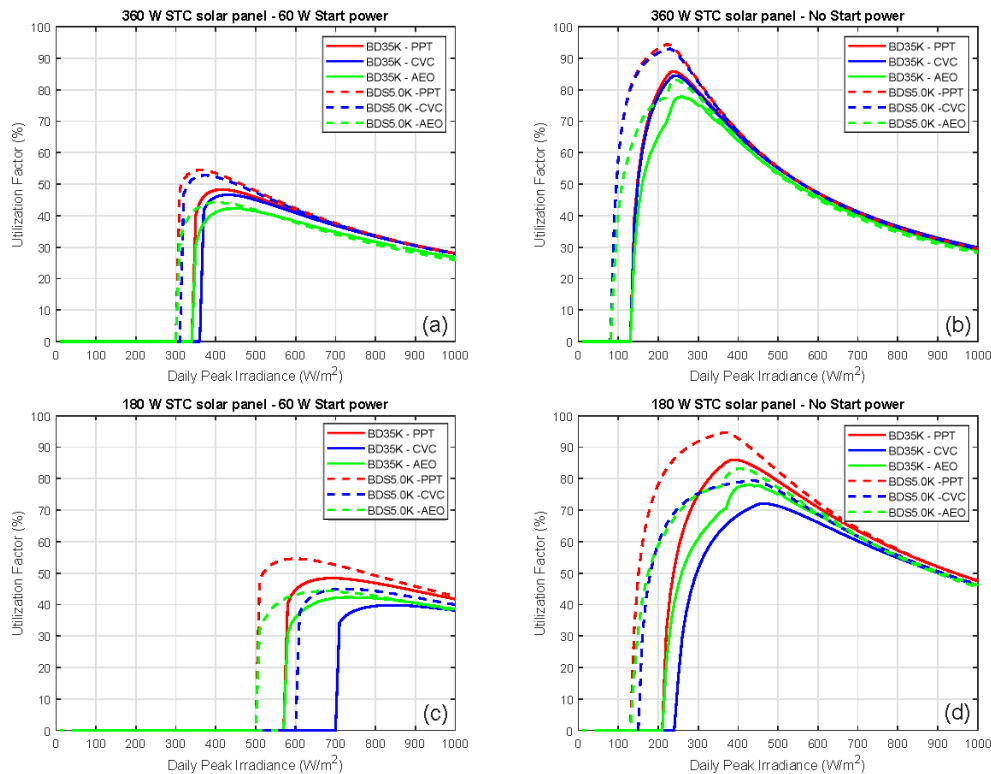


Figure 44 Utilization factor for the BD35K and BDS5.0K compressors under the PPT, CVC and AEO control strategies using both the 180 W and 360 W PV panels and with and without compressor start power delivered from the PV panel.

As seen in Figure 44 (a), the utilization factor increases rapidly after the minimum peak irradiance was attained and peaks shortly hereafter. Here the BDS5.0K attained the highest utilization factor with the PPT or CVC with a value of approximately 55 %. Here only 45 % was attained for the AEO. The BD35K utilized less of the available power, peaking at around 48 % for the PPT and CVC and around 42 % for the AEO. As the daily peak irradiance increases, the differences between the utilization factor of the two compressors and the different control strategies diminished, and at a daily peak irradiance of a  $1000 \text{ Wm}^{-2}$  the utilization factor was approximately 28 % for all six options.

As seen in Figure 45 (a), then although there was only a minor difference between the utilization factor of the two compressors, the accumulated daily cooling load differs significantly. Here the BDS5.0K was capable of

delivering more cooling load than the BD35K, as the BDS5.0K compressor was more efficient. Again, it may be seen that the PPT and CVC attain comparable cooling loads while the AEO delivered slightly less.

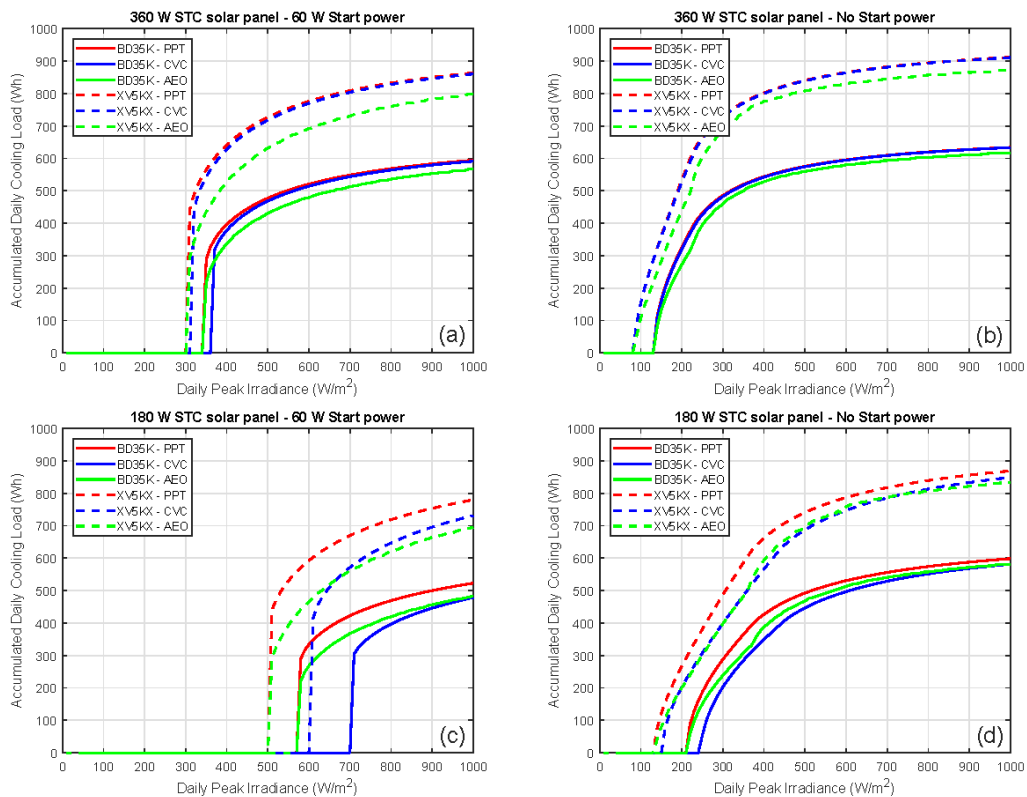


Figure 45 Daily accumulated cooling for the BD35K and BDS5.0K compressors under the PPT, CVC and AEO control strategies using both the 180 W and 360 W PV panels and with and without compressor start power delivered from the PV panel.

Assuming that the need for compressor start power can be alleviated but keeping the PV panel size of 360 W results in the utilization factor and accumulated daily cooling loads seen in Figure 44 (b) and Figure 45 (b). As seen, this allowed the compressors to run at significantly lower daily peak irradiances. Here all three strategies delivered a cooling load already from a daily peak irradiance of 90 W for the BDS5.0K and to 120 W for the BD35K. Again, the utilization factors show a rapid increase as soon as the minimum irradiance was attained. Here the BDS5.0K with the PPT and CVC peaks at a utilization factor of 94 % while the AEO reached around 83 %. The BD35K again utilized less of the available power peaking at around 84 % for the PPT and CVC and 78 % for the AEO. Again, the differences between the utilization factors of the two compressors and the three control strategies diminishes with increasing peak irradiance reaching approximately 30 % with a peak irradiance of 1000 Wm<sup>-2</sup>. As shown previously, the BDS5.0K delivers significantly more cooling load than the BD35K, see Figure 45 (b). As it was also shown earlier, the AEO delivers less cooling load compared to the CVC and PPT. However, when the need for start power was alleviated, the AEO approaches the load delivered by the CVC and PPT.

When the PV panel size was reduced to 180 W while still supplying the 60 W of start power, the minimum peak irradiance increases significantly, see Figure 44 (c) and Figure 45 (c). As seen, the BDS5.0K with either the PPT or AEO requires a peak irradiance in excess of 500 Wm<sup>-2</sup>, while the CVC requires 600 Wm<sup>-2</sup>. For the BD35K this was 590 Wm<sup>-2</sup> for the PPT and AEO and 700 Wm<sup>-2</sup> for the CVC. In light of these results, this configuration was deemed infeasible as it would result in the lack of cooling load for too many days.

However, if the need for compressor start power was alleviated for the 180 W panel, the minimum peak irradiance was again significantly reduced, see Figure 44 (d) and Figure 45 (d). Here the BDS5.0K will be able to

deliver a cooling load from around  $120 \text{ Wm}^{-2}$  while the BD35K would require slightly more than  $200 \text{ Wm}^{-2}$ . Generally, it may be seen that the utilization factor for this configuration was higher than the remaining configurations. Even at  $1000 \text{ Wm}^{-2}$ , almost 50 % of the available power was utilized. As seen, the accumulated daily cooling load was actually comparable to that of the 360 W with 60 W start power when both are running. As such it can be concluded that if the compressor start power can be alleviated, the PV panel size can be halved without reducing the delivered cooling load. Actually the cooling load can be delivered at lower irradiances with half the PV panels if start power was avoided. Finally, it may seem that for this configuration there was a slightly higher difference between the applied control strategy.

### 6.3 Dynamic compressor control

Figure 46 compares the simulated results to the measurements performed at SECOP. It depicts the condenser and evaporator pressure and saturation temperature, the compressor power, and the compressor control frequency, which is a measure of the compressor speed.

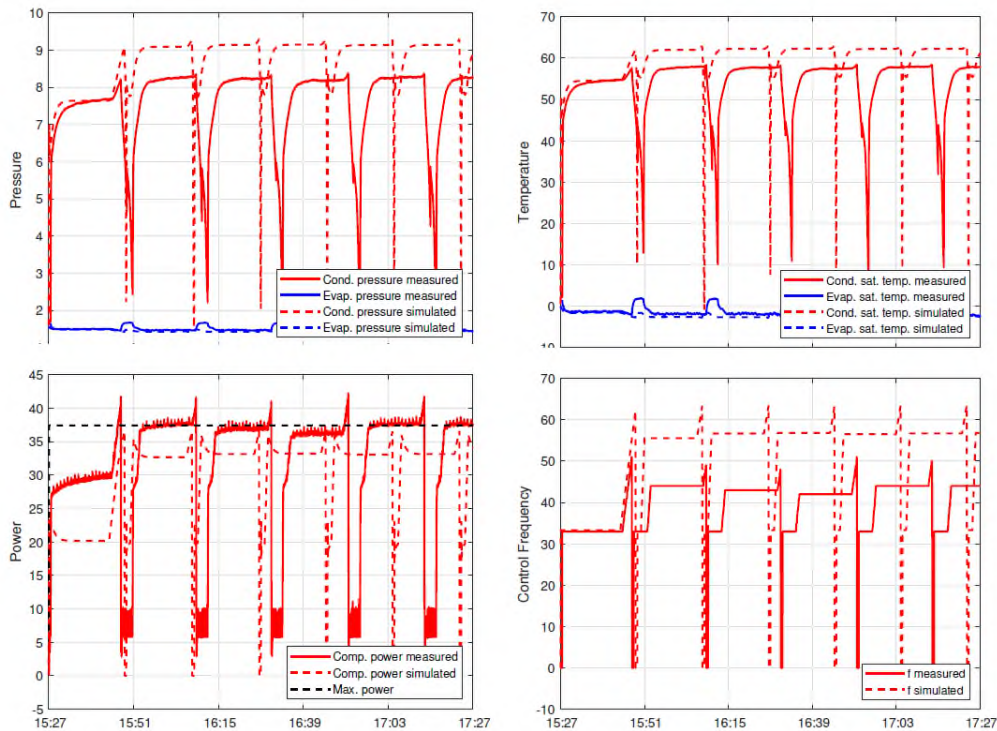


Figure 46 Comparison of the simulated results and measurements performed at SECOP. The abscissa is showing time and is the same for the lower and upper graphs.

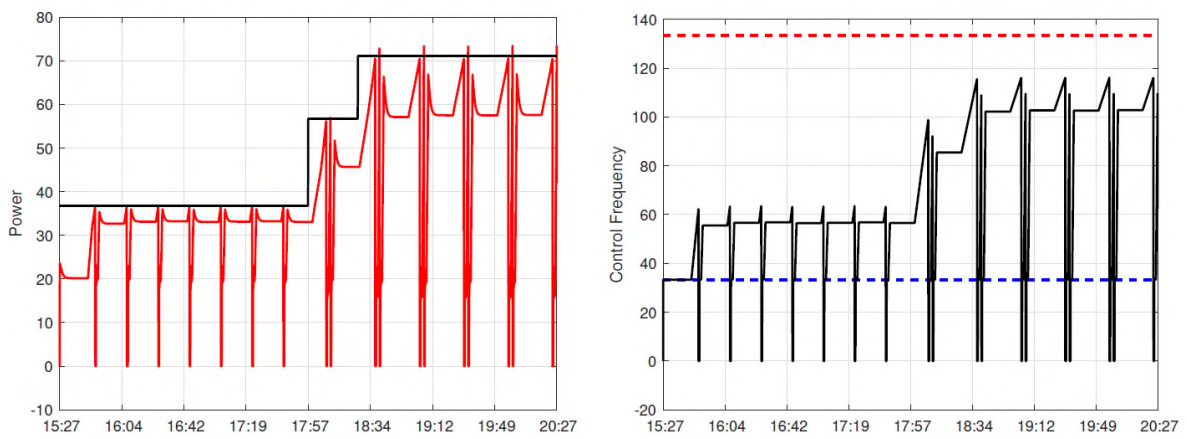


Figure 47 Compressor power and control frequency for the WHO irradiance profile and the AEO control strategy.

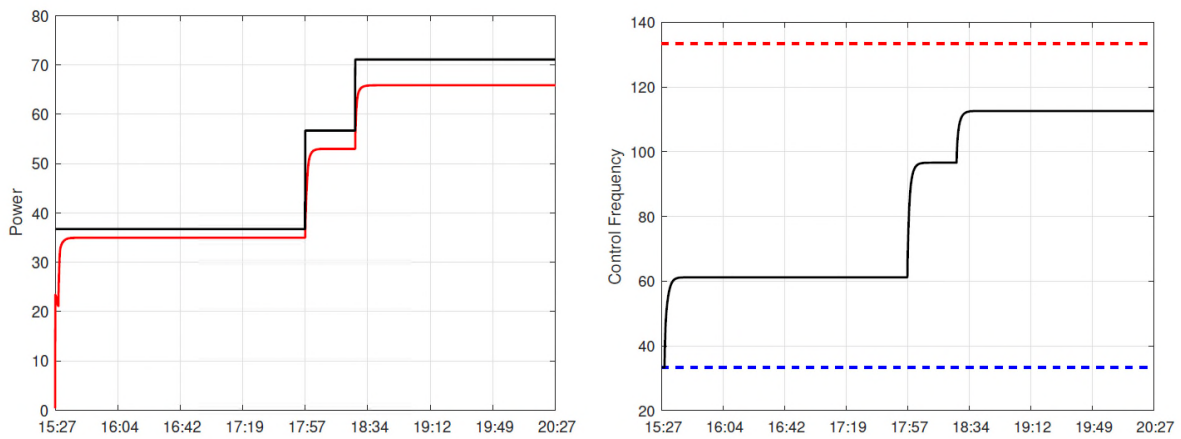


Figure 48 Compressor power and control frequency for the WHO irradiance profile and the CVC control strategy.

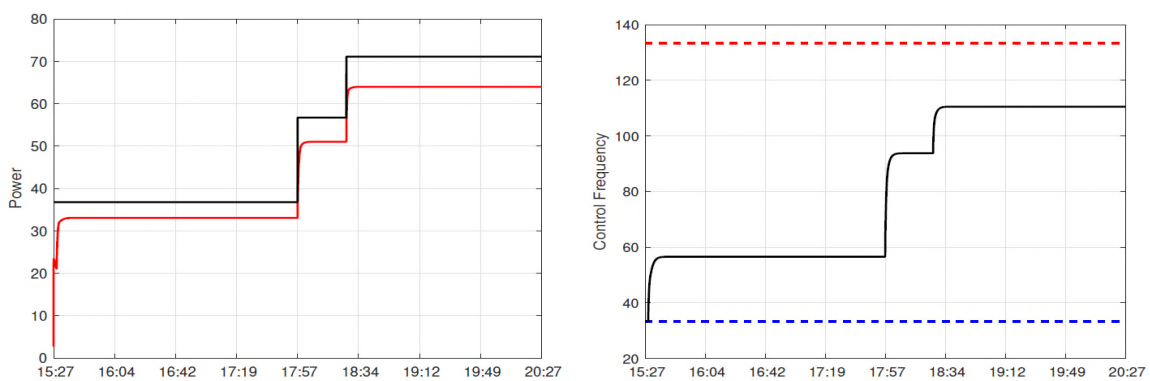


Figure 49 Compressor power and control frequency for the WHO irradiance profile and the PPT control strategy.



It may be seen that although there are some discrepancies between the simulations and the measurement, the simulations seem to catch the overall operation of the system and give a reasonable approximation to the characteristics of the operation.

It should be noted that the model seems to underestimate the compressor power. Consequently, the compressor can run at higher speeds in the simulations without collapsing the PV panel. This infers that the simulations generally have a higher control frequency, which further entails the higher condensation pressure. The underestimation of the compressor power may stem from the fact that the model applies compressor polynomials for the AC version of the XV5KX compressor, while the measurements were performed with a prototype DC version of the same compressor. It is uncertain if this AC/DC conversion may be the source of the increased power consumption in the measurements.

Figure 47, Figure 48 and Figure 49 present the simulation for the three compressor control strategies for the first half of the WHO irradiance profile. As seen, all three control strategies ensure reasonable utilization of the available power from the PV panel which was also suggested by the steady state results.

On the other hand, Figure 50, Figure 51 and Figure 52 present the simulations of the three compressor control strategies for a 1,5 hour time series of measured solar irradiance. These measurements were performed with intermittent cloud covers resulting in large fluctuations in the peak power. As seen, under these conditions the CVC and PPT control strategies both ensure a significantly higher utilization of the available power compared to the AEO control. For the PPT control, the PV panel only collapsed once while two collapses occurred for the CVC control.

## 6.4 Economic assessment

The results of the steady state simulations indicate that a reduction of the compressor start power, either by an improved start algorithm or by a super capacitor, may result in a up to 50 % reduction in the needed PV panel area and thus in a significant reduction of the capital investment.

Additionally, both the steady state and dynamic simulations have indicated the CVC and PPT control result in a comparable performance of the system. However, the CVC control can be realized with less measurement equipment and thus with less investment. Consequently, the results indicate that the PPT may not be a viable option compared to the CVC control.

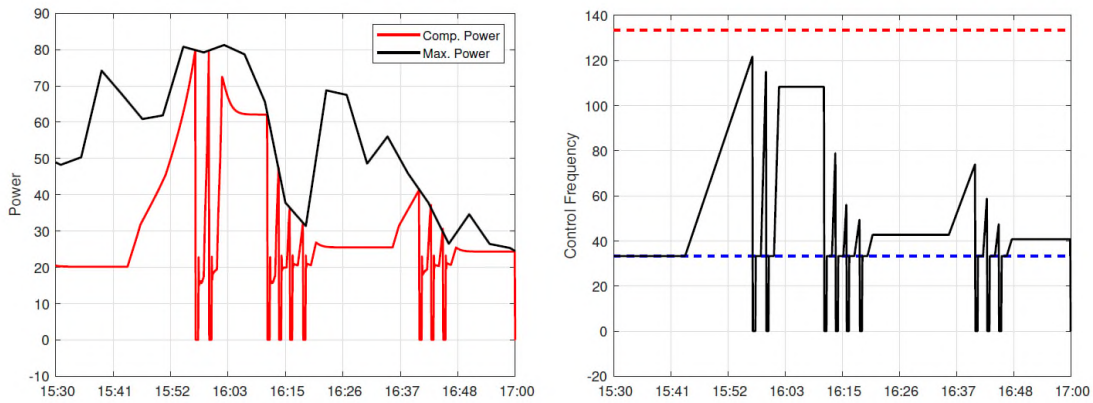


Figure 50 Compressor power and control frequency for the measured irradiance profile and the AEO control strategy.

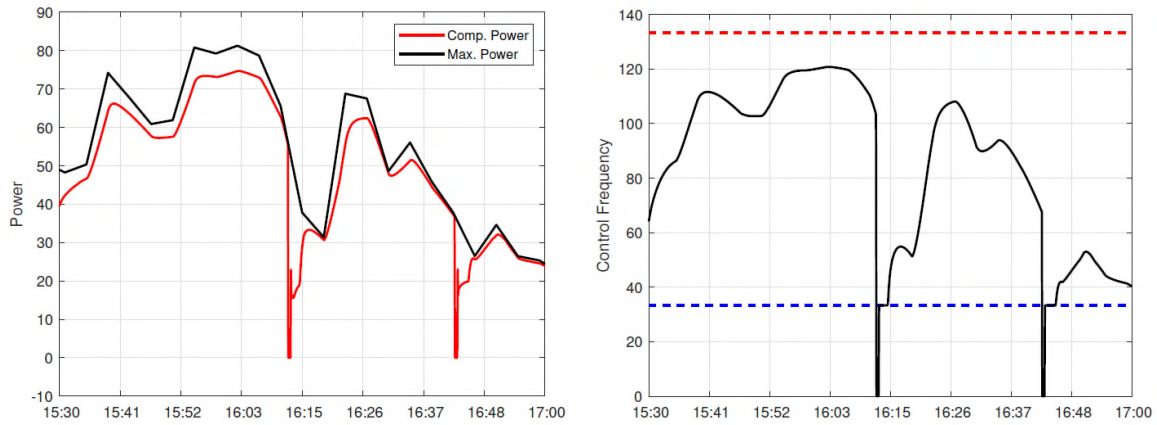


Figure 51 Compressor power and control frequency for the measured irradiance profile and the CVC control strategy.

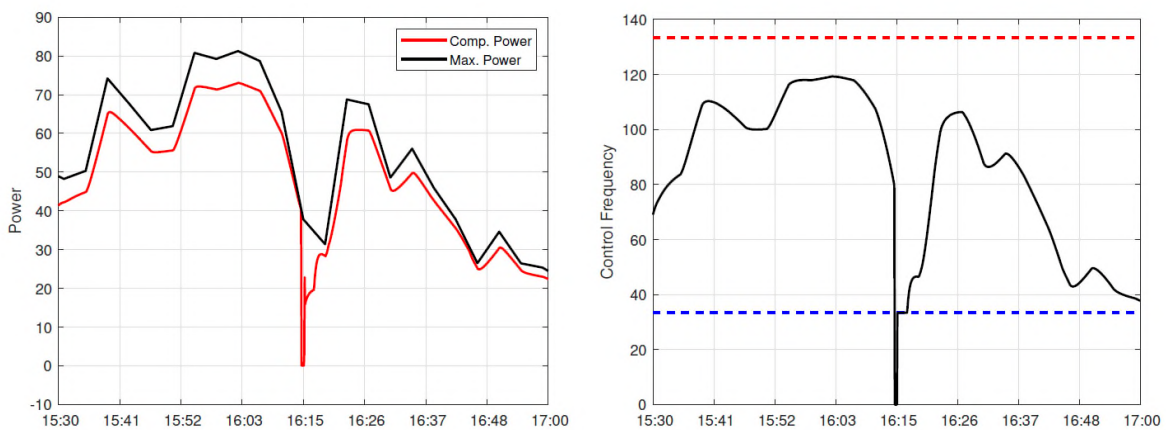


Figure 52 Compressor power and control frequency for the measured irradiance profile and the PPT control strategy.

## 6.5 Summary of guidelines based on the simulation models

A dynamic model of an ice-lined vaccine cooler cabinet was used to investigate the autonomy time and the steady state temperature of the air during phase change of the ice. A baseline model representing an existing cabinet was calibrated against experimental results from three different measurement setups. The calibrated baseline model showed a good agreement with the measurements. It was investigated how different parameters related to the cooler cabinet and ice storage affected the autonomy time, while making sure that the steady state temperature stayed in an acceptable range between 2 °C and 8 °C. The results showed that the mass of ice in the storage was the most promising parameter to consider for prolonging the autonomy time. Furthermore, it was shown that a reduction of the thermal bridges in the cabinet also is of great importance.

The influence of compressor type and compressor control strategy on the performance of a solar direct drive refrigeration system was investigated using a steady state numerical model. The Utilization Factor and Accumulated Daily Cooling Load were determined for a full day under varying daily peak irradiances. Two compressor types, the BDS5.0K and BD35K, and three compressor control strategies, PPT, CVC and AEO, were investigated. Furthermore, four configurations were included: a 360 W and a 180 W PV panel both with and without compressor start power delivered from the PV panel. Results showed that both the choice of compressor and the applied control strategy affected the system's ability to utilize the available power from the PV panel, especially under lower irradiance conditions and when the PV panel was downsized. Generally, the PPT strategy delivered the highest Utilization Factor and thus the highest cooling load. The CVC was comparable to the PPT for the 360 W PV panel, while performing worse than the PPT for the 180 W configurations. The AEO generally had a lower performance than the PPT and CVC. However, compared to the simplicity of this control strategy, the AEO actually performed well compared to the more challenging PPT and CVC controls. The BDS5.0K performed better than the BD35K due to both the increased efficiency and the increased speed range. Finally, results show that if the need for compressor start power delivered by the PV panel was alleviated, the size of the PV panel can be halved without a significant reduction in performance.

The three control strategies were also compared using a detailed dynamic model of the system. The dynamic model was applied both to the WHO PQS irradiance profile and for a measured irradiance profile with intermittent cloud covers. The results for the WHO profile are in good agreement with the results of the steady state analysis, thus showing only minor differences in the performance of the three strategies. However, for the measured irradiance profile both the CVC and PPT attain a significantly higher performance than the AEO control strategy. Again, only minor differences were observed between the PPT and the CVC control.

## 7. Project conclusion and perspective

A new Solar Direct Drive compressor, BD-Nano 50K, has been developed and tested. SECOP plans to start mass production of this new compressor in November 2021.

A new vaccine cooler cabinet has been developed and tested, and Vestfrost Solutions plans to market this cabinet in the fall of 2021. Vestfrost has also developed and tested a new remote monitoring system (EMS), and this will also be marketed in the fall of 2021.

### Compressor development

Two new Solar Direct Drive compressors have been developed and tested in this project.

The first one is based on the relatively new SECOP XV compressor platform. This was developed and tested with success. Because of a change of ownership and a change of strategy at SECOP, it was decided to stop the further development of this compressor because it is based on a household compressor platform. The new strategy for SECOP is to focus on compressors for professional appliances.

A new compressor platform has been developed for all DC compressors, including compressors for the automotive sector and for the Solar Direct Drive sector. The name is "Nano-Compressor". The SECOP BD-Nano50K Direct Drive compressor is more efficient since it has bigger cooling capacity compared to the existing BD35K DD compressor.

For freezing applications ( $T_{\text{evap}} = -25\text{ °C}$ ), the cooling capacity has increased from 36W to 50.8W (+41 %), and the energy efficiency (COP) has increased from 0.87 to 1.19 (+36.8 %).

For refrigerator applications ( $T_{\text{evap}} = -10\text{ °C}$ ), the cooling capacity has increased from 83.8W to 109.1W (+30.2 %), and the energy efficiency (COP) has increased from 1.39 to 1.66 (+19.4 %).

SECOP plans to start the production of the new compressor in November 2021. Later on, a new version of the compressor controller will be set into production. This will include the new AEO control strategy developed in this project.

The price for the new compressor is not yet known.

### Cabinet development

A new cabinet with longer hold-over time has been developed and tested. An enlarged ice storage prolongs the hold-over time to 89h 32 min according to the latest version of the WHO PQS protocols.

A more precise temperature regulation has been developed and tested. This consists of a new technology which includes a small electrical heater and a more sophisticated control. In addition, a new freeze protection has been developed and tested.

The new cabinets will be more robust since the control sensors are coated, and the wires are protected against humidity and influence from rodents.

The increased robustness supplied by the new remote monitoring device (EMS) is expected to reduce the need for service and to prolong the lifetime of the coolers. Vestfrost plans to increase the guarantee period from 2 to 3 years for the new coolers.

Vestfrost has developed and tested a new remote monitoring device: "EMS". It has the size of an iPhone, and it is connected to GSM mobile phone net. It includes a GPS that makes it possible for the administrative authority to see where the unit is placed. The EMS sends periodical reports to the authority, and it sends an alarm, if something gets wrong.

Energy Harvesting will be possible using the new EMS device. Two USB slots (5V) are built in.

The new cabinet with the new temperature control and the EMS remote monitoring device has been in field test in Africa with good results.

The new cooler has been tested at Danish Technological Institute and approved according to the WHO specifications.

The price for the new cabinets is expected to be slightly higher compared to the existing Solar DD vaccine cabinets due to increased costs for the remote monitoring device (EMS) and a larger ice bank.

It is, however, expected that the new cooler will be very competitive according to the better temperature regulation, the prolonged hold-over time and the remote monitoring possibility.

### **Discussion**

The new compressor will ensure:

- Reduction of the necessary PV panel size for Solar Direct Drive vaccine coolers.
- The Solar DD technology will expand to slightly bigger cabinets.

The new Solar DD vaccine cooler will ensure a more stable vaccine storage temperature and reduce the loss of vaccines in the field. It is expected that the increased robustness combined with the new remote monitoring device will prolong the lifetime of the cooler. The new remote monitoring device will also ensure fast service if something happens with the cooler. This will also reduce loss of vaccines.

There will, however, in the near future be a need for an even bigger cooling capacity for Solar Direct Drive compressors for commercial cabinets for cooling food and drinks and for freezing ice and food.

## 8. Appendices

## 8.1 Appendix A: Temperature control experiments

Test of Vestfrost SDD with Secop XV compressor **IK September 2020/rev June 20121**

### Temperature control experiments

DTI has tested a vaccine cooler from Vestfrost in the project “Second generation vaccine cooler”. The unit has a special power supply made by Secop with 30-70 V input range.

Purpose: SDD appliances in field operation monitoring have sometimes shown a strongly fluctuating temperature pattern, probably when the ice bank is not frozen at all or is fully frozen. Full freezing could result in too low wall temperatures so that grade A freeze protection cannot be achieved.

If we can reproduce the observed behaviour in the laboratory, we could try to move the thermostat and do other modifications to see if it has any effect on temperature stability.

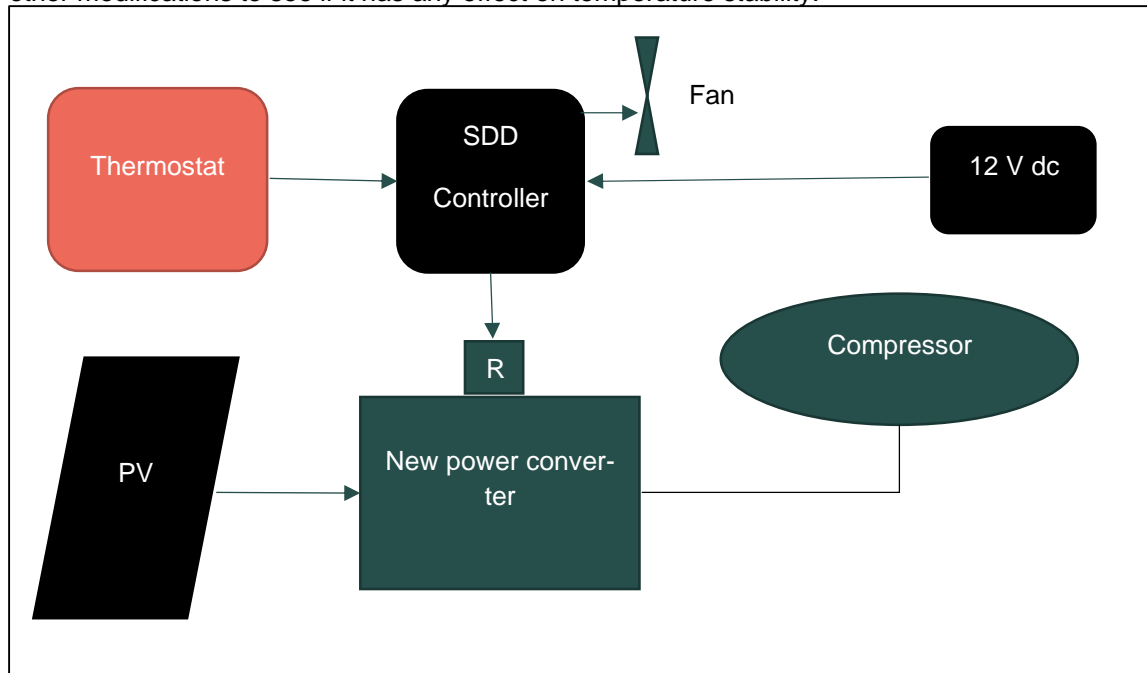


Figure 53: Test setup

The internal thermostat and display are powered by a 12 V dc supply which also powers the fan. The Secop special converter is active when the thermostat is on, i.e. the relay R is triggered.

Test conditions:

- The PV simulator is set up to simulate a single standard PV module with 72 cells and nominal power 150 Wp.
- Thermostat initially set to 4 °C (factory setting)
- Running with WHO test cycle day/night
- Laboratory temperature 15-20 °C

Photo documentation and results:



Figure 54 Compressor with external power supply

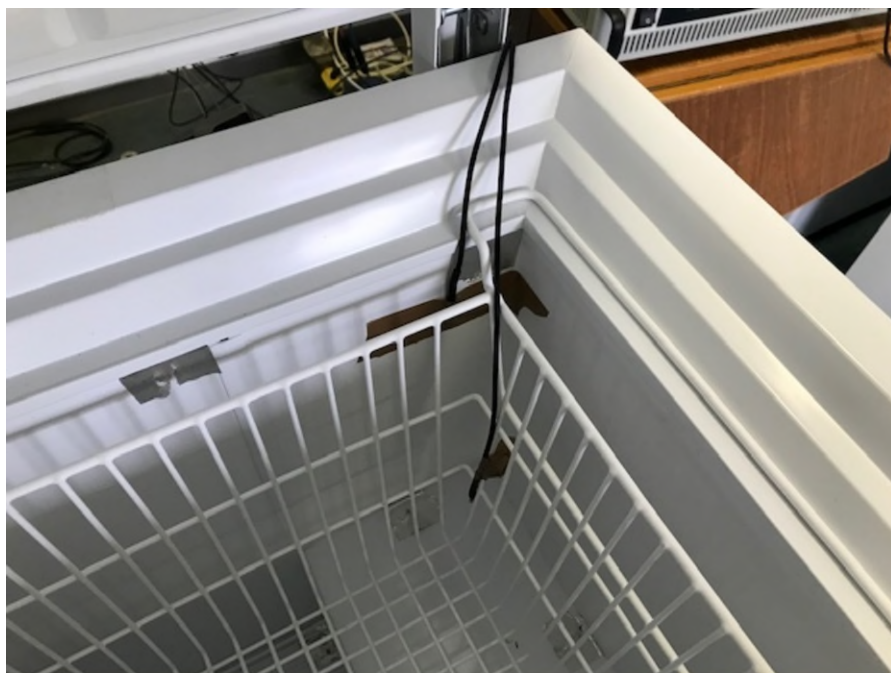


Figure 55 Internal temperature sensors mounted in the cabinet.



**Run#1 11-09-2020:**

PV simulator 150 Wp / 72 crystalline cells  
 Running with WHO 3.5 kWh/day test profile 24 h cycles  
 Thermostat set to 4 °C  
 Available solar energy per day:

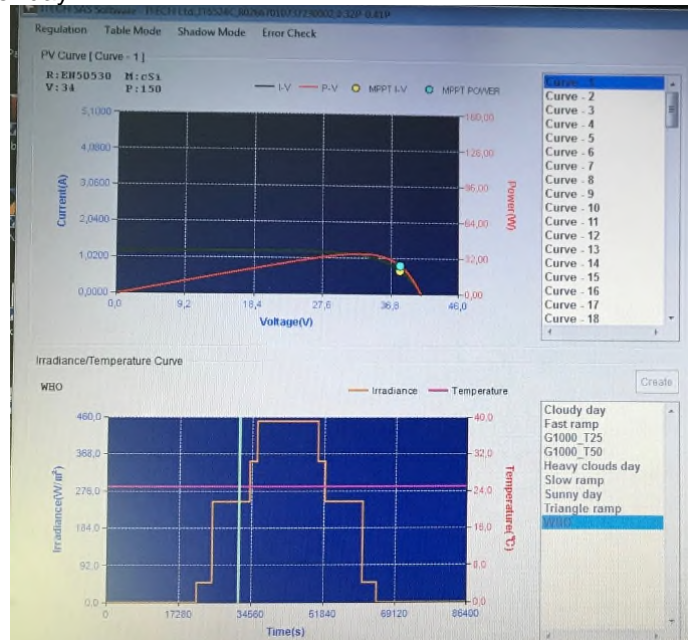


Figure 56 Screen dump of solar PV simulator. Lower graph shows the irradiance profile. The dot on the I-V curve shows the actual point of operation at a slightly higher voltage than the MPP voltage. At 450 W/m2 the corresponding maximum PV power is  $0,45 \times 150 \text{ Wp} = 67.5 \text{ W}$

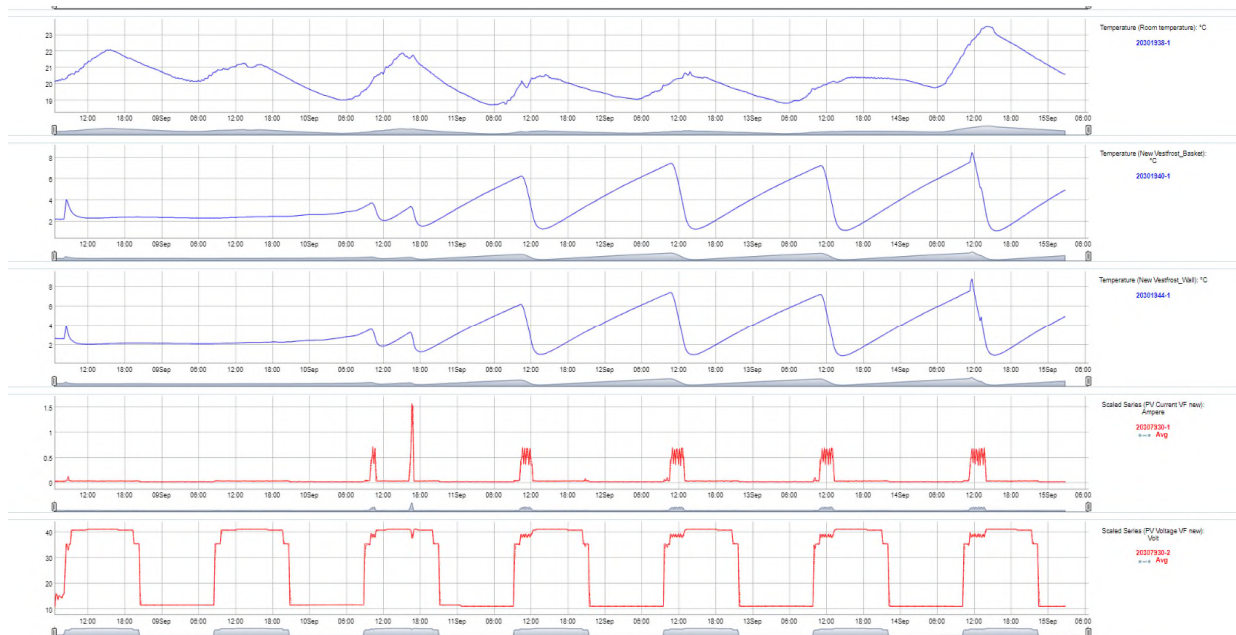


Figure 57 Short daily runtime(current draw 2 h/day) and strong cycling indicates that the ice bank is not sufficiently frozen. It will not be possible to adjust the thermostat to a lower setting without reaching too low minimum temperatures since it already goes below 2°C. Peak power is  $1.5 \text{ A} \times 38 \text{ V} = 57 \text{ W}$  but mostly around 20 W.

Evaluation of daily runtime: For a 90% freezing of 15 litres of storage volume, the demand is:

Tank volume	0,015	m3
Ice ratio	0,9	

	917	kg/m <sup>3</sup>
Ice mass	12,38	kg
Energy content	1,15	kWh

The electricity demand can be estimated to half of this i.e. 0,6 kWh.

Measured average current is 0.6 A and voltage 38 V

Runtime= 0.6 kWh/(38\*0.6)/1000 = 26 hours!

Conclusion: Full freezing takes several days with the WHO power profile. The thermostat cuts out far too early causing very short daily runtime and no freezing of the storage. Inspection of water tank showed liquid water above 0°C.

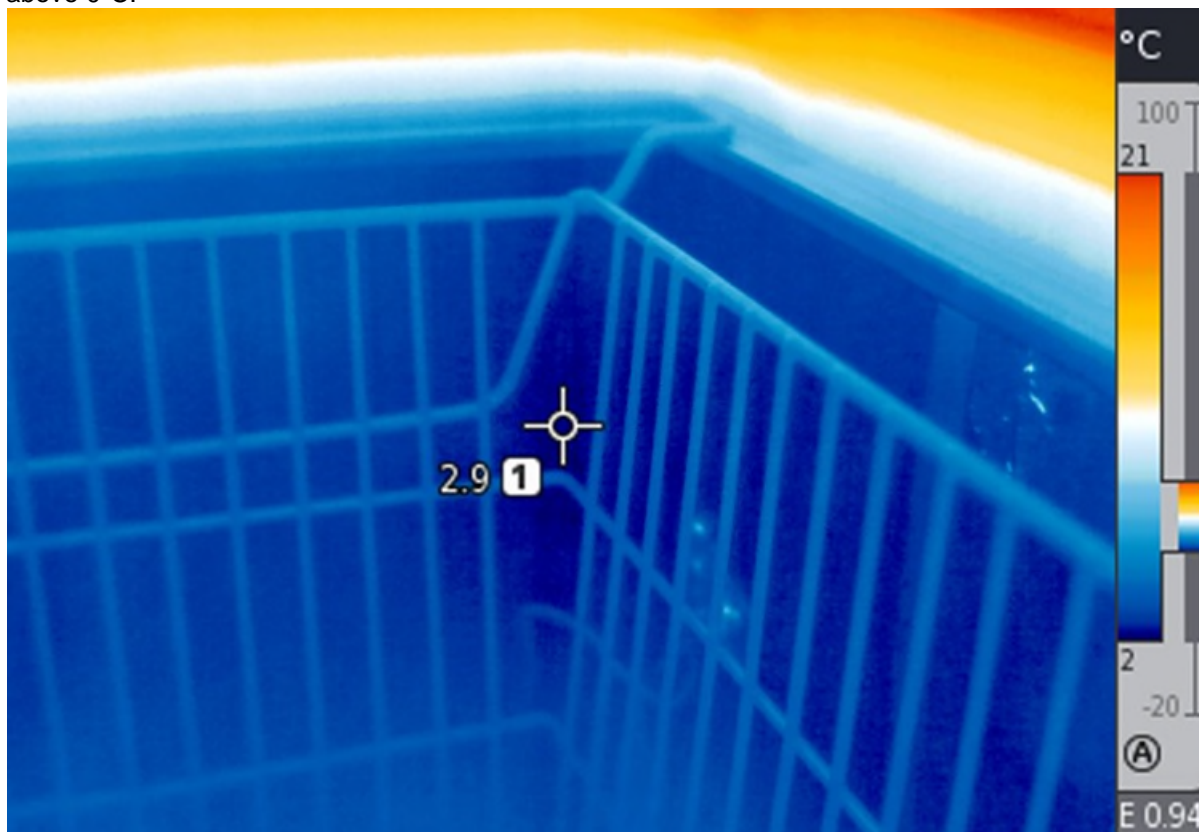


Figure 58 Thermal image showing very uniform internal temperature, also when running.

**Run#2 16-09-2020**

New position of thermostat sensor 21 cm over the cabinet floor.

17-09-2020: Wall sensor moved to ice tank hole.

Thermostat was set to its minimum adjustment = 1°C. The graph shows that the runtime is strongly increased the first day after change, and all temperatures become much more stable. This indicates formation of ice is taking place. There is partial freezing in the cabinet, which is not desired.

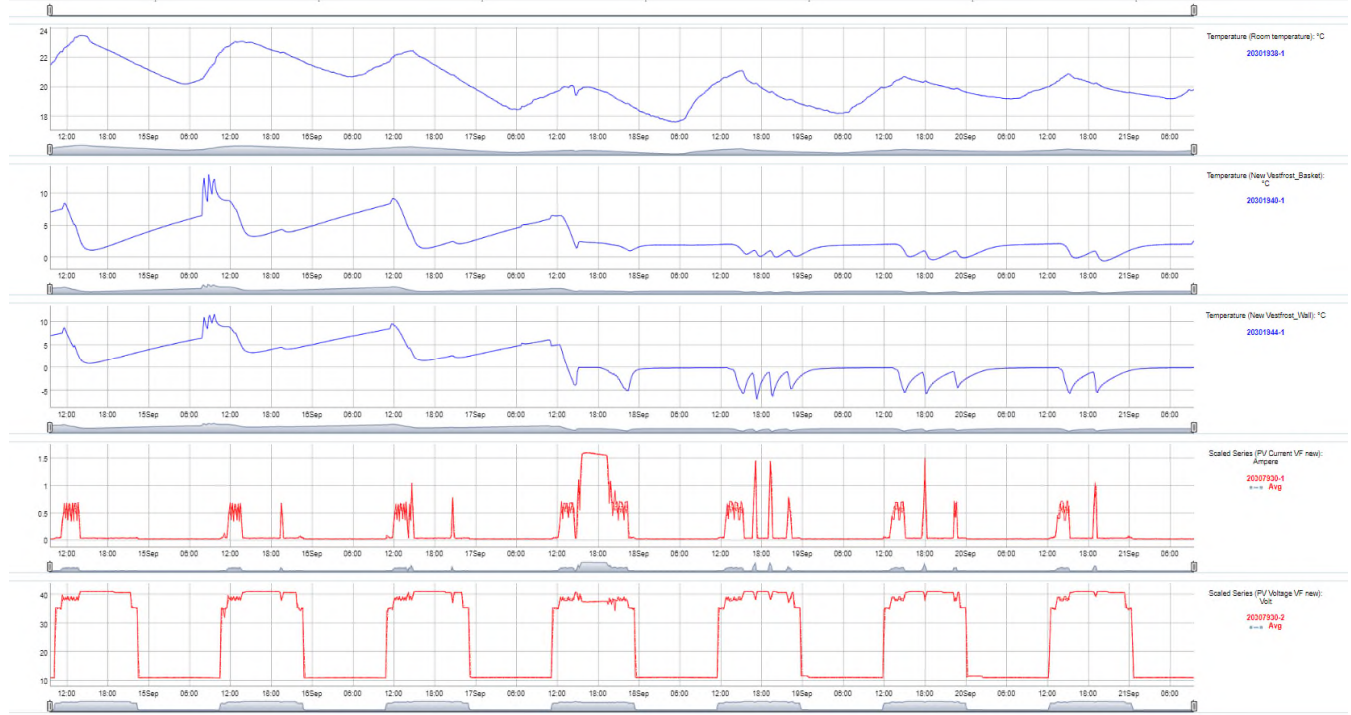


Figure 59 Long runtime and freezing from day 1 stabilizes temperature.

**Run#3 21-09-2020**

Thermostat adjusted to 2 °C. With this setting there is no freezing any longer and the measured average basket temperature is quite stable around 1.7 °C:

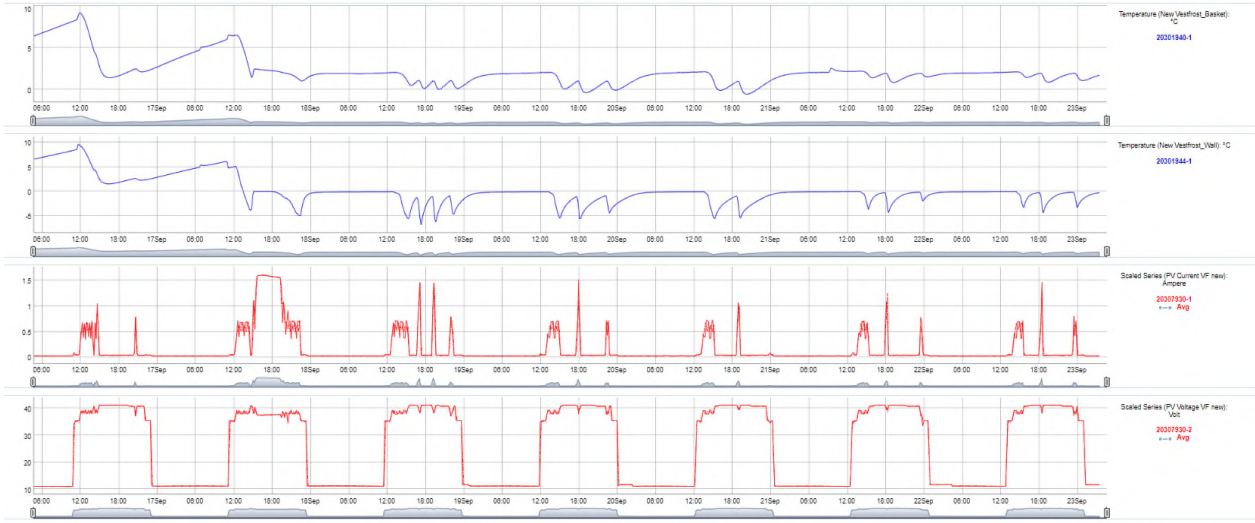


Figure 60 Improved stability due to higher minimum temperature in the basket. Regular run pattern.

**Run#4 23-09-2020**

Thermostat adjusted to 3 °C: Passive compressor for 5 days, then strong cycling starts again.

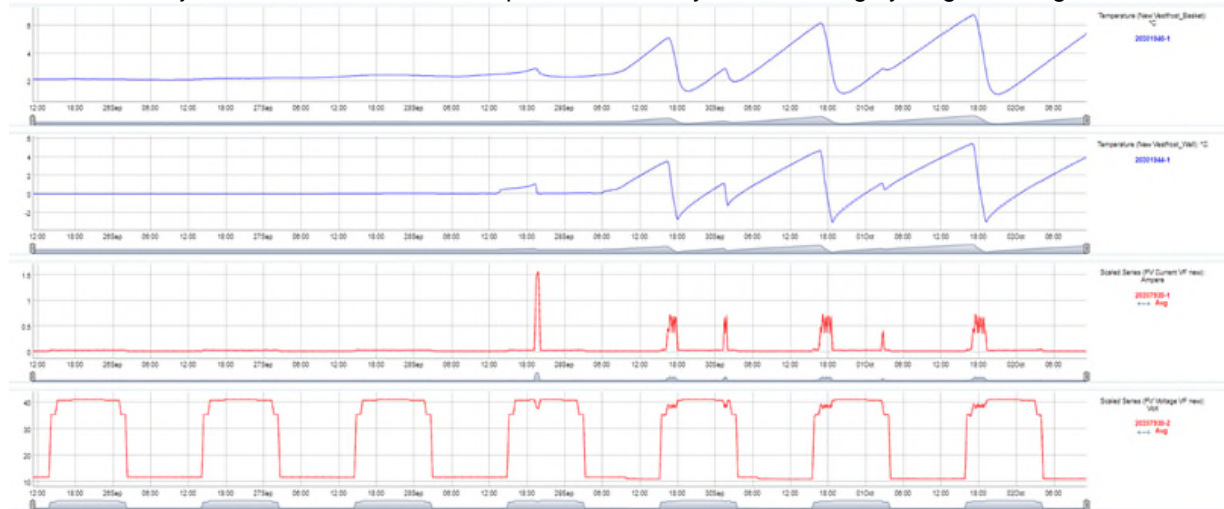


Figure 61 The graph shows that the temperature setting is too high and after melting of ice the temperatures become unstable again.

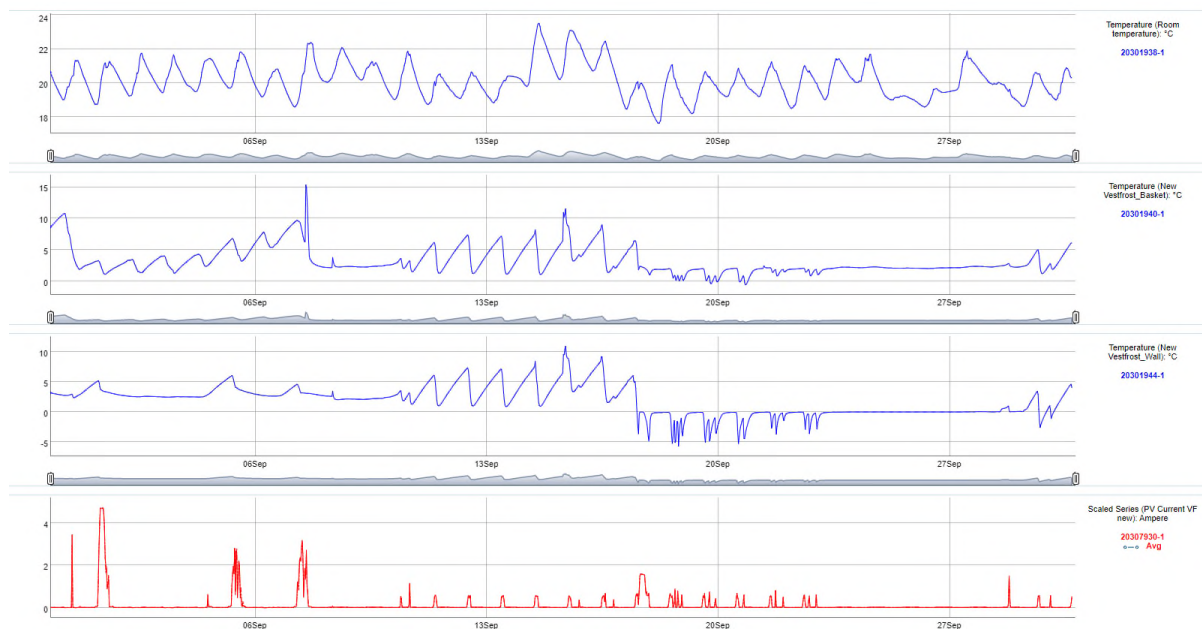


Figure 62 Longer sequence showing data for runs 1-4.

**Run#5 02-10-2020**

1 kg warm mass added to the inner space

Will it force the compressor to run longer and build up ice? Stopped- no useful results.

**Run#6 05-10-2020**

Thermostat again set to 1°C (minimum)

Good thermal contact to the wall near ice bank and furthermore the sensor was insulated with foam tape. This could ensure cut-out when the ice temperature becomes too low and therefor risk of negative compartment temperature.

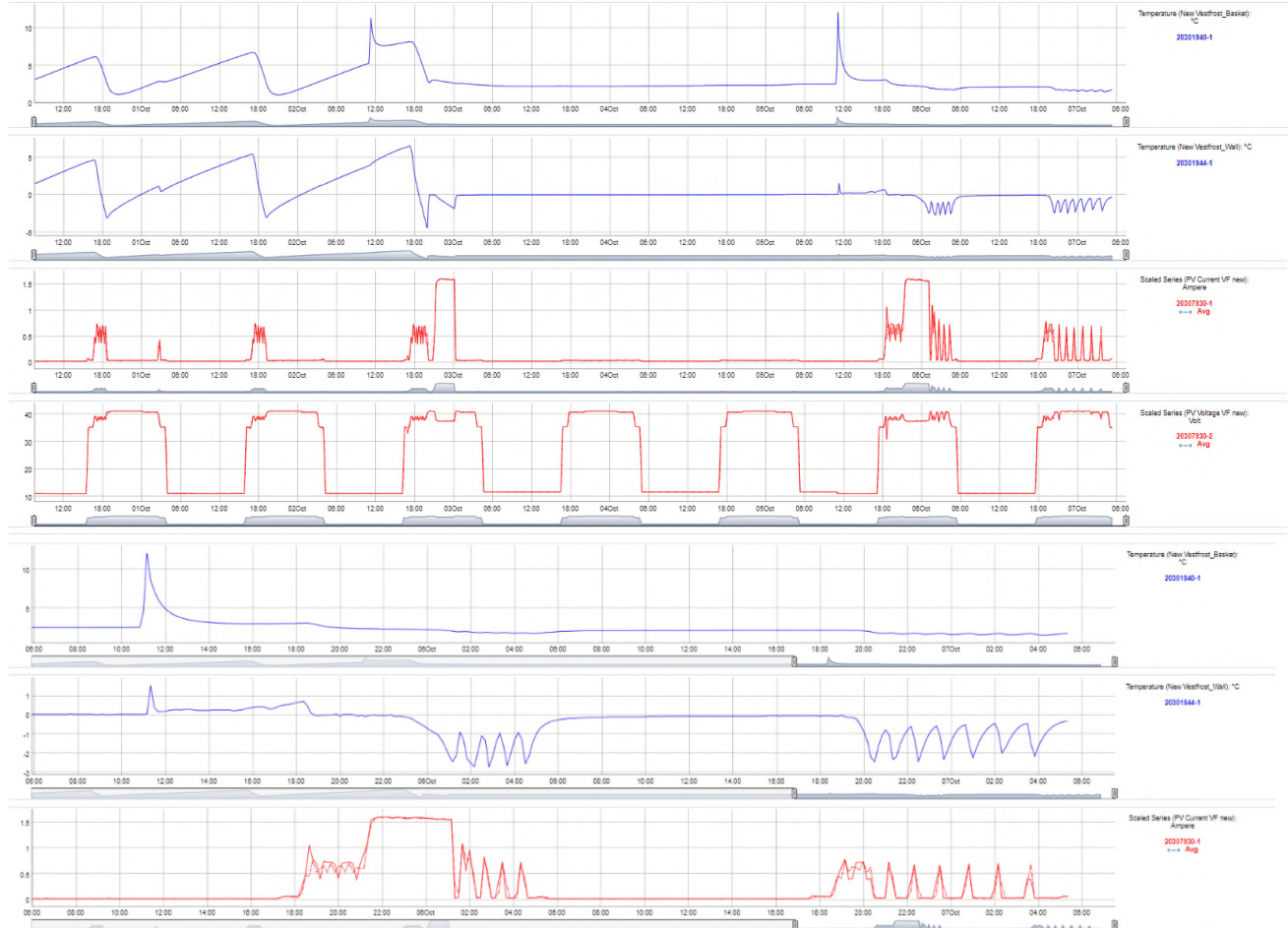


Figure 63 The unit is running with several daily cycles and maintain a very stable temperature in ice bank(wall) and basket. However, the basket temperature is slightly lower than 2 °C which is the limit set by the relevant WHO PQS standard.

- THERMOSTAT ADJUSTED TO 1.5 °C 07-10-2020 9:44
- SET BACK TO 1.0 09-10-2020 13:00 due to missing freezing

**Run#7: 12-10-2020**

THERMAL INSULATION ADDED ON ICELINER (3 SIDES) for prevention of low vaccine temperature. The insulation was polymer foam taped to the inner surface.

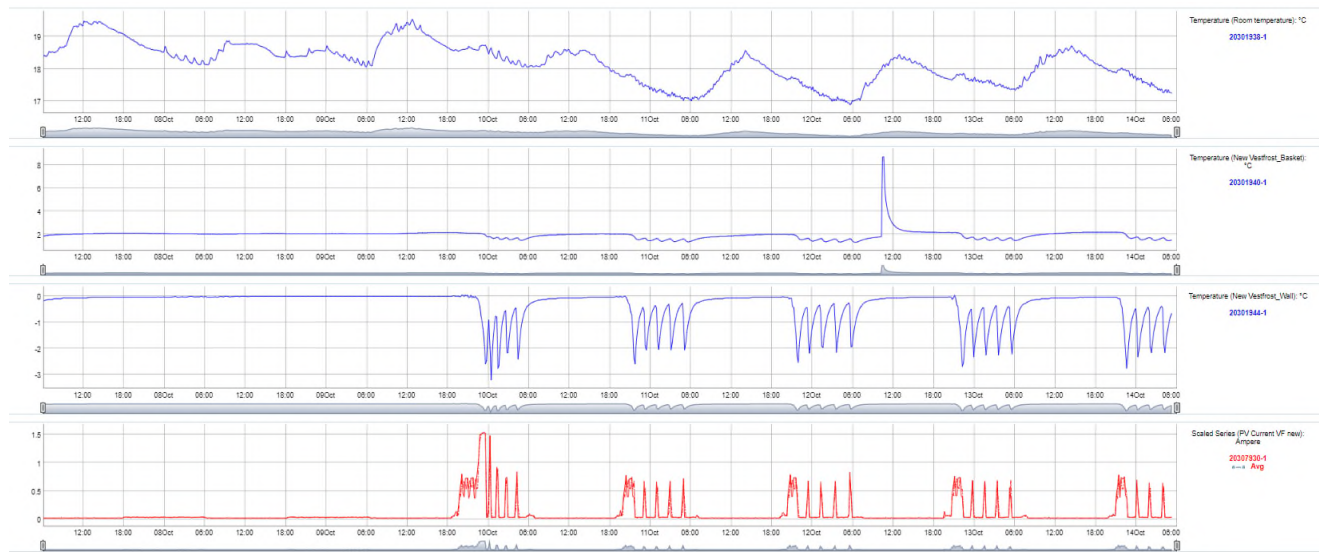


Figure 64 Disappointing result. The temperature is almost the same as before insulation. Maybe poor contact between sensor and wall.

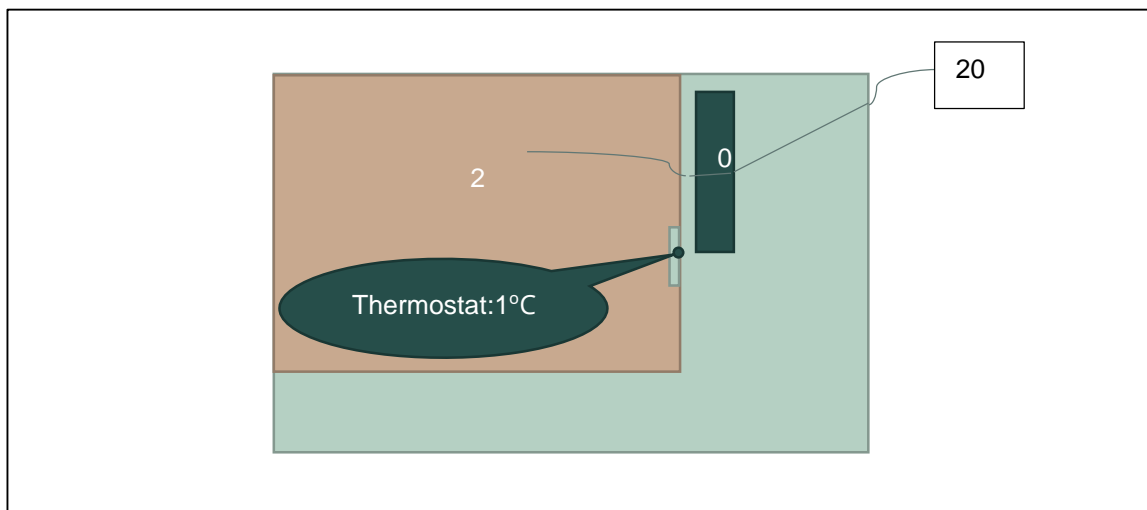


Figure 65 Cross section with assumed temperature profile

**Run#8 14-10-2020**

THERMAL INSULATION ADDED ON last side for prevention of low vaccine temperature. More insulation was added over the sensor.

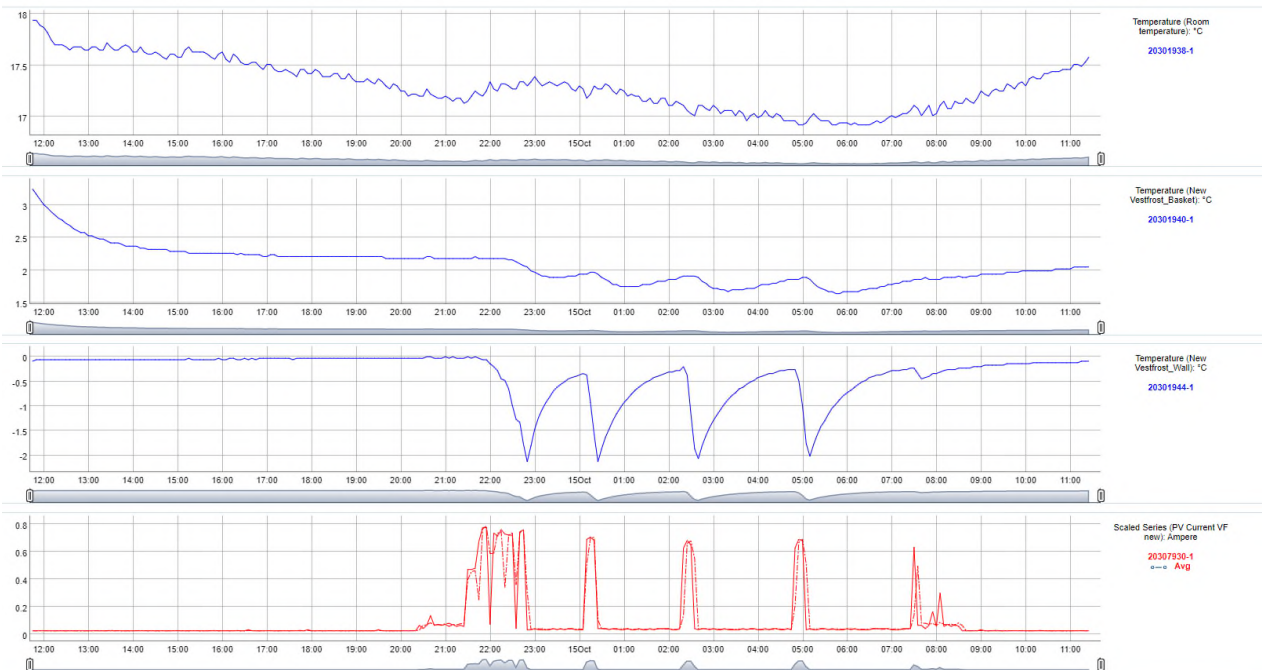


Figure 66 Cycling with additional inner insulation and set point 1 degC. The basket temperature is still going below 2°C.

Conclusion on insulation experiments: The effect on compartment temperature is very limited. The position at setting of the thermostat sensor is more important.



**Run#9: 21-10-2020 Capacity test**

In this test of cooling capacity 37 warm cans added to basket, a sensor (basket) placed in one of them:

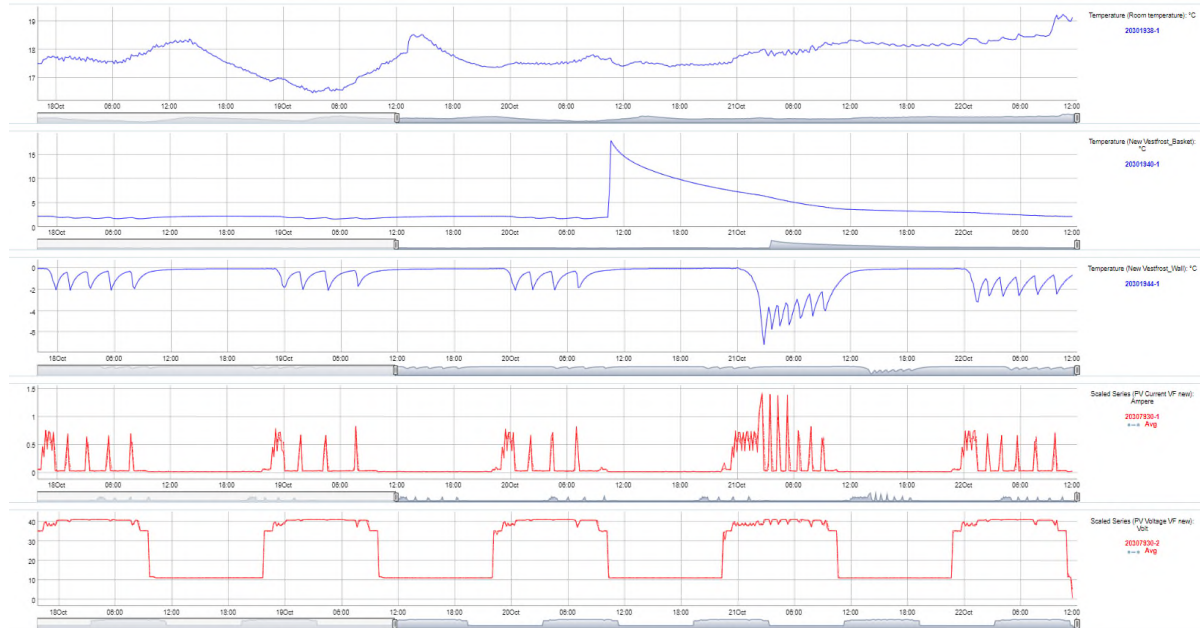


Figure 67 Cooling of 37 canned beverages. On the first day after load the runtime increases significantly.

Observed cooling rate: From 18°C to 4°C in 24 hours.

$$M = 37 \times 0,33 = 12,21 \text{ kg}$$

$$C = 4186 \text{ J/kgK} \times 12,21 = 51111 \text{ J/K}$$

$$P = 51111 \times (18 - 4) / (24 \times 3600) = 8.3 \text{ W heat transfer from the cans in average}$$

The only partial running the day after load indicate the maximum cooling capacity is not reached.

**Run#10: 22-10-2020 14:25**

Experiment with active temperature control.

100 Ohm heater mounted in bottom of cabinet and cans removed. The heater is connected in parallel to the PV panel and should adjust the daytime temperature in the basket at a slightly higher level without affecting the ice storage.

Estimated power at PV voltage 35 V :  $P=U^2/R = 35 \times 35 / 100 = 12 \text{ W}$

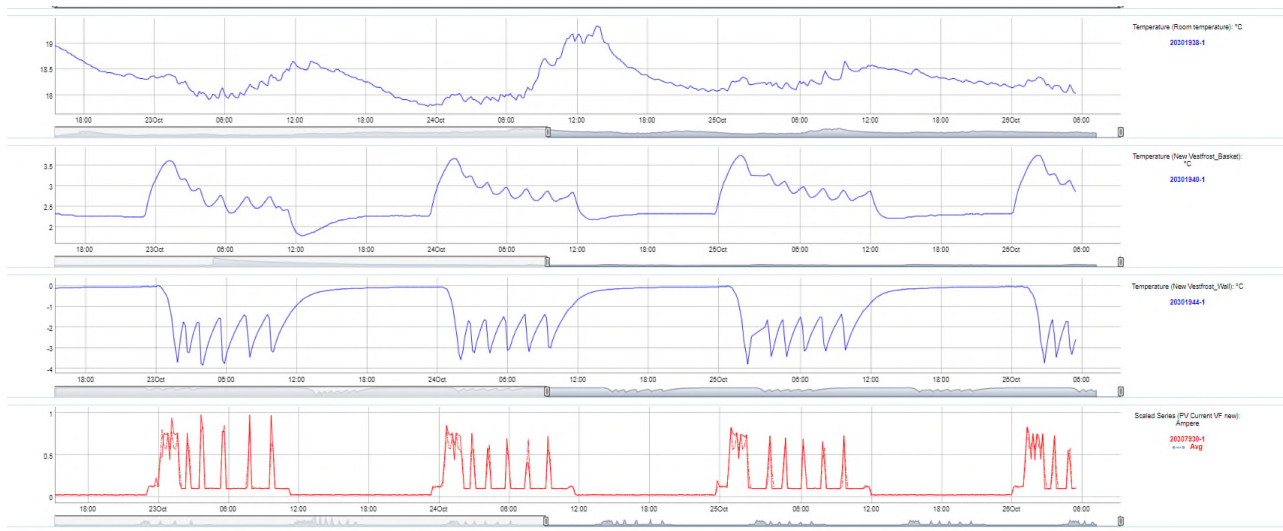


Figure 68 Application of a heater causes the basket temperature to rise a bit during daytime. WHO criteria are met.

**Run#11: 28-10-2020 Thermostat set to 2 C**

No positive impact on night temperature, only day temperature rises a bit.

**Run#12: 30-10-2010 6 icepacks inserted at bottom of basket for prevention of cold night temperature of basket.**

There is a more uniform temperature the last two days:

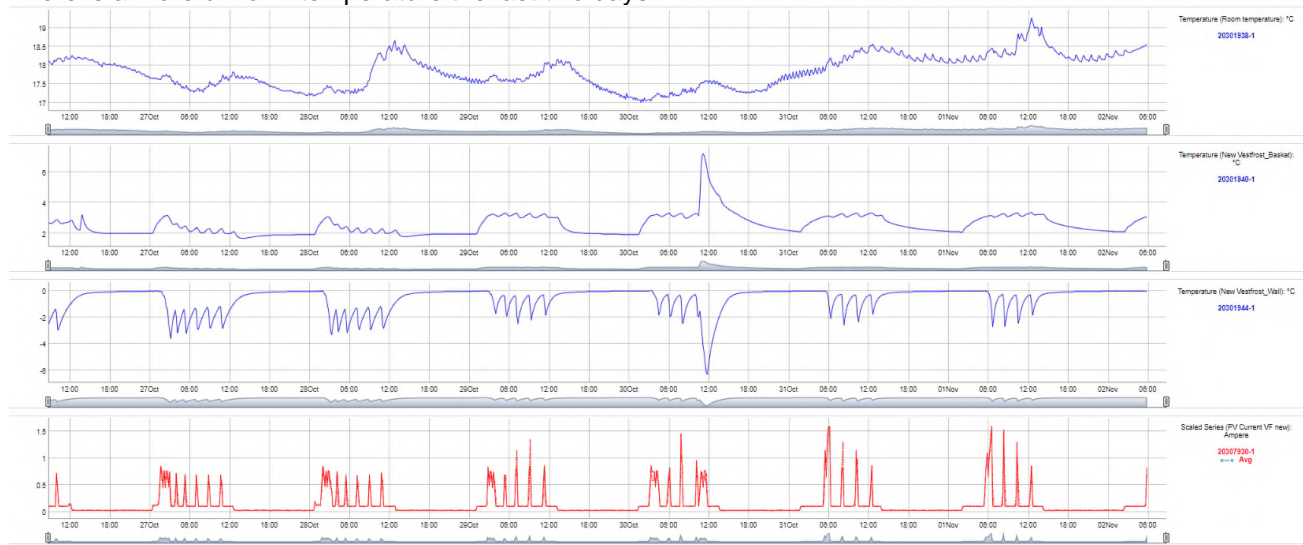


Figure 69: Test 12.

Conclusion: Electric heating is a viable solution for freeze prevention. The load of 12W works very well with the current cabinet.

**Summary:** The many experiments and modifications have shown that there is no easy way to achieve the perfect temperature balance in a SDD appliance relying on ice as only means of energy storage. Compared to the original construction the result is a significant improvement of the temperature stability by the following actions:

- 5) Re-positioning of the inner thermostat sensor so it becomes in closer contact with the ice storage.
- 6) Insulate the sensor surface (or move it to the inner side of the cladding)
- 7) Lower the thermostat setting to 1-1.5 C which is just sufficient to initialize freezing
- 8) Install a small heat load to counteract too low temperatures when ice is generated during daytime

## 8.2 Appendix B: Subcooling Experiments

Ivan Katic (November-December 2020)

### Background

Laboratory and field experiments have shown that the current Vestfrost cabinet does not always freeze the ice storage, especially when the ambient temperature is low. This may be caused by the phenomenon subcooling. Subcooling of water is not desired in the case of ice formation for energy storage. This is because negative water temperatures trigger the thermostat to stop the cooling cycle before ice has been built up and thus the state of charge of the energy storage remains very low – only sensible heat capacity of water is activated.

A literature survey has shown that there are different ways to accelerate the formation of ice but that some of the mechanisms are not fully understood. Methods mentioned in literature are:

- Mechanical impact
- Application of a DC electric field
- Application of a magnetic field
- Certain proteins (e.g. testosterone)
- Alcohols with long carbon chains (Pentanol and above)
- Small particles of solid matter

### Experiments in the lab

Some of the ideas have been tested by DTI with the following results:

- 6) Two electrodes with a voltage difference of 12 V was submerged in the ice bank without any measurable effect on ice formation. The electrodes were switched on in parallel with the thermostat.
- 7) A freezer was set up for more controlled experiments and comparison of methods. First run was with the solid matters kaolin powder and saw dust. In both cases there was a positive effect compared to pure tap water, with sawdust as the best. The test used plastic cups with externally mounted sensors.
- 8) Next test compared the alcohols pentanol and hexanol with pure water and water with plastic foam granulate. About 10 drops of alcohol was used in each cup. The granulate performed best while the cups with pure water and with alcohol added all exhibited subcooling.
- 9) The same test was repeated, but this time in small and closed plastic bags without free air surface. Only one drop of alcohol was used. In this case the bags with added alcohol had no subcooling, while pure water and water with granulate had.
- 10) Experiment no.3 was repeated with only one drop of alcohol per cup. This time the hexanol and the granulate worked best, while both water and pentanol exhibited some subcooling. Submerged sensors (incl. dust or other foreign object) for better accuracy may have influenced on results.

Photo documentation and results:

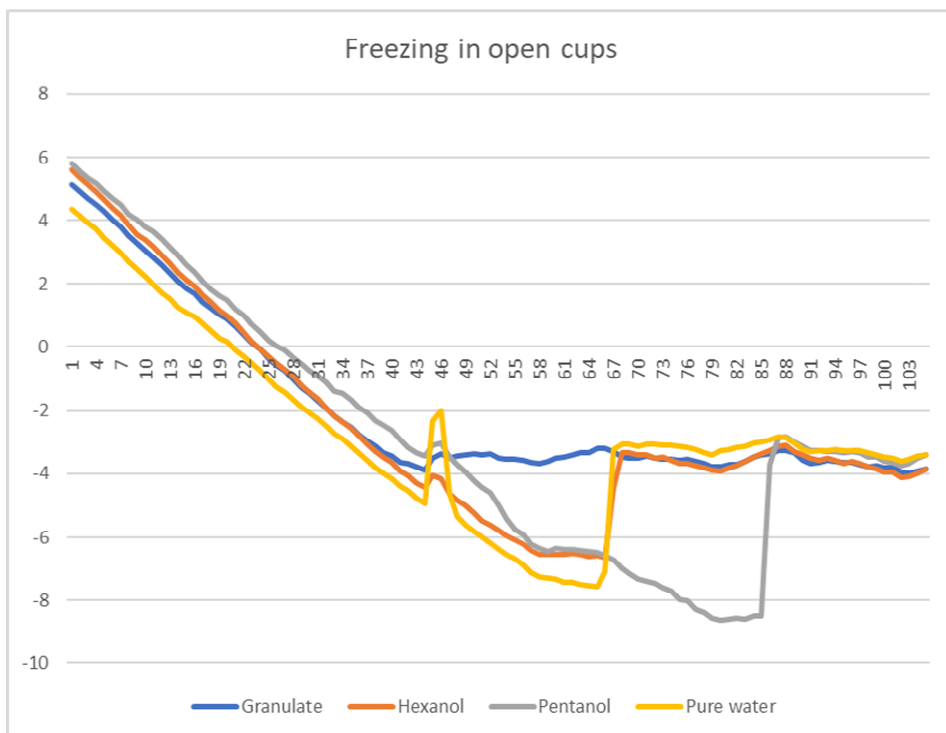


Figure 70 The first experiment showed a strange behaviour but a clear effect of added granulate. Sensors mounted on the outer surface explain the low temperature readings. More than 10 drops of alcohol were used.



Figure 71 Freezer with water filled cups and various additives. External mounting of sensors. A vibration damping mat was used to avoid vibrations from the compressor that could possibly trigger freezing.

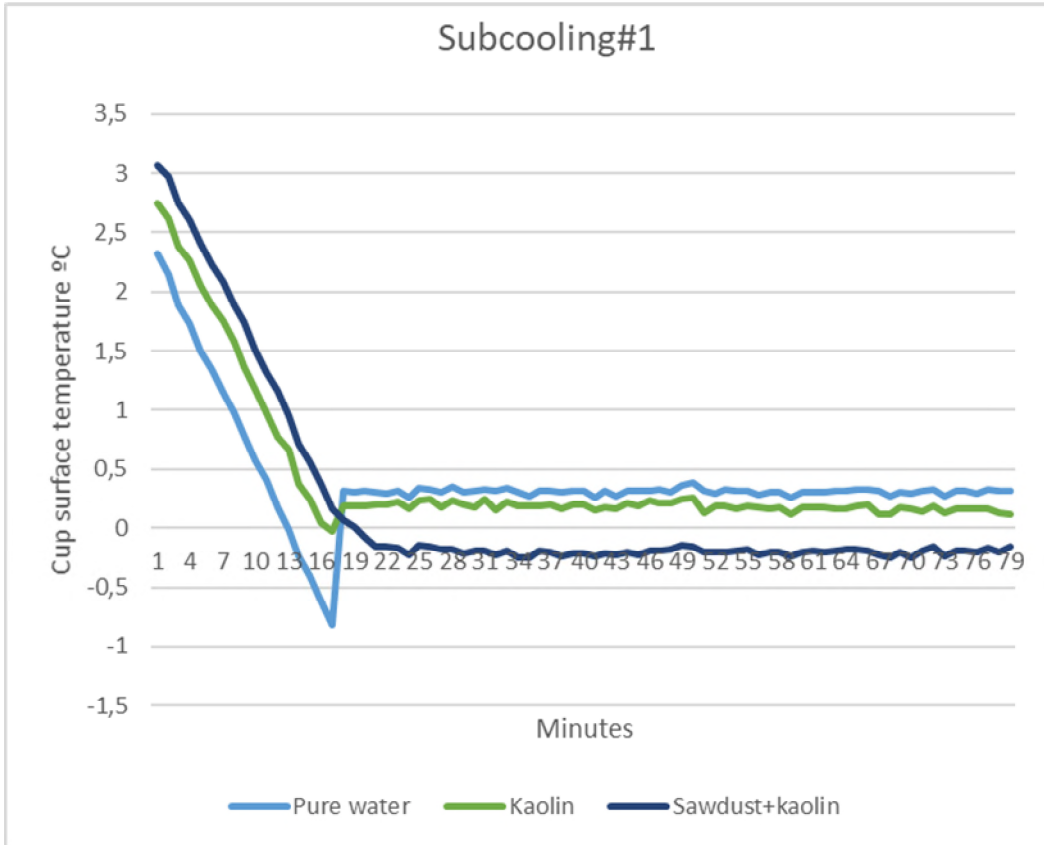


Figure 72 Effect of solid matter. A teaspoon of kaolin powder was added. (Sank to the bottom).

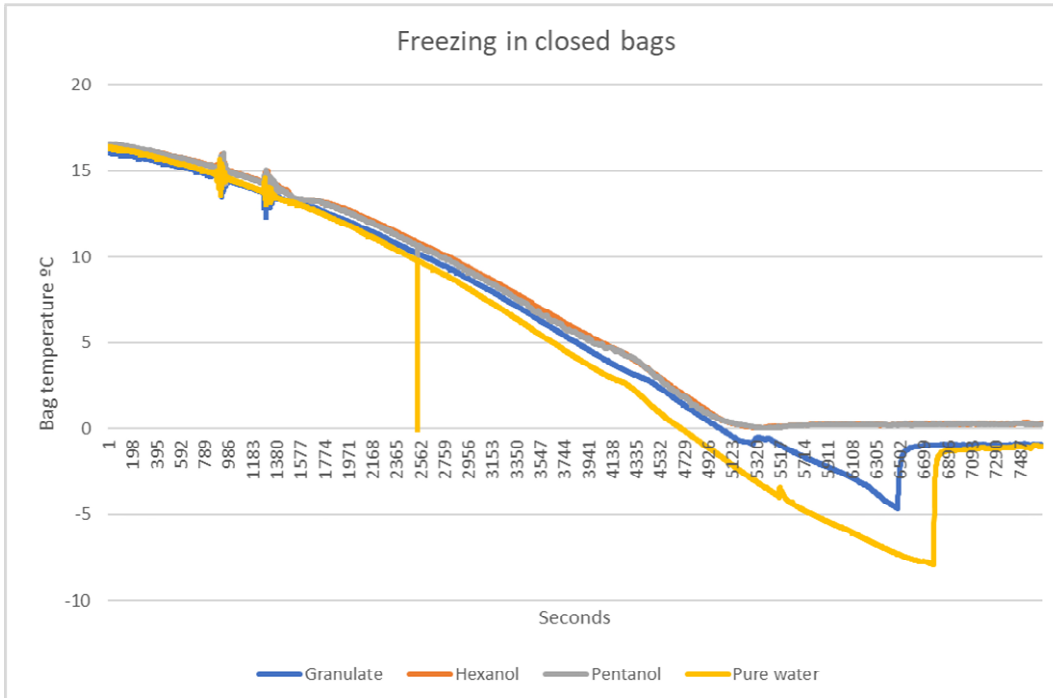


Figure 73 Effect of solid matter (foam granulate) and alcohols without an open surface to the air.



Figure 74 Plastic bags with temperature sensors taped to the lower surface.

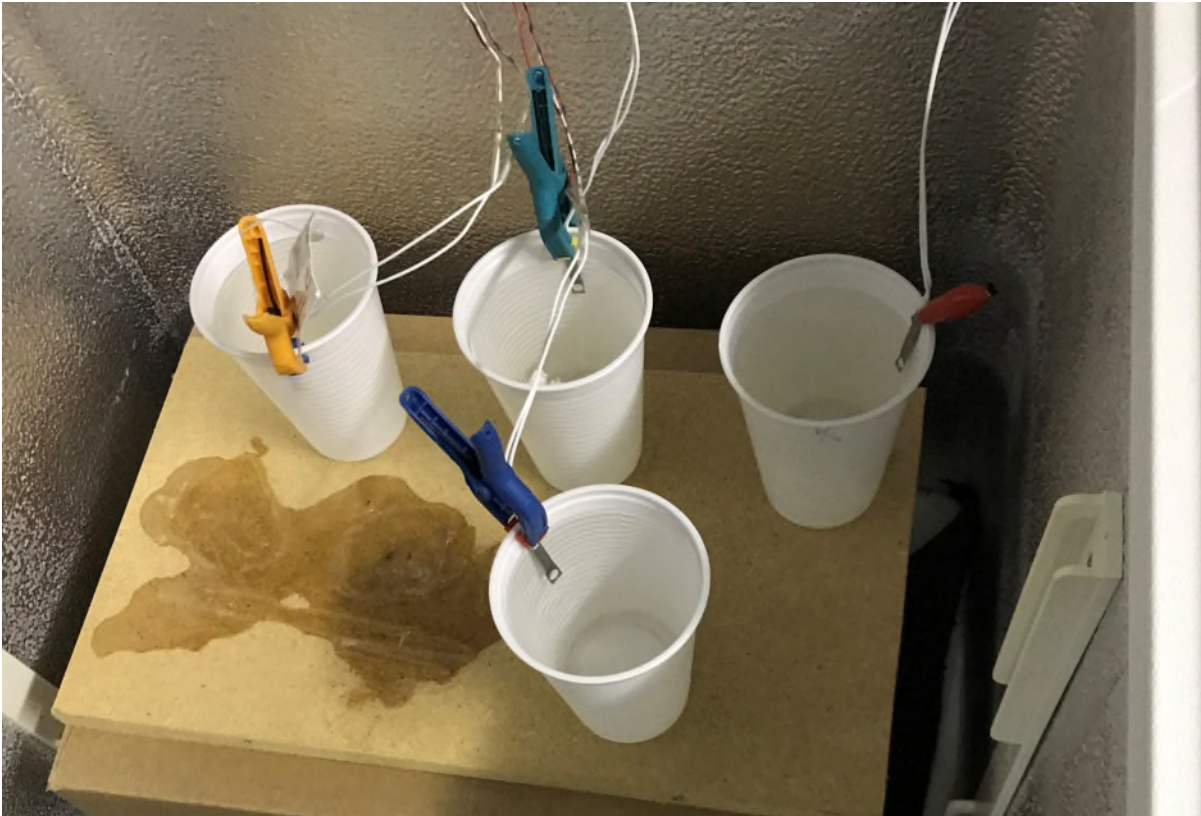


Figure 75 Freezing with submerged temperature sensors. Presence of sensors may have influenced on the results due to impurities/capillary effects.

In the last experiment, only a single drop of hexanol and pentanol was added to the cup:

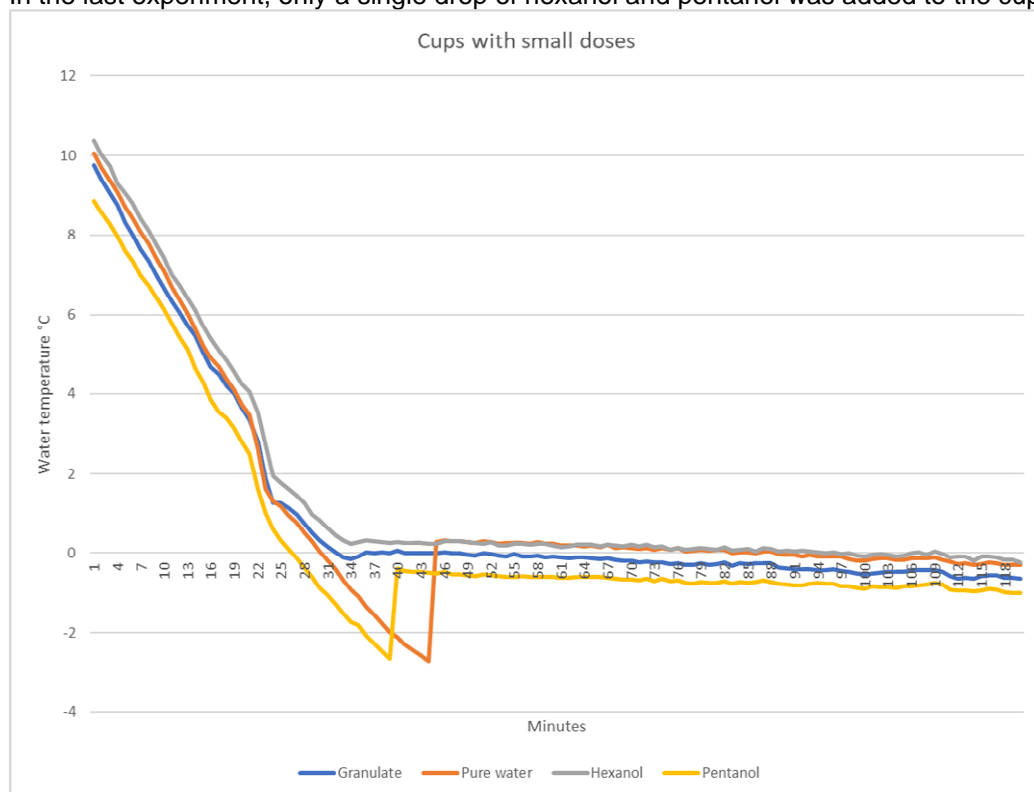


Figure 76 Effect of foam granulate and alcohols (1 drop) with an open surface to the air.

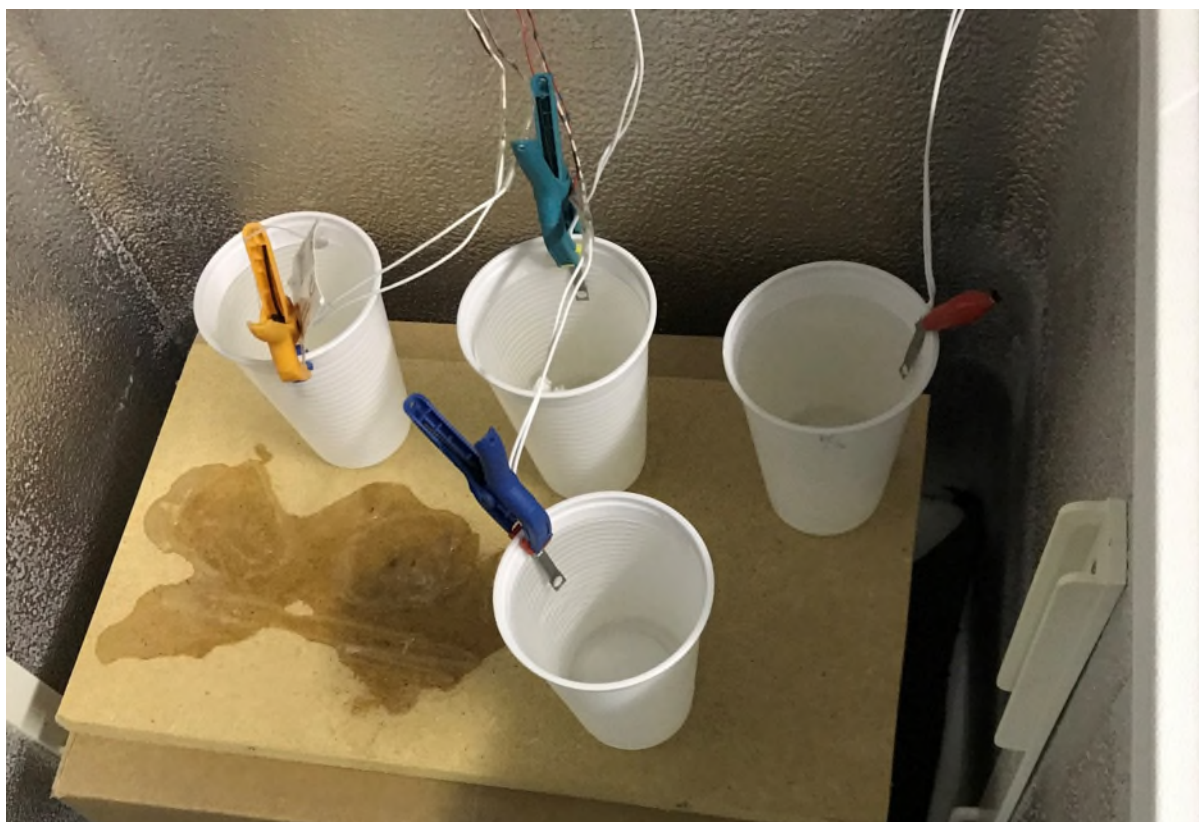


Figure 77 Freezing with submerged temperature sensors. Presence of sensors may have influenced on the results due to impurities/capillary effects.



Preliminary conclusion

There is a clear effect of floating granulate as ice nucleation agent on an open surface. This effect disappears when the granulate is submerged in the water. Both tested alcohols have a positive effect, but the optimum dose is not clear and there seem to be some randomness in the results. It looks like very small doses has the best effect, maybe because larger amounts change the general surface tension in the open cups? It is suggested that the concentration should be specified as drops per surface area of the ice bank because these alcohols are not easily soluble in water and stay as droplets on top of the water. It is not clear if the alcohol will evaporate over time.

Based on these experiments it was decided to add some of these additives to the ice bank of the Vestfrost cabinet and restart with improved instrumentation.

**RESTART 10-11-2020 Subcooling experiments**

Reference data showing that after melting the ice bank is not freezing again and temperature strongly fluctuating:

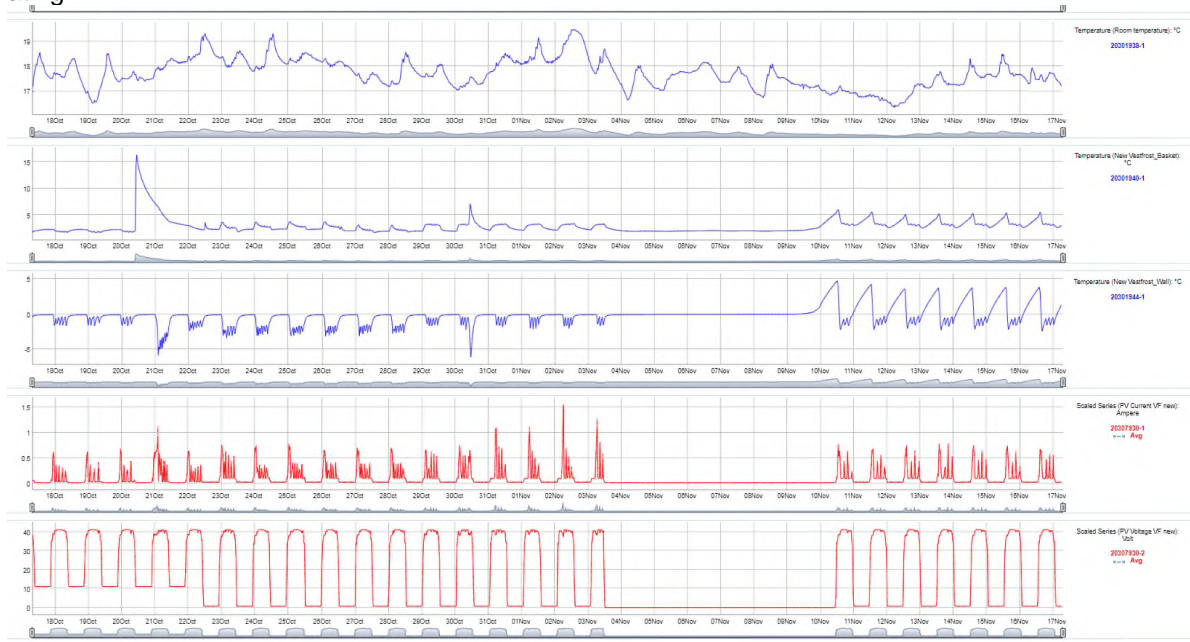


Figure 78 Shift from normal run through standby phase and at last reconnection.

After many days, spontaneous freezing occurs (two last days with power. Hereafter disconnected).

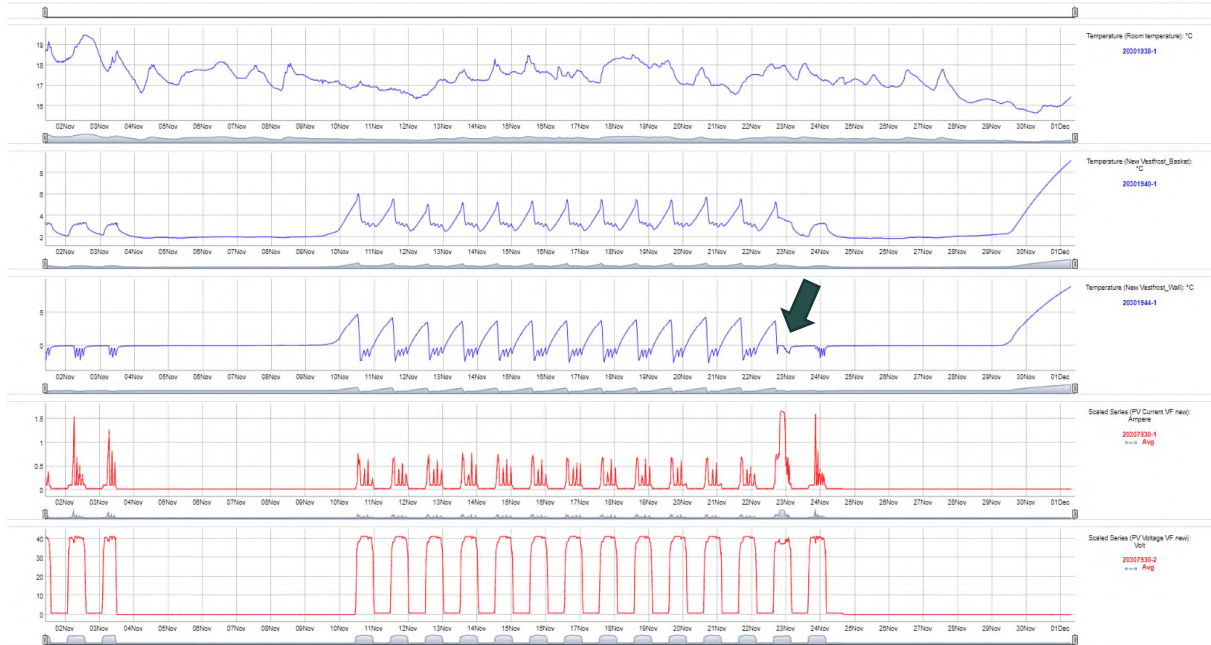


Figure 79 Stable running and sudden shift due to freezing.

**09-12-2020 New instrumentation**

Hexanol added (10 drops directly in the ice bank):

3.8 degrees subcooling and icebank freezing. Almost no change compared to the reference/initial results.

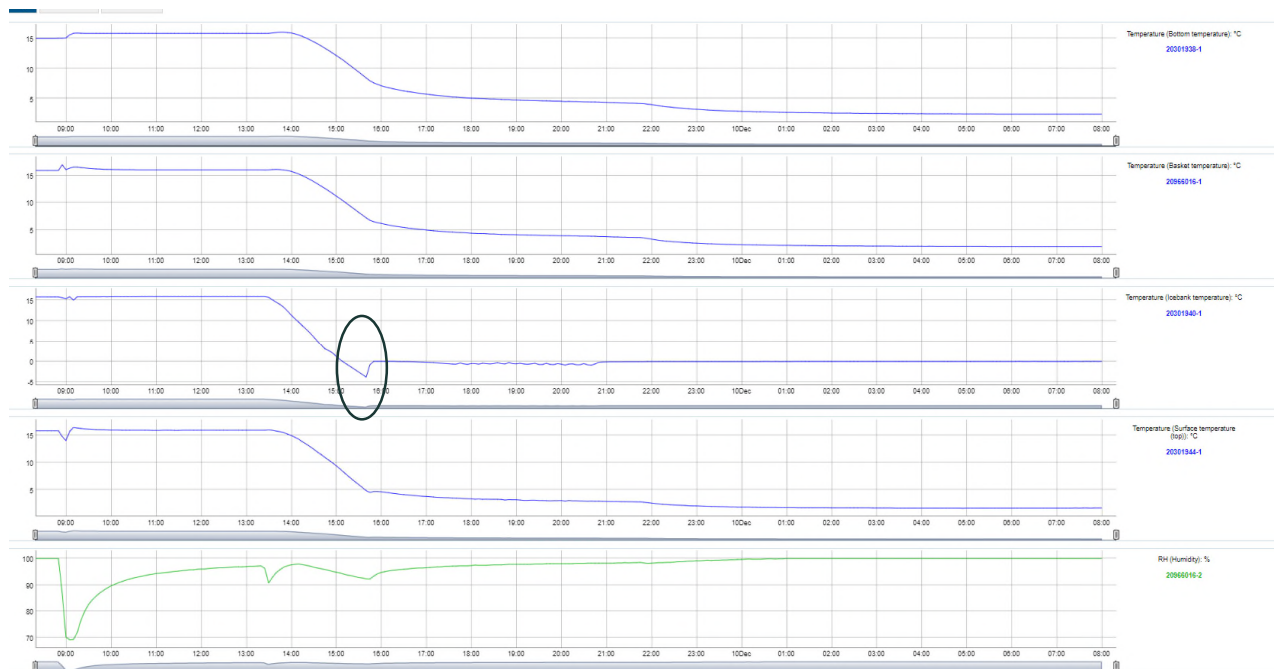


Figure 80 Subcooling of the ice bank.

**Summary:**

Literature study and tests have shown that the phenomenon of subcooling of water is difficult to fully understand but that additives may have a certain effect on the degree of subcooling. The test with hexanol in the ice bank was not successful for unknown reasons. It has to be tested in practice if the additives are stable and functional in production.

**Sources:**

- [https://www.researchgate.net/publication/244603680\\_Effects\\_of\\_Electric\\_and\\_Magnetic\\_Field\\_on\\_Freezing\\_and\\_Possible\\_Relevance\\_in\\_Freeze\\_Drying](https://www.researchgate.net/publication/244603680_Effects_of_Electric_and_Magnetic_Field_on_Freezing_and_Possible_Relevance_in_Freeze_Drying)
- <https://www.mdpi.com/2073-4352/7/10/299>
- <https://lifelife.stackexchange.com/questions/17653/how-to-freeze-water-more-quickly>

## 8.3 Appendix C: Humidity Control

Technical note IK 2021-06-07

Ivan Katić

Refrigeration and Heat Pump Technology, Danish Technological Institute

### **Dehumidification of solar direct drive (SDD) vaccine refrigerators.**

#### **Background and scope**

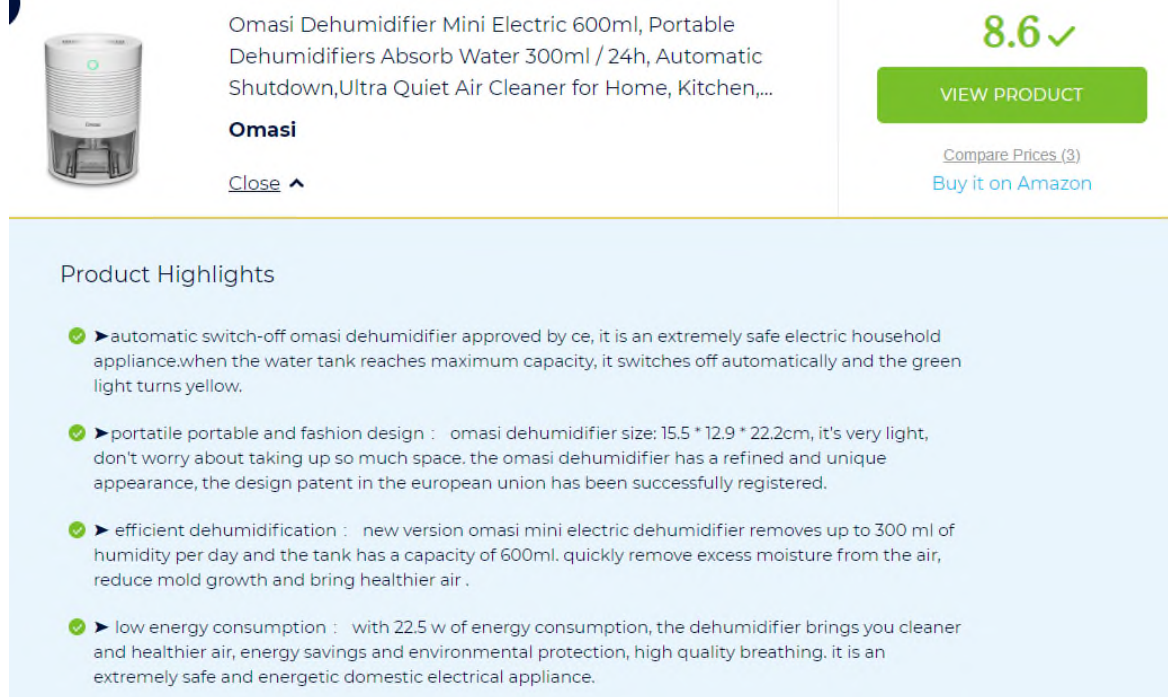
Solar direct drive refrigerators have been in the market for more than two decades and have generally proven as a reliable solution in areas without stable grid power supply. However, there is evidence from some health clinics that high internal levels of humidity can sometimes cause problems like mould growth and /or destruction of labels and vaccine packaging materials. WHO is constantly working to refine the qualification criteria and test methods for such refrigerators, lately with the draft protocol *WHO/PQS/E003/TPP05.1 Humidity Control for Vaccine Refrigerators*. DTI is part of a project aiming to improve the technical performance of SDD refrigerators, so it was suggested to investigate dehumidifier technologies within the project framework and compare results with the WHO draft requirements. The main findings of these investigations are reported in this document. The project "*2nd generation solar-powered vaccine coolers*" is supported by the Danish EUDP programme (Under Danish Energy Agency).

#### **Experiments with dehumidification of Vestfrost VLS 054 SDD**

As partner in the project Vestfrost have kindly delivered a VLS 054 SDD chest type vaccine refrigerator for the experiments. Apart from a special compressor it is the same model as sold to the health care sector globally. It would be a market advantage if the refrigerator could pass the set criteria for dehumidification, so this was set up for a test in a laboratory at DTI. Humidity can generally be removed from air if there is access to a surface with lower temperature than the dew point temperature. DTI has suggested that a simple way to implement humidity control would be by a small electric dehumidifier placed in the cabinet. Such devices are commercially available at low cost and are based on thermoelectric cooling. Such a dehumidifier was purchased to see if it could have two beneficial effects on the refrigerator's behaviour: Firstly, prevent high humidity which can cause condensation on surfaces, and secondly deliver some excess heat, which could force the compressor to run for a longer period and thus ensure that the ice bank freezes during all operating conditions. In some cases, under special circumstances, Vestfrost have experienced cut-off by the thermostat before the ice was frozen and this causes unwanted temperature excursions.

**Dehumidifier**

The dehumidifier of the brand Omasi was purchased from eBay. It is based on the Peltier principle and is powered by a 9V 2.5A DC external power supply. To make it turn on and off in sync with the available solar power, a relay was built in which connect when there is voltage from the solar PV supply. This required an intervention and bypass of the manufacturer's control system but was relatively easy to implement.



Omasi Dehumidifier Mini Electric 600ml, Portable Dehumidifiers Absorb Water 300ml / 24h, Automatic Shutdown,Ultra Quiet Air Cleaner for Home, Kitchen,...

**Omasi**

Close ^

8.6 ✓

VIEW PRODUCT

[Compare Prices \(3\)](#)

[Buy it on Amazon](#)

**Product Highlights**

- ▶ automatic switch-off omasi dehumidifier approved by ce, it is an extremely safe electric household appliance.when the water tank reaches maximum capacity, it switches off automatically and the green light turns yellow.
- ▶ portatile portable and fashion design : omasi dehumidifier size: 15.5 \* 12.9 \* 22.2cm, it's very light, don't worry about taking up so much space. the omasi dehumidifier has a refined and unique appearance, the design patent in the european union has been successfully registered.
- ▶ efficient dehumidification : new version omasi mini electric dehumidifier removes up to 300 ml of humidity per day and the tank has a capacity of 600ml. quickly remove excess moisture from the air, reduce mold growth and bring healthier air .
- ▶ low energy consumption : with 22.5 w of energy consumption, the dehumidifier brings you cleaner and healthier air, energy savings and environmental protection, high quality breathing. it is an extremely safe and energetic domestic electrical appliance.

Figure 81 Description of [Omasi Dehumidifier Mini Electric 600ml, Portable Dehumidifiers Absorb Water / | eBay](#)

The condensed moisture is collected in a small container / drawer under a cooling element. There is a fan at the top that removes excess heat and circulates air around the cooler.



Figure 82 Photo of the dehumidifier.



Figure 83 The dehumidifier was placed at the bottom of the cabinet under the storage basket.

### Initial test run

In the initial test the system was started from ambient temperature (15°C uncontrolled lab temperature) and ice was produced during the first days. A wet napkin was placed in the basket as a first experimental humidity load. After rising to 100% the relative humidity undergoes a day-night cycle and eventually decreases to a much lower level than the initial value of 80%. It should be mentioned that the RH of the room is not regulated, and the air was relatively dry due to winter conditions.

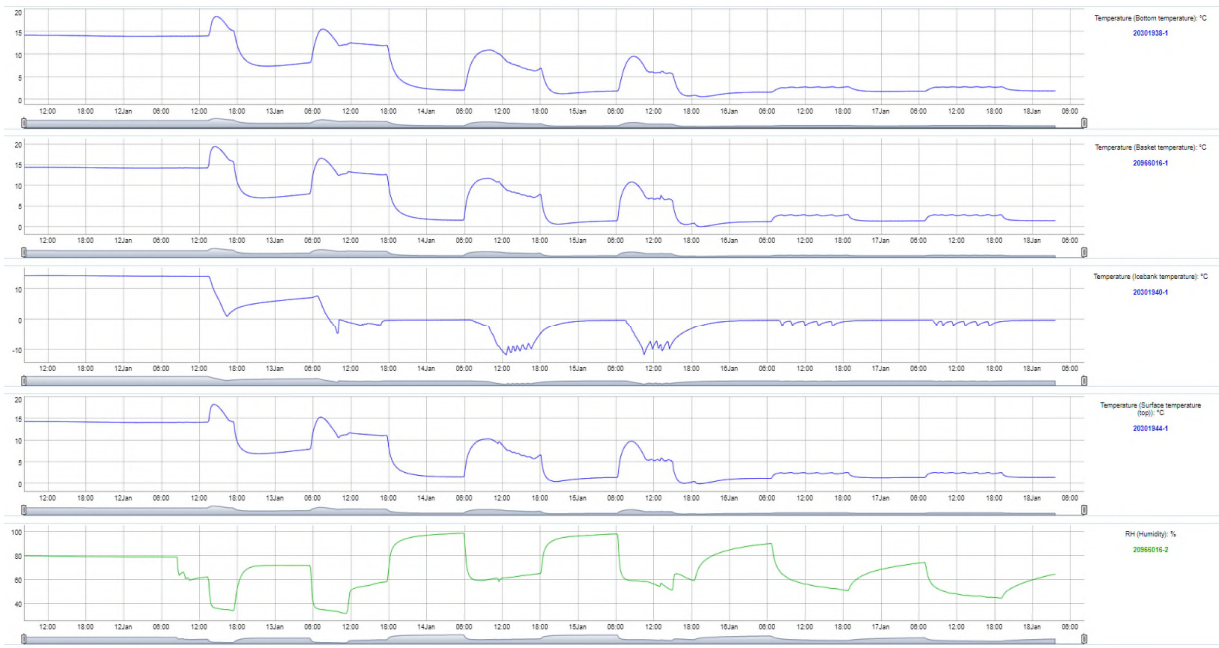


Figure 84 Temperature and humidity cycles (lower curve). There is a clear effect of the dehumidifier.

After some days, the humidity level drops significantly, so the test was deemed successful. However, the excess heat from the device causes temperature fluctuation of the cabinet. Therefore, the supply voltage was reduced from 16 January to limit the power uptake from nominal 22 W to about 10 W which is the level that was found appropriate at a previous thermostat control test. After this adjustment, the temperature becomes very stable, and the humidity is approximately 55% RH as daily average value. In field tests made by DTI in warm and humid conditions the compartment humidity is mostly found to be in the range of 90-100% RH. The higher RH during daytime (active compressor) is because cold air can contain less water vapour than the warmer air at night.

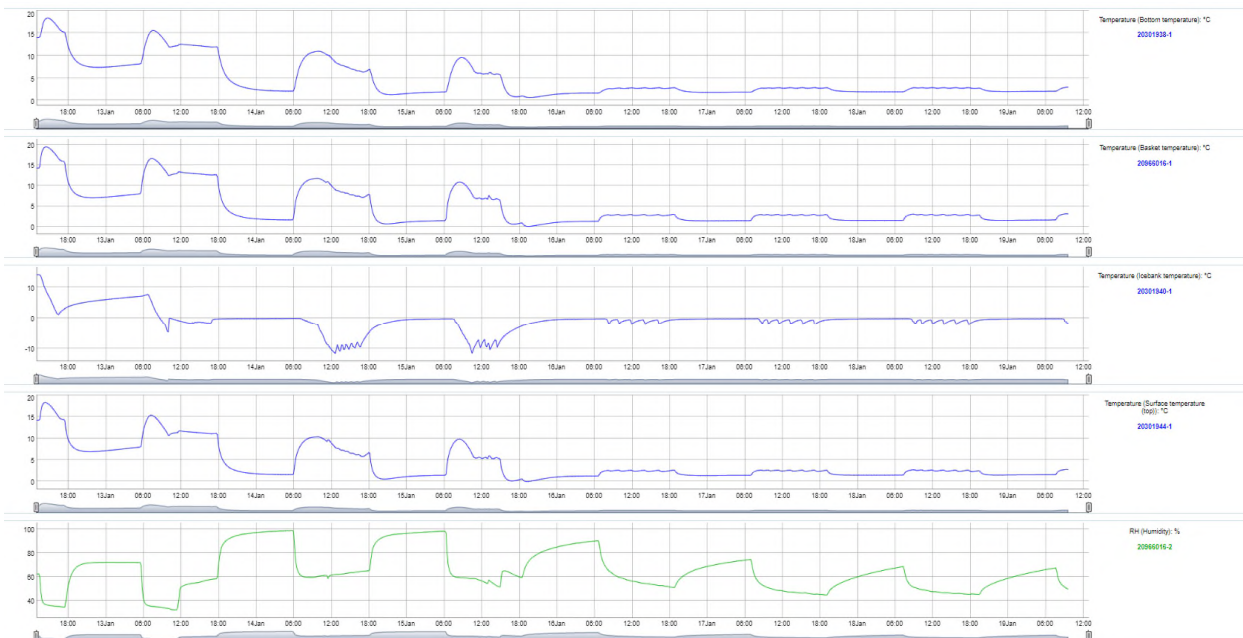


Figure 85 Gradually lower relative humidity. At the end of the test a very stable temperature is achieved. (Curve no 3).

**Test with open water surface**

The WHO draft test procedure prescribes a certain water volume with a specific area depending on the refrigerator size to be placed in the cabinet. An 18 cm diameter bowl of water was inserted to see how fast humidity can be removed. The open water surface area=  $9^2 \times 3.14 = 254 \text{ cm}^2$ .

19-01-2021 12:00 Start of experiment.

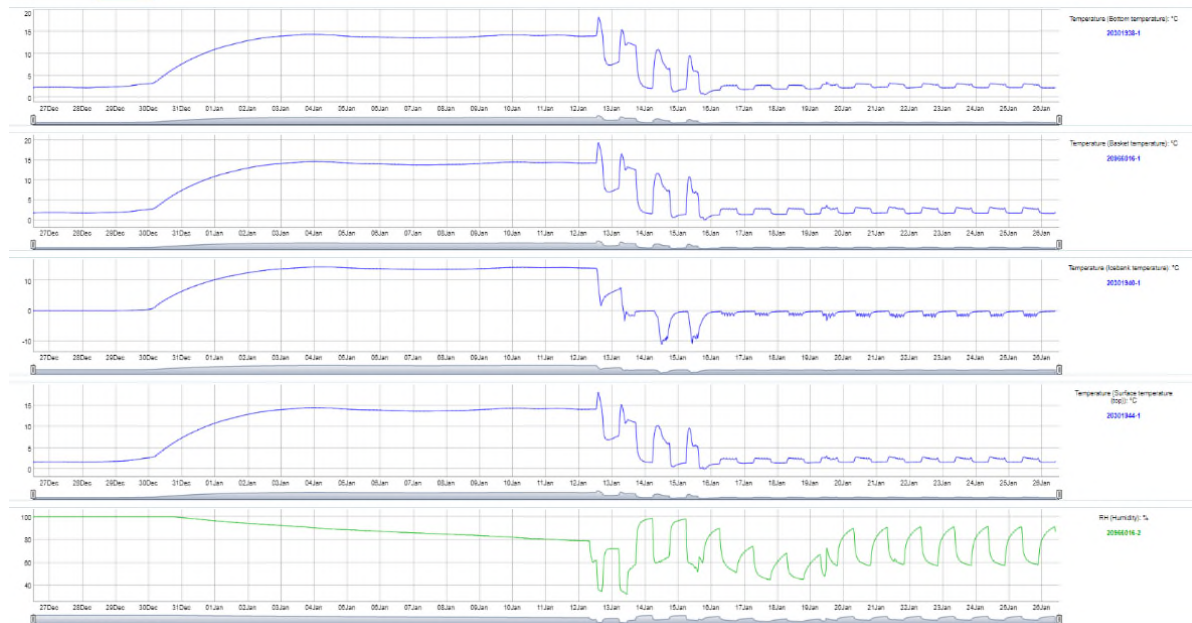


Figure 86 The RH oscillates between 60 and 90% while the water level sinks. RH is highest at night.

It was found that the daily oscillations are uniform if there is water left in the bowl.

**Modification**

In a field installation the dehumidifier should be driven directly by the PV panels, but since they have a typical voltage of 30-40V a converter must be inserted in the line. A very flexible DC-DC converter was found from a Danish supplier. The circuit was changed on 26-01-2021 so that the power goes directly from the PV simulator through a DC-DC step down converter and on to the dehumidifier. The low-cost converter can accept a wide voltage range and the output is adjustable. The output voltage was set to 5.5 V in the experiment.

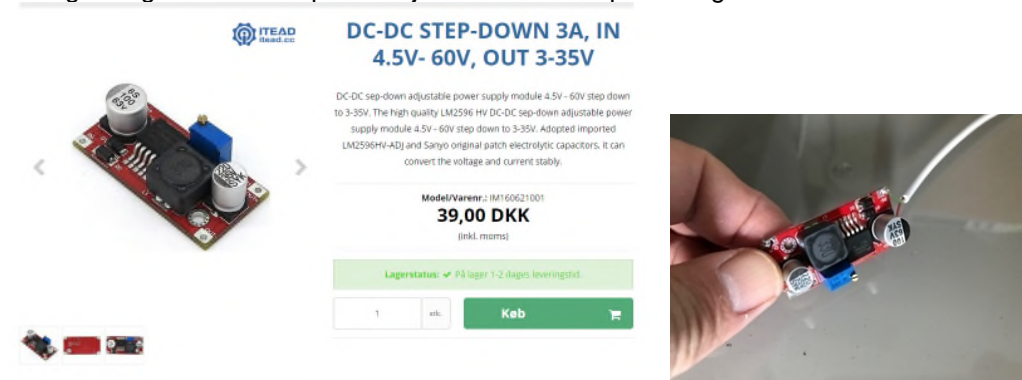


Figure 87 DC step down converter from Let-Elektronik.dk.

**Test in climate chamber at 43° C**

The purpose of the test was to see how much water the dehumidifier would remove during normal operation in a hot and humid climate. The device was placed in the climate chamber and running for a week. After some days the signal from the datalogger was lost, probably due to the closed room (Faraday's cage) and high humidity. The fridge was therefore moved to another position allowing the sensor cables to go through the wall and the data logger placed outside the room. This improved signal strength to normal level.





Figure 88 Mounting in climate chamber with high temperature and humidity.



Figure 89 Collected amount of water after one week and without additional humidity load (only some door openings).

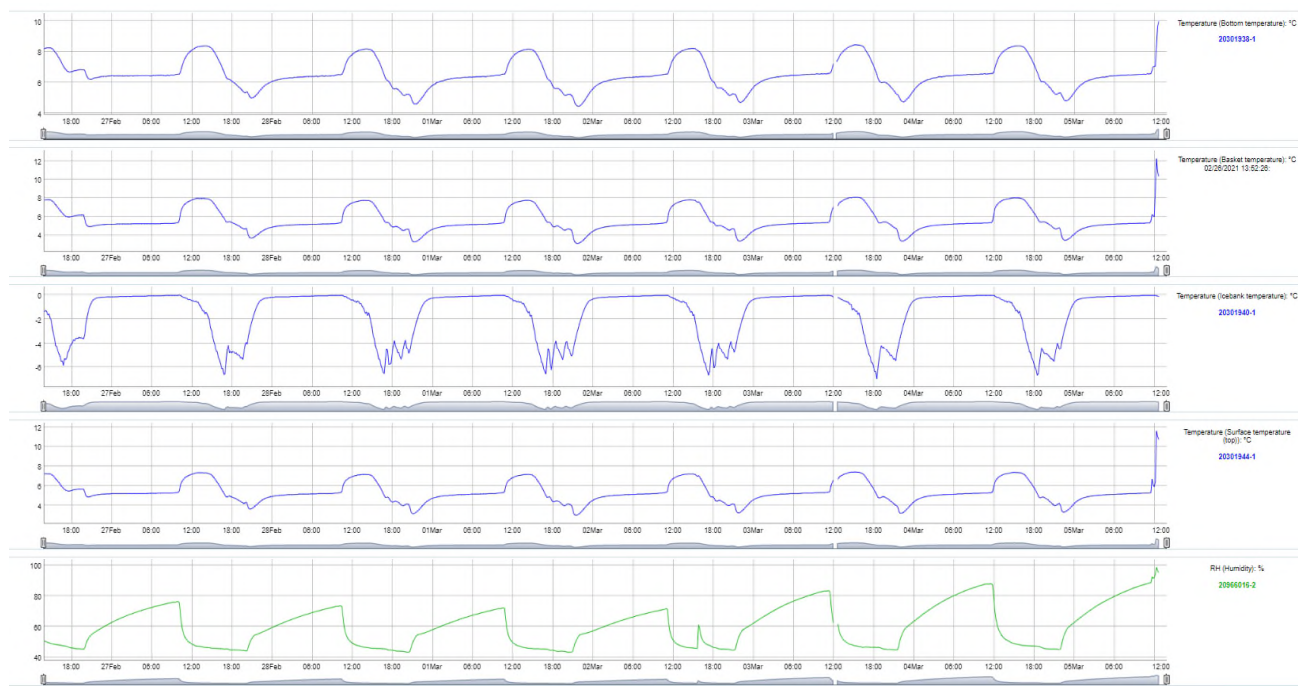


Figure 90 The humidity level rises due to door opening the last day.

From 5<sup>th</sup> of March the water has not been collected but drained through a plastic tube going from the dehumidifier to a drainage hole in the bottom of the cabinet.



Figure 91 Water collector modified with drain tube.



Figure 92 Drainage through bottom plug.

### Drying of a wet cardboard box

On 8<sup>th</sup> March 14:30 a water soaked cardboard box was placed in the basket to measure how fast it would dry out. This would be a more realistic way of using the fridge than filling it with open containers containing large amounts of water.

Measurement results:

- 8<sup>th</sup> March 14:30 Dry weight: 90.9 g. Soaked weight: 186.9 g
- 10 March 16:20 New weight 144.9 g
- 12 March 13:00 New weight 119.0 g
- 15 March 10:30 New weight 94.9 g

After almost complete drying the internal air humidity level drops to a much lower level than before:

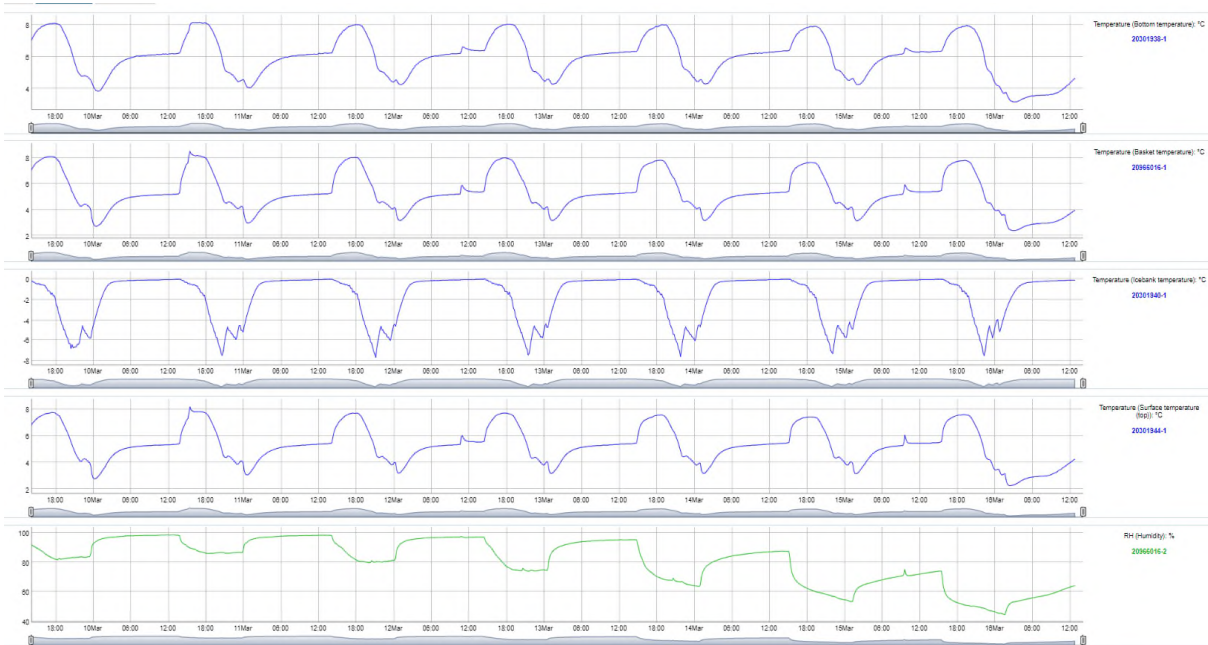


Figure 93 RH drops sharply after 4-5 days.



Figure 94 Soaked cardboard box on the scale.

**Reference test run**

Following the run with active dehumidifier a reference experiment was made with disconnected dehumidifier giving the following result:

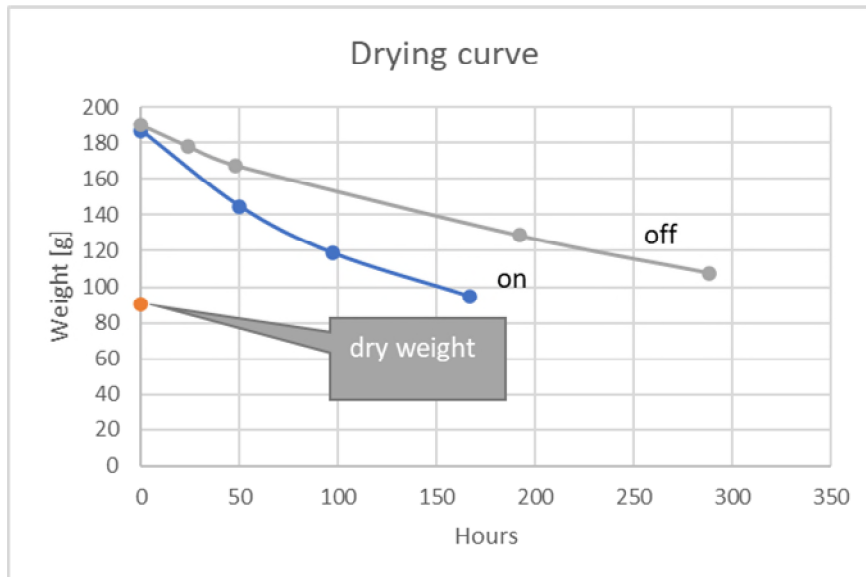


Figure 95 Drying time is almost halved when the dehumidifier is active. Furthermore, the RH of the chamber is generally lower.

**Assessment of WHO draft specifications for SDD vaccine refrigerators.**

In the draft specifications WHO/PQS/E003/TPP05.1 the following information is found:

**Acceptance criteria:**

If the following acceptance criteria are met, the vaccine refrigerator will be recognized as having humidity control.

1. Stabilized internal temperatures maintained between +2°C and +8°C in the vaccine storage compartment and below -3°C in the water-pack freezing compartment (if present).

**Dummy evaporative load:**

A dummy evaporative load will be used in place of the dummy vaccine load for the humidity control test. General test conditions of the dummy vaccine load will apply to the dummy evaporative load.

Prepare a dummy evaporative load using open-top glass containers.

- The internal height of the container shall be at least 2.0 cm.
- Measure the surface area of the container opening in cm<sup>2</sup> (length x width for rectangular dishes, diameter x diameter x 0.785 for circular dishes). If the container has drafted walls, measure the length, width, and/or diameter at a height of 0.5 cm below the top rim.
- Select the number of containers required to build a dummy evaporative load whose surface area in cm<sup>2</sup> is equal to the measured vaccine net storage capacity in liters multiplied by six, ± 10%.
- Estimate the volume required to fill all the dummy evaporative load containers to within 0.5 cm of their tops. Fill a separate water storage container with at least that much water.
- *Test dummy load container size and water depth must be confirmed in final version of verification protocol.*

These criteria could not be met in the simple test at DTI but compared to the situation without dehumidifier there is a strong and positive effect on relative humidity. It is questionable if it is necessary to be able to remove as much water as specified in the document. If the WHO draft test procedure is strictly followed it is necessary to evaporate a water column of at least 1.5 cm on a surface of 6 cm<sup>2</sup>/litre x net Volume(l). This within a 24-hour test period.

The cabinet is VLS 054 SDD with a net volume of 55.5 L

In our case A = 55.5 L x 6 = 333 cm<sup>2</sup> and water volume = 333 x 1.5 = 499.5 ccm (1/2 L)

This is a very high volume and according to the manufacturer, the Omasi dehumidifier can only remove up to 0.3 L/day when grid connected.

The test procedure may also be interpreted as having an equilibrium between the free water and a certain RH level below 65% but this would require a device that was also active at night and therefore impossible in a SDD appliance.

Humidity sources

Each time the cabinet is opened there is a risk that humid ambient air can enter and humidity condensate on surfaces. The maximum amount of water to be removed due to exchange of humid ambient air can be evaluated if we assume that the entire volume of cold air at 4°C and RH 55% is replaced by 43°C warm air with a RH of 65%. The difference in water content can be read from a Mollier diagram or calculated with EES Cool-Pack software:

Reading 1: 2.8 g water/kg dry air

Reading 2: 36.5 g water/kg dry air

Difference = 34 g water/kg dry air. The weight of the air is approximately 1.2 kg/m<sup>3</sup> x 0.108 m<sup>3</sup>(gross volume) = 0.13 kg. Thus, the water removal rate must be 0.13 x 34 = 4.4 g water per full air exchange. This is a factor 100 less than the test volume used in the WHO draft procedure. Unless free water is placed in the cabinet there seem to be no reason for such a high rate of dehumidification.

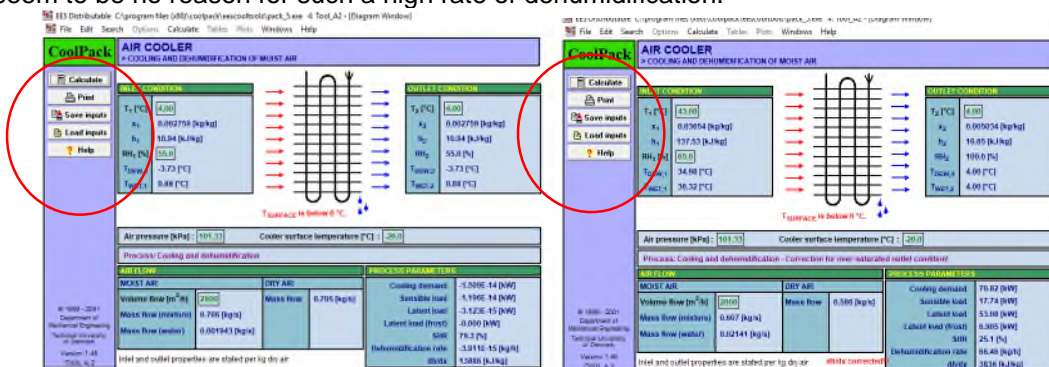


Figure 96 Coolpack calculator.

**Efficiency and power consumption**

The minimum energy required for condensation of water is equal to heat of evaporation = 2270 kJ/kg and for the entire water volume of 500 ml this becomes:

$$E = 0,5 \text{ kg} \times 2270\text{kJ/kg} = 1135 \text{ kJ} = 0.32 \text{ kWh}$$

Estimating a daily runtime of maximum 10 hours the cooling power should be 32 W and with Peltier technology the required electric power would be around 15W in best case (see following figure). This relatively high power input causes the temperature to fluctuate more than in the ideal case where it was found that a power dissipation of approximately 10 W gave a very good temperature regulation and also a safe freezing of the ice storage.

The following shows a typical efficiency curve for a Peltier cooler:

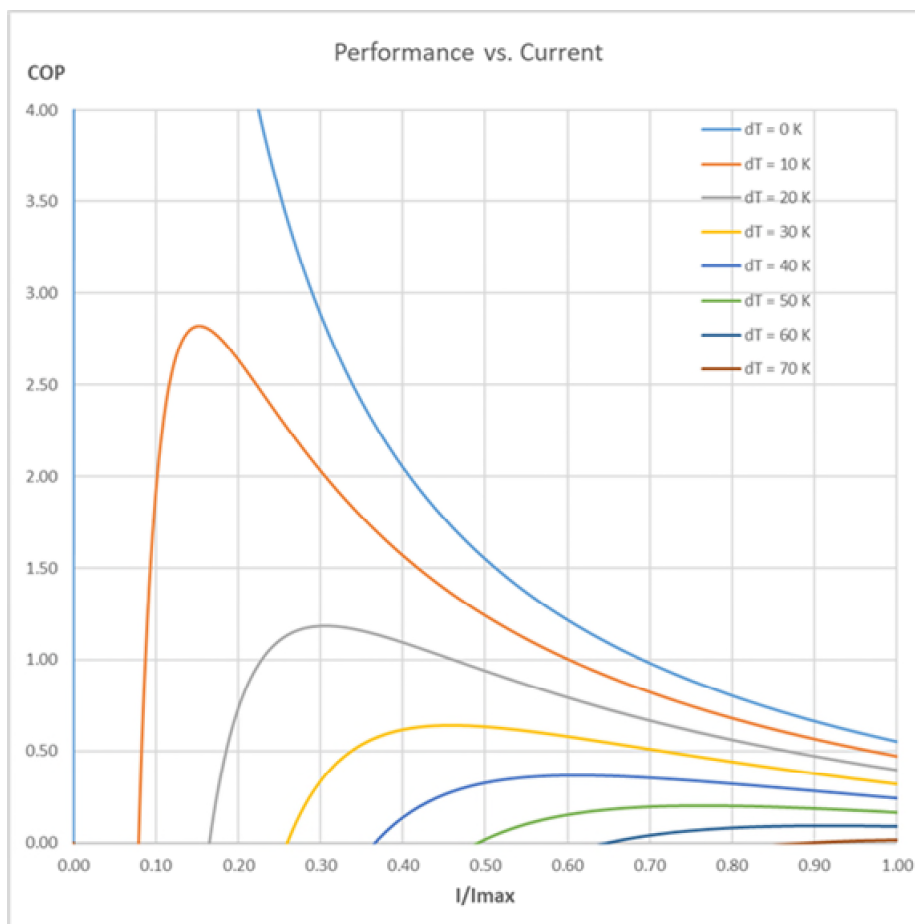


Figure 97 COP for Peltier cooling (example). Peltier Element Efficiency [3].

The example shows that the current should be limited to get the best COP. There is unfortunately no specific information available for the actual dehumidifier except power supply data:

Nominal voltage 9 V

Nominal current 2.5 A

The current uptake as a function of supply voltage was measured to:

Current[A]	1,02	1,25	1,6	1,82	1,99
Voltage[V]	4,23	5,01	6,03	6,85	7,51
Power[W]	4,31	6,26	9,64	12,46	14,94

The converter became relatively hot at high currents, so measurements stopped at 2A.

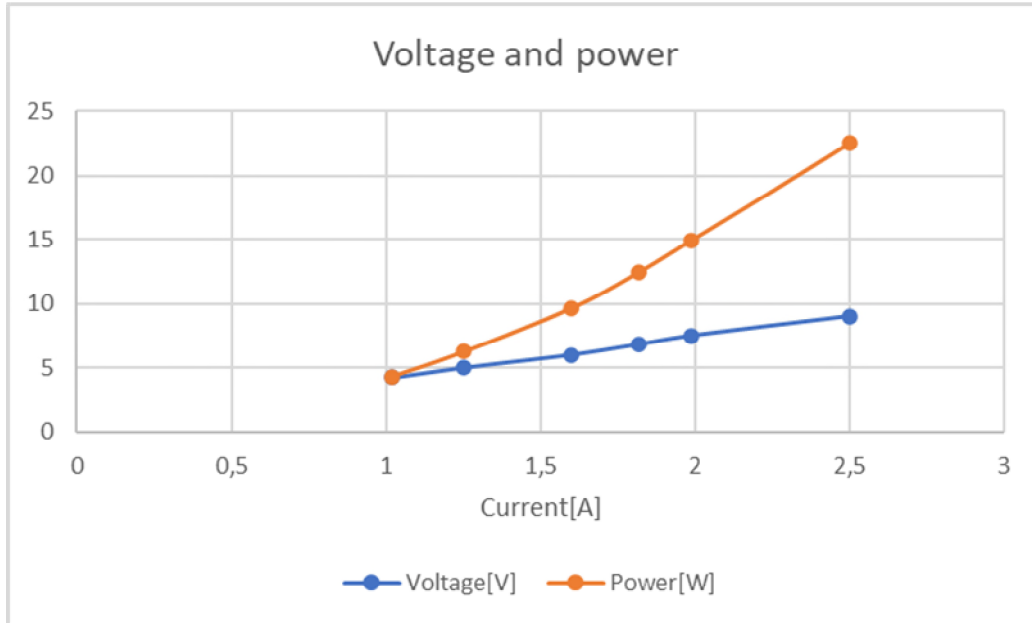


Figure 98 Measured electric parameters.

With water volume 0.3 l/day (Omasi specs) the minimum energy for condensation is  $0.3 \times 2270 / 3600 = 0.19$  kWh per day.

Nominal consumption =  $2.5A \times 9V \times 24 / 1000 = 0.54$  kWh

Thus, the nominal efficiency of the process is  $0.19 / 0.54 = 35\%$

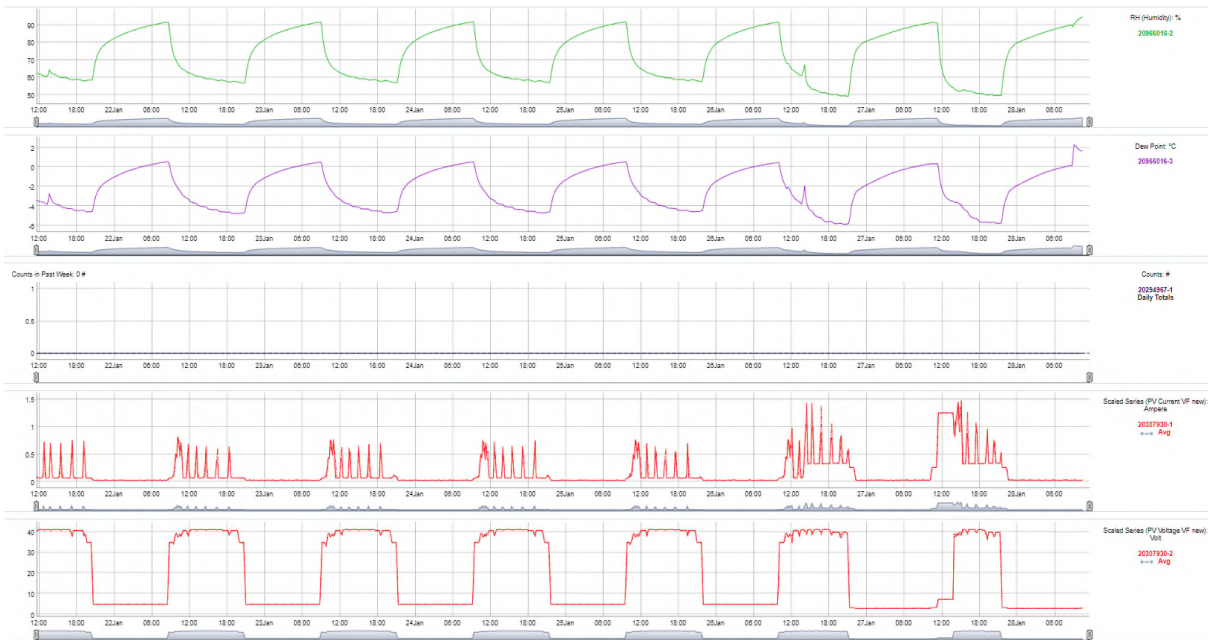


Figure 99 The current and runtime increases significantly on the last two days where the supply voltage to the dehumidifier was increased. There is also a dip of the RH during daytime.



**Proposed design.**

If the cabinet will be modified to have an integrated dehumidifier it should have a compact size and be mounted in a way that does not disturb normal use of the refrigerator.

The dehumidifier could for example be mounted over a drain hole or channel in the bottom corner of the cabinet so water drops can be extracted continuously. It should be possible to remove the unit for easy cleaning.

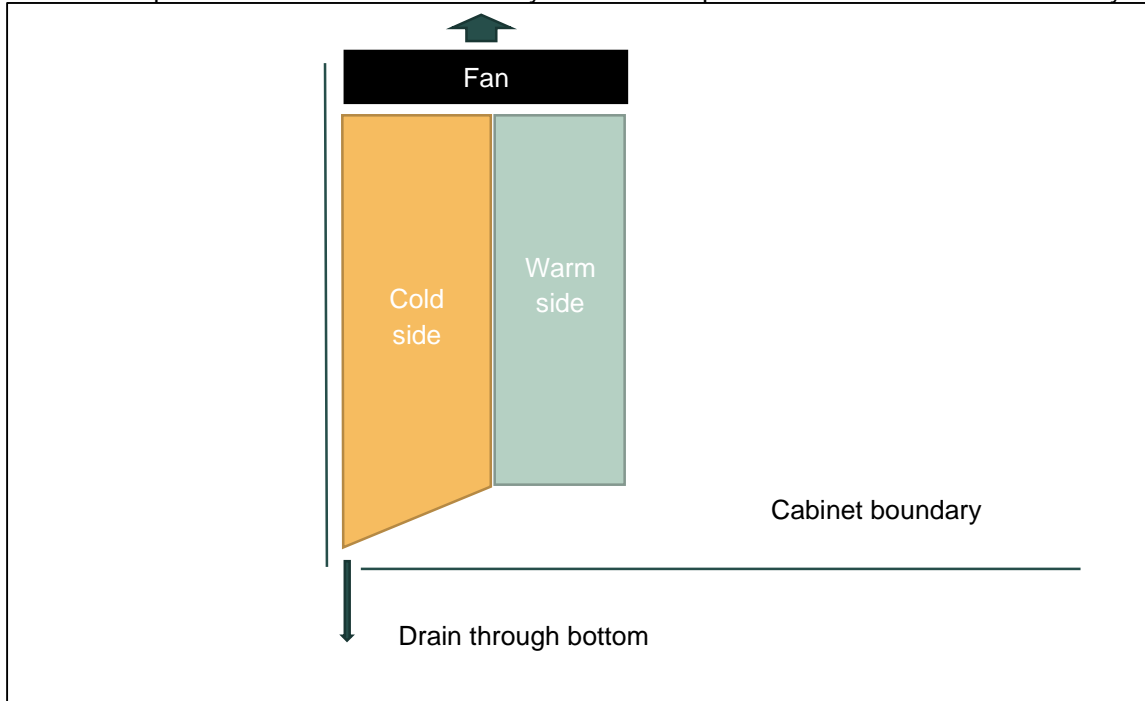


Figure 100 Design idea for integrated dryer. Alternatively, cooling and condensation could be provided by part of the evaporator coil of the refrigeration circuit.

**Optimum regulation**

The control of the dehumidifier must first of all deliver the right amount of heat to trigger the thermostat and ensure correct freezing of the ice while maintaining 2-8°C in the vaccine compartment. This function is needed if the ambient temperature is low (less than about 25°C) but can be kept inactive at high ambient temperatures where the compressor is running much more, and ice is generated every day without premature thermostat cut-out. It is suggested to control the runtime of the dehumidifier as a function of the internal temperature. When the temperature is close to 8°C the dehumidifier should not run because it generates excess heat and threaten to exceed the maximum temperature limit (a higher temperature also lowers the RH). Contrary it should run at full power when the temperature is approaching 2°C which indicates there is plenty of power available. The RH will then drop to a very low level due to active dehumidification so there is some buffer before a critically high RH is reached.

## Conclusion

The Peltier principle has been demonstrated to work well as a practical solution for temperature and humidity control at the same time. Since the power of a Peltier cooler can be regulated continuously, it is possible to find a voltage setting that suits a specific thermal balance. The dehumidification can be considered as a by-product. The water removal rate of the tested device is sufficient to keep content dry and to dry out wet packaging materials, but too low to pass the draft test criteria set by WHO. It is the author's impression that the humidity control draft PQS requirements are far too strict and will be difficult to implement in a cost-effective way. The proposed design and control strategy will assure a stable temperature and dry surfaces in the tested appliance and can likely be implemented at low cost.

It has been demonstrated that an alternative test method using a soaked cardboard box as humidity load works well and can be documented by simple means. It is suggested to modify the WHO draft criteria for humidity control to a less strict and more realistic level, for example:

RH should drop below 90% after 72 hours with a humidity load of xx grams of water soaked in a cardboard or fabric surface of area YY cm<sup>2</sup>. This should be enough to assure condensation free interior surfaces which is the main problem to be avoided. More work is needed to find appropriate and realistic levels.

## References

[1] WHO/PQS/E003/TPP05.1 Humidity Control for Vaccine Refrigerators

[2] Coolpack tool <https://www.jpu.dk/products/coolpack/>

[3] Peltier cooling: <https://www.meerstetter.ch/customer-center/compendium/71-peltier-element-efficiency>

## 8.4 Appendix D: Energy harvesting

### Experiments with charge controllers in parallel operation with a SDD refrigerator.

A simple test was carried out in the laboratory at DTI with the aim to observe how it would work if a SDD refrigerator was not only connected to a PV panel but also to a charge controller and a battery. The battery could provide electricity for light, phone charging etc. like in common solar home systems. The refrigerator should not be affected by the added components according to the WHO PQS test method for energy harvesting devices.

The setup:

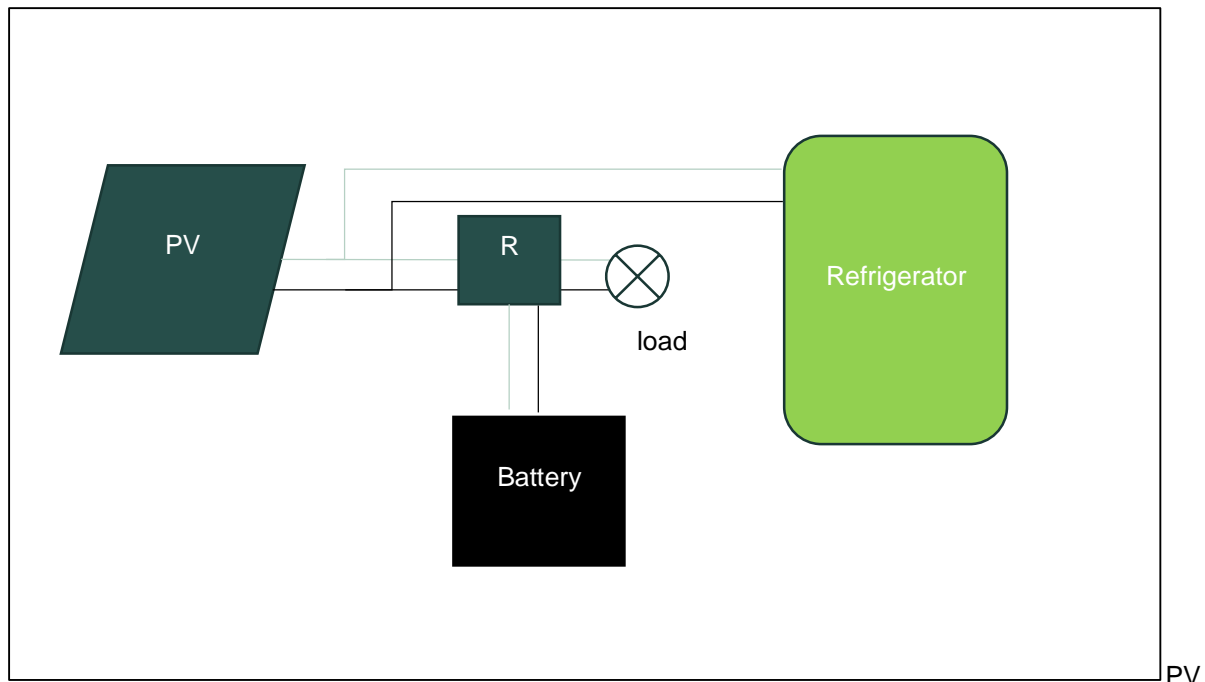


Figure 101 Test setup.

The charge controller R is a DC/DC converter with MPP function, and it is connected to the PV power cable and a 12 V battery. When the refrigerator calls for power it lowers the voltage of the PV module output and the current flow to the battery stops. It seems to work well, but it is not 100% clear if some potential power will be “stolen” from the refrigerator. It was checked that the compressor could start without any problems on a simulated 100 W PV panel both with the regulator mounted and removed.

In a second test with another type of charge controller the system failed. This controller is a shunt type regulator, which controls the battery charging by shorting the PV input and consequently also the fridge. It is evident that this type cannot be used because it stops the fridge whenever the battery is charged.

There is a third type of regulator, the simple series type, which disconnect the PV panel to stop battery charging. This type may also work, but it locks the PV operating voltage to the battery terminal voltage – usually 12-14 V - and may therefore reduce the PV panel power output compared with the optimum operating voltage.

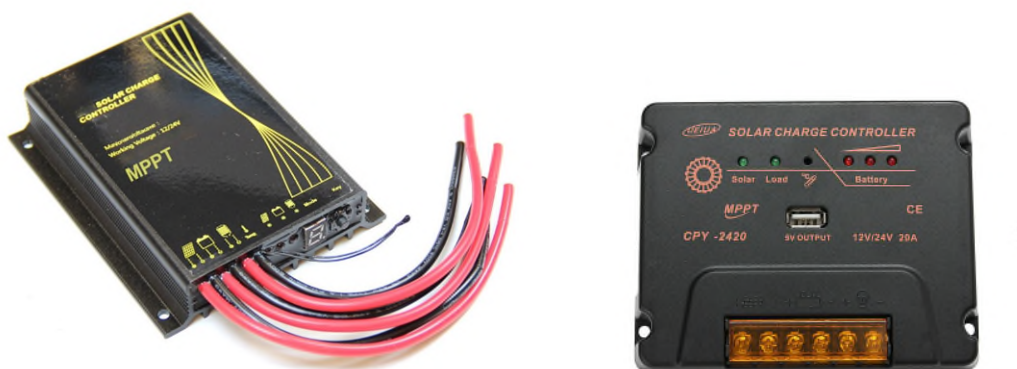


Figure 102 Examples of small PV MPPT charge controllers.

Some measurement results from the experiments are illustrated below:

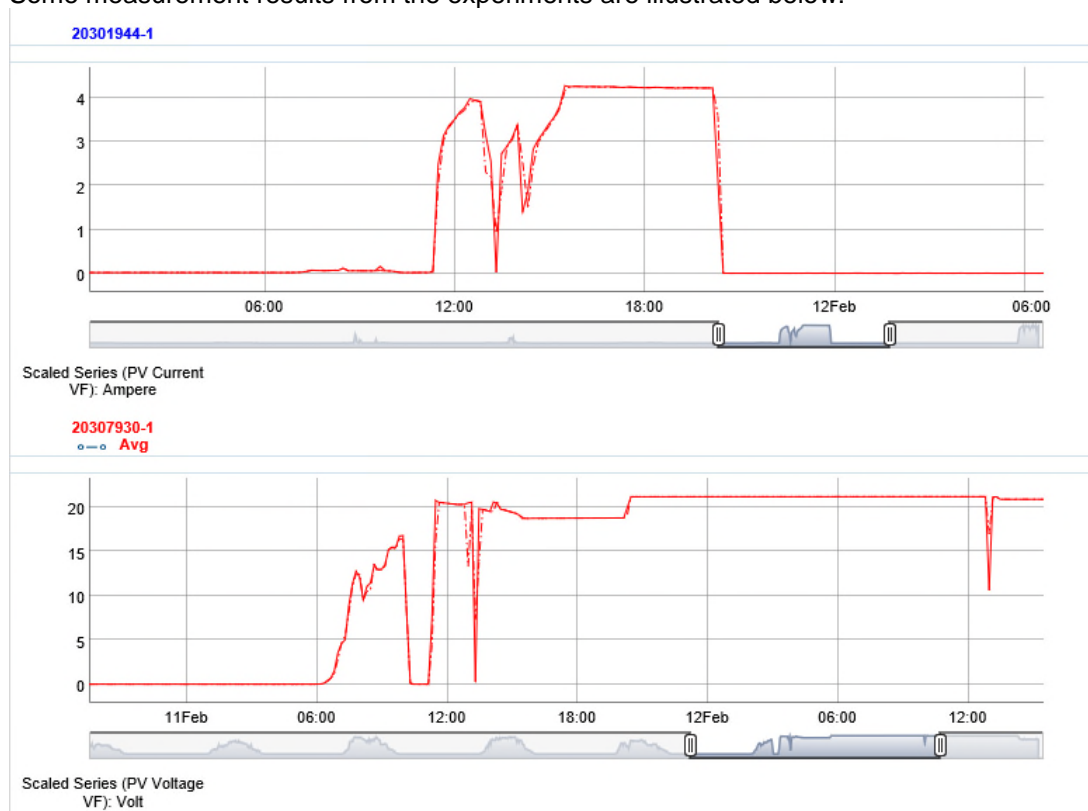


Figure 103 With 100 W potential PV output the compressor runs at full speed until thermostat cut-off. In this experiment there is no load on the battery.

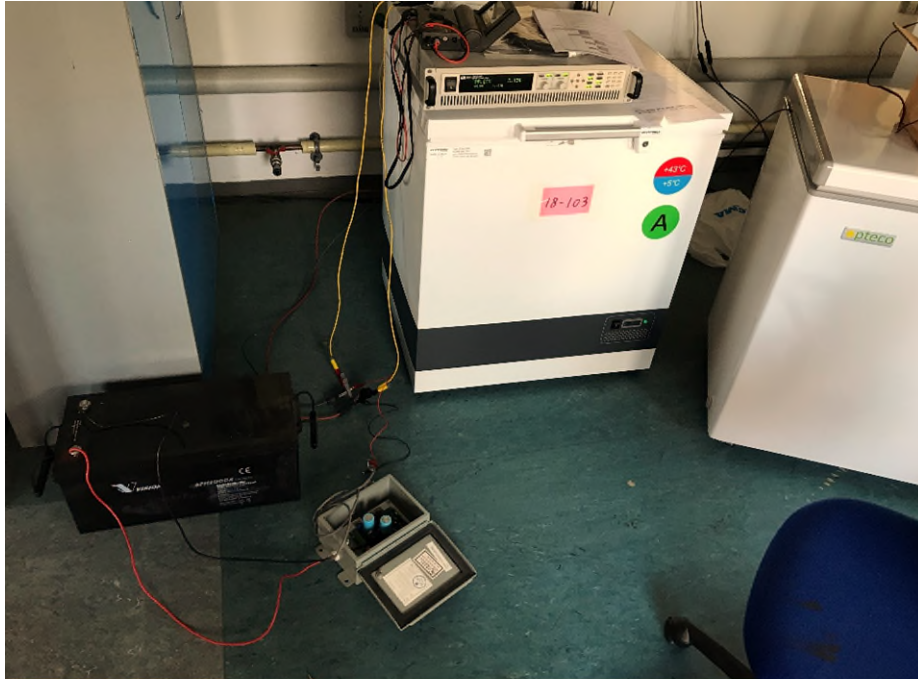


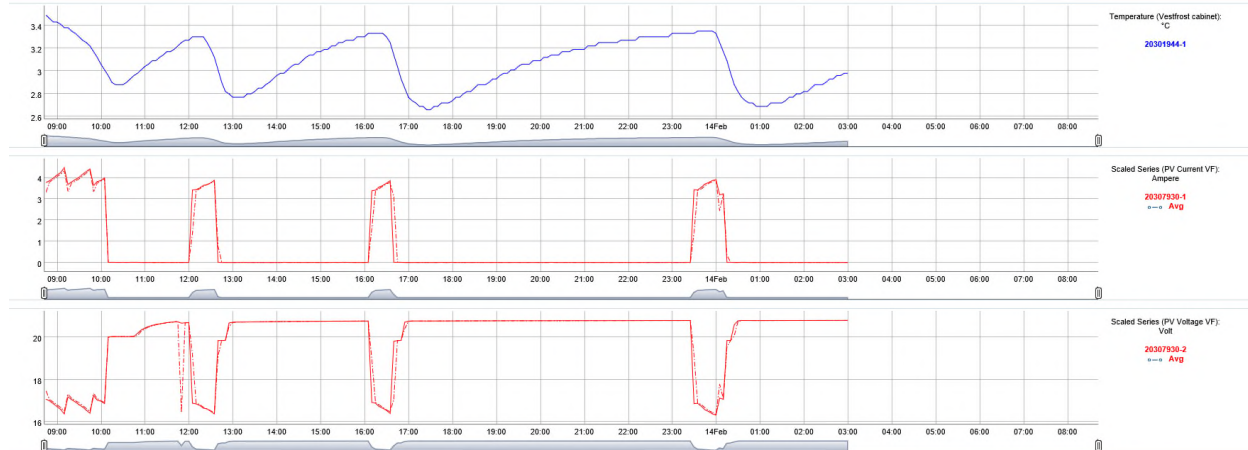
Figure 104 Charge regulator and battery connected. The PV simulator is seen on top of the refrigerator cabinet.

Later the PV output was reduced to 75Wp and a load of 10W (lamp) connected to the battery(controller). Even with this reduced power availability the compressor started, this time at low speed and ramping up:



Figure 105 Start and ramping up. Restarting three times because it can't reach full speed.

With 65W and MPPT charger on:



With 50W PV and MPPT charger on:

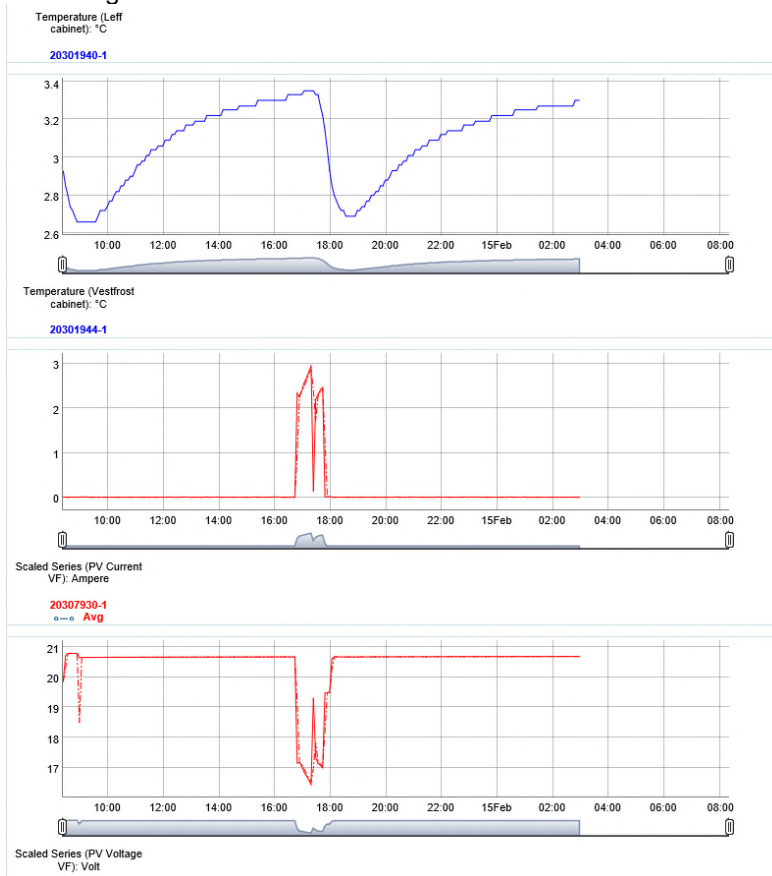


Figure 106 Start sequence and ramping up current with power limit 50 Wp. This was the lowest useful setting on the PV simulator.

**Summary:**

The experiments prove that with the right type of charge regulator a SDD appliance can operate in parallel with a battery system without any technical problems. It has to be tested if there are challenges if other voltages than 12 V (Lead acid) is used.

## 8.5 Appendix E: Paper: Direct Drive Solar Cooling

Manuscript ID: 1024  
DOI: 10.18462/iir.icr.2019.1024

### DIRECT DRIVE SOLAR COOLERS

Per Henrik Pedersen<sup>(a)</sup>, Ivan Katic<sup>(a)</sup>, Jonas Kjær Jensen<sup>(b)</sup>, Wiebke Brix Markussen<sup>(b)</sup>, Hendrik Moeller<sup>(c)</sup>, Claus Cording<sup>(d)</sup>

<sup>(a)</sup>Danish Technological Institute  
Gregersensvej 2, DK-2630 Taastrup, Denmark,  
prp@teknologisk.dk

<sup>(b)</sup>Technical University of Denmark, Department of Mechanical Engineering  
Nils Koppels Allé, Building 403,  
2800 Kgs. Lyngby, jkije@mek.dtu.dk

<sup>(c)</sup>Nidec Global Appliance Germany GmbH  
Mads-Clausen-Str. 7, 24939 Flensburg, Germany  
[hendrik.moeller@mail.nidec.com](mailto:hendrik.moeller@mail.nidec.com)

<sup>(d)</sup>Vestfrost Solutions  
Falkevej 12, DK-6705 Esbjerg Ø,  
CLC@vestfrostsolutions.com

#### ABSTRACT

For many years, photovoltaic power has been used in areas without grid electricity for vaccine refrigerators with a lead-acid battery to store electric energy and to provide the start current for the compressor. The problem with this technology is that the lifetime of the battery is short due to deep discharging of the battery during periods with low irradiance and high ambient temperature. The development of solar “direct drive” refrigerators started in 1999 at Danish Technological Institute (DTI).

It was demonstrated that the energy density of ice produced by a compressor is at the same magnitude as the lead-acid battery. As of to date (January 2019), 40 direct drive vaccine coolers from eight different manufacturers are listed on the WHO website, with the technology being one of the fastest growing technologies in the vaccine cold chain.

This paper describes the status and new development and discusses how the technology can be used for other purposes in the future. The paper also discuss how remote monitoring can help to prevent destruction of vaccines by early warning and automatic call for service.

**Keywords:** Photovoltaic, Direct drive, Vaccine coolers, Natural refrigerant, Isobutane, Remote monitoring.

#### INTRODUCTION

Health organizations have developed a cold chain system with health centres in regions without grid electricity, and correct storage of vaccines has been a challenge for them. Many vaccines must be kept at temperatures between +2 °C and +8 °C. Some deviations in the upper end can be allowed but freezing would immediately destroy the vaccines resulting in the loss of potency.

The vaccines used in immunization programmes are stored in a dedicated special vaccine cooler approved and prequalified by WHO and listed in the PQS. New and traditional vaccines used in country immunization programmes are expensive and often much more expensive than the refrigerators themselves in the long run.

Since the early 1980s, photovoltaic power has been used for such refrigerators with a lead-acid battery to store power and provide start and operating current to the compressor. The problems with this solution are the relatively high cost and the limited lifetime of the battery due to high ambient temperatures and deep discharging of the battery during periods with little sun as well as the lack of timely planning for the recurrent budget for the replacement of the batteries.

Therefore (and because of lower investment costs), gas and kerosene powered absorption refrigerators have been standard in the remote setting health facilities until recently. Absorption refrigerators need a constant fuel supply, and they are, therefore, expensive to run over its lifetime. Moreover, the temperature control is often poor, which results in expensive vaccines being destroyed. The above challenges formed the background for developing and testing solar “direct drive” refrigerators, where the energy is stored in ice instead of a battery and thereby eliminating the practical and financial difficulties with battery replacement.

The development of solar “direct drive” refrigeration started in 1999 at Danish Technological Institute (DTI). Here, a prototype was produced with funding from the Danish Energy Agency. A normal DC compressor (with high start current) was used and a big capacitor helped to start the compressor. It was demonstrated that the energy content in ice produced by this compressor was higher than the energy content in a lead-acid battery, in terms of both volume and weight. (Pedersen and Katic, 2016).

Contact was established to international organizations, and after a meeting in Frankfurt the “SolarChill Partnership” was established with UNICEF, WHO, UNEP, GIZ, PATH, Greenpeace International and DTI as partners. The goal was to develop and implement PV-powered vaccine refrigerators without batteries but using natural refrigerants. (Pedersen and Maté, 2007).

At the same time, a compressor manufacturer developed a DC-compressor for R600a and with “soft start”, which made it possible to wire the compressor directly to the PV-panels (DD – direct drive). In 2004, with additional field tests carried out in three countries (Indonesia, Senegal and Cuba), the results were so promising that the partners chose to continue the further development of the solar direct drive refrigerator to pre-qualify the product for WHO PQS standards for safe storage of vaccines. (Pedersen and Maté, 2010).

## CURRENT STATUS

This section describes the current status for vaccine coolers for health stations in rural areas in developing countries.

### Ice storage versus batteries

Relief organizations want to avoid lead batteries as the main source of energy to keep the vaccines cold during night-time and periods with little solar power. Previous experience has shown that additional costs are related to the batteries in that high ambient temperatures and frequent deep discharging result in a fast degradation and short life cycle of the batteries. This by itself is one key reason why the solar battery powered refrigerators have often been more expensive than kerosene or LPG-powered absorption refrigerators.

In the SolarChill project, ice bank “batteries” have been developed as an alternative source of energy storage. In (Pedersen and Katic, 2016) there is an analysis and comparison between the energy storage in a typical lead battery and in ice.

The conclusion is that the cooling energy capacity of ice storage is in the same order of magnitude as that of a traditional lead battery on volumetric and mass basis. The cooling energy capacity of ice storage is approx. 123 % higher (for the ice storage) on weight basis and approx. 21 % higher on volume basis.

Commercialization of long-life lithium based batteries with high energy density might change the role of battery storage in solar refrigeration. However, the ice storage in SolarChill is the simplest and most cost-efficient solution so far. A disadvantage when using ice storage is that the ice has to



be stored inside the insulation of the cabinet. Thus, the net volume inside the refrigerator will be smaller.

## Compressor for “Direct-Drive” (DD)

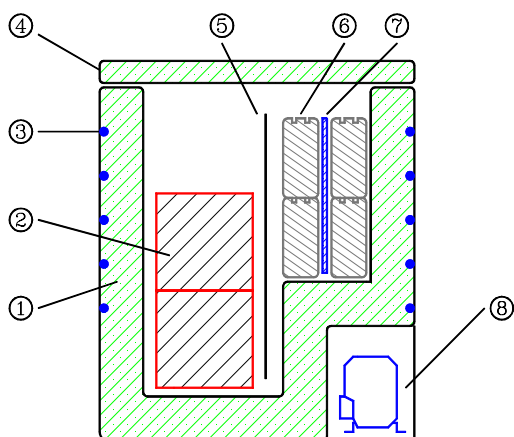
There are only very few PV direct drive compressors available on the market today. The most common model is the BD-35K. The compressor manufacturer also developed a new integrated electronic control for the compressor, which ensures that the photovoltaic panels can be connected directly to the compressor without external control. The electronic control also ensures a “soft start”, which is important when no battery is used.

The electronic control is equipped with an adaptive speed control (Adaptive Energy Optimizer – AEO). By using this control, the compressor will stepwise speed up from low speed to maximum speed in steps of approx. 12.5 RPM/min. If the photovoltaic panels cannot provide enough power, the compressor will stop and after a short while it will try to start again. The compressor will try to start every minute, and once the power from the panels is sufficient, the compressor will start at a lower speed. The first start in the morning is at approx. 2500 RPM. After a thermostat cut-out, the compressor will start up at the latest speed minus 400 RPM. The speed range is from 2000 to 3500 RPM.

The controller accepts a voltage between 10 and 45 V. The voltage from photovoltaic panels can vary, and a wide voltage range is an important and crucial feature for solar powered refrigerators and freezers. When using 12 V modules, the starting current of the compressor is less than 3 A; typically, there will be sufficient power a few hours after sunrise. The compressor runs continuously at about 3 A at lower speed. Using a standard compressor control, the start current would be much higher, which requires much bigger PV-panels or the use of a big capacitor to help start the compressor.

In the prototypes (chest and upright), the expansion device is a capillary tube with a heat exchange to the suction line. In the chest type cabinets, integrated skin condensers are used as in most chest freezers.

The evaporator in the vaccine chest refrigerator is a wire-on-tube-type placed in the ice storage as shown in figure 1a. The evaporator in the upright-type is a box-type roll bond-aluminium evaporator as known from old refrigerators with a small freezer compartment.



- 1 – Cabinet
- 2 – Vaccine compartment
- 3 – Skin condenser
- 4 – Lid
- 5 – Internal wall, insulated
- 6 – Ice storage (26 „ice packs“, 600 ml)
- 7 – Evaporator, wire on tube
- 8 – Compressor.

Figure 1a: Figure with basic principles for the first prototype vaccine cooler.

Figure 1b: Photo of a DD solar compressor. The integrated solar electronic control is placed on the left-hand side of the compressor.

## Field test experience and commercialization

DTI has been running an extensive field test program, where the performance of the first series of solar DD appliances was documented in terms of practical use in health clinics.

Pedersen and Maté (2007) explain how the field test of this vaccine cooler took place in Indonesia, Senegal and Cuba using 180 W photovoltaic panels (3\*60 W peak). Moreover, the tests show the hold-over time of about five days without any energy available. The field test lasted about one year and the ice banks were never completely melted, except when the connections to the PV-panels were disconnected intentionally. However, the vaccine temperature was not always within the preferable range of 2-8 °C in connection with this early prototype.

Vaccine specialists have developed new criteria for DD vaccine coolers. This work was done in cooperation with the partners of the SolarChill partnership and other technical experts.

The first generation of the WHO PQS (Performance Quality Safety) criteria for DD vaccine refrigerators was introduced in 2010, and the first test for WHO approval was conducted at DTI in 2010.

The WHO PQS prequalification is a condition in most tenders for the procurement of cold chain equipment for organizations that procure cold chain equipment used for storage of vaccines. This ensures the quality of vaccines stored in these products as safe for use in immunization programmes.

Currently there is a new field test going on with a selection of WHO approved DD vaccine coolers in a GEF (Global Environmental Facility) project.

## Two main types of DD vaccine refrigerators

The WHO website holds an increasing number of approved DD vaccine coolers. In January 2019, it contained 40 units from eight different manufacturers. 37 of the units use the natural refrigerant isobutane (R600a). Three of the units use a HFC-refrigerant (R134a).

Today, there are two main types of DD vaccine coolers on the market.

The first type is the ice-pack type, where the ice storage (and/or PCM-materials) is built into the walls of the cabinet or in a special compartment close to the evaporator. This type of DD vaccine cooler is often based on a chest type cabinet. Such types of cabinets are relatively cheap to manufacture, but precise temperature control may be a challenge.

This (or a very similar) technology is applied in 34 of the 40 DD vaccine coolers on the WHO list in January 2019.



Figure 2: Ice pack type of DD vaccine cooler.

The other main type of vaccine refrigerator is the tank type using a mixture of ice and water surrounding the vaccine chamber. Water has the highest density at about +4 °C and with a top-mounted ice storage. This ensures that water in the bottom of the tank and in thermal contact with the vaccine storage is about +4 °C, which is ideal for storage of vaccines, and it eliminates the risk of freezing.

The DD vaccine refrigerators using this technology ensure a very stable temperature and a long hold-over time, but they can be more expensive to manufacture if the special tank is manufactured in smaller quantities.

This technology is applied in six of the 40 DD vaccine coolers on the WHO list in January 2019.



Figure 3: Tank type DD vaccine cooler.

## FUTURE PERSPECTIVES

The existing refrigeration technology in solar direct drive vaccine coolers is about 17 years old. Therefore, a new R&D project has been started involving the Technical University of Denmark, a compressor manufacturer, a manufacturer of vaccine coolers and Danish Technological Institute, who is the project manager. The Danish Energy Agency is funding the project.

The project started in 2017 and the aim is to develop:

- Concept for a new compressor
- Concept for a new cabinet, new ice storage and remote monitoring.

The compressor is supposed to be more energy efficient compared to the present DD compressors. In addition to this, the variable speed compressor is supposed to have higher cooling capacity and a broader span in capacity. This will give possibilities to use this compressor for bigger cabinets and for new applications in addition to the present use of this type of compressor.

Furthermore, efforts are made to develop a more efficient control strategy (Jensen, Moeller, Katic, Pedersen and Markussen, 2019).

DTI hosted a meeting with the WHO PQS working group in November 2018. In a discussion about future generation of direct drive compressors for vaccine coolers it was the impression that the group wants to avoid dependence on batteries for energy storage – also in the future.

The future cabinet is supposed to have a longer “hold-over time”, which can be met by using bigger ice storage and/or better insulation. The future vaccine coolers are supposed to be remote monitored to ensure safe storage of vaccines and early warning if something goes wrong.

According to the WHO PQS working group, high relative humidity and even presence of water inside the vaccine compartment is a problem. In some coolers creation of mould has taken place. Thus, the next generation of vaccine coolers are supposed to solve this problem.

### Remote monitoring

Refrigerators used for vaccine storage need to be extremely robust and must be able to keep the temperature within the limits specified by WHO. A spoiled load of vaccine costs thousands of dollars, and manufacturers and users are therefore looking for methods to send early warnings in case of malfunction. In the past, monitoring had to be based on manual readings and download of data, but today IoT technologies are available from many providers of monitoring systems and are already used by some appliance manufacturers. DTI has investigated a range of systems using GSM mobile network for data transmission in connection with a large field test project (SolarChill) for solar direct drive refrigerators.

Ideally, the data acquisition system should have the following characteristics:

- Robust and reliable automatic data acquisition not relying on grid connection or internet
- Easy download of data, preferably automatic transmission
- Not too expensive and simple to install and operate.

In the SolarChill project, the following values are being monitored:

Table 1: List of data monitored by the advanced datalogger and the simple datalogger in the ongoing SolarChill project.

Advanced data logger	Basic data logger
Solar irradiance in plane of array	
Ambient temperature	Ambient temperature
Internal temperatures (4)	Internal temperatures (4)
Relative humidity	
Current	
Voltage	
Open/close events	

Both data loggers are uploading data with a user defined frequency to the manufacturer's server. The user can see and download data from a web portal, and alarms can be sent automatically by email.

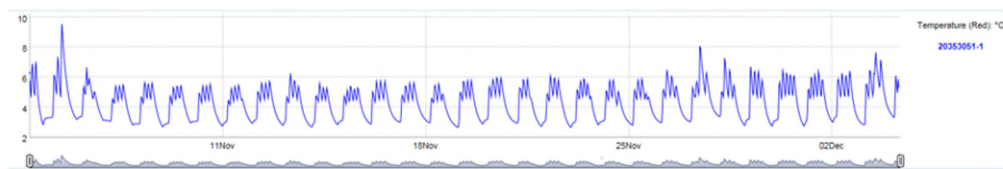
Because the project is about solar powered refrigeration in remote areas, there is no grid power nor regular internet connection available at the installation sites. Therefore, mobile network or satellite communication are the only options for daily long distance access to the measurement systems.

For short distance, there are several other wireless technologies available, they may be used for internal communication between sensors and a GSM base station, also called Remote Terminal Unit (RTU) or cellular gateway.

Type A



Type B



Type C

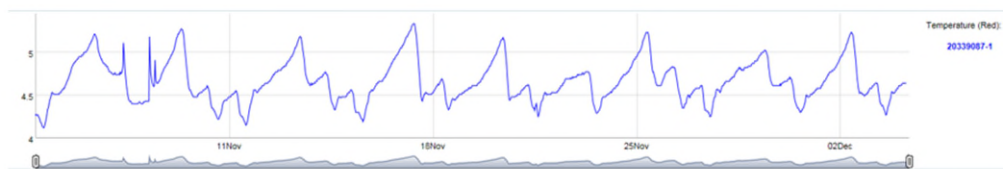


Figure 4: Example of field test data. Every type of refrigerator has its own temperature “fingerprint” that may be useful in preventive maintenance.

There are several remote monitoring systems in the market that can be used for temperature monitoring alone. These are either single channel devices (some disposable) or multichannel with replaceable battery power supply. For collection of other data, like solar irradiance and voltage, there are not as many options. These systems are mostly configured with a central GSM gateway or base station that can be connected with or without wire to a range of different sensors. The gateways usually have a considerably higher energy consumption than the integrated sensor systems and needs external power supply for long term operation (Option for PV panel). Some are always connected to the GSM network for near-realtime monitoring, others are only calling and updating hourly or daily.

Internal power supply of the DAQ system may be provided by either:

- Drycell batteries (single use)
- Rechargeable batteries (To be occasionally charged from grid or a vehicle)
- PV power from the systems under measurement (Parasitic power)
- Separate PV supply.

The software for cloud based data collection and monitoring is mostly offered as a subscription service per month or per year for each connected device. It could therefore add up to a considerable amount. Most software is proprietary and can only be used with the company's own data loggers. There is also software paid with a onetime license per user/PC and this could be a cheaper solution in the long term.

### **Vaccine coolers - future perspectives**

Since the first solar DD refrigerator project in 1999, the cost of PV modules have dropped from about 4 USD/W to 0.4 USD/W or a factor of 10. In the same period, the unit size of a typical panel has increased from less than 100 W to about 300 W nominal power. This means that the same SolarChill refrigerator can now be run with a single PV panel instead of 2-3 panels, translating to simpler mechanical support and circuitry with the invention of plug and play MC connectors. In comparative terms, the retail cost of a single panel of 150 W, which provides enough energy for these products in most tropical climates, would typically be 500 USD, which is about the same cost as a set of high quality batteries. With even cheaper PV modules foreseeable in the future, new refrigerators will not have to focus that much on energy efficiency, but rather on the overall system costs and performance.

The interaction between the PV panel and the compressor can be further improved. Instead of the current "trial and error" method for adjustment of the compressor speed, it would be better if a maximum power point tracker could continuously adjust the compressor speed.

### **Other applications - DD coolers for food and drinks**

Besides the need for vaccine storage refrigerators, there is a huge need for cooling of food and drinks in regions without a grid. There are only few battery-free coolers available on the market so far, and it is difficult to bring the costs down to a level that is comparable with the conventional household appliances. The power demand for such appliances is much higher than for vaccine refrigerators, and the current DD compressors are not always sufficient. It would be interesting if new and bigger devices could be developed for this market. As an alternative solution, the current models may be used in parallel-configuration.

On an even larger scale, there is a growing interest to use the solar DD technology for commercial cooling demands such as milk cooling, ice production for the fishing industry, cold stores etc. For such applications, it might be better to include a (small) battery bank, so that the PV power can be used for light and other secondary power needs as well.

## **CONCLUSIONS**

The SolarChill field test has shown that DD solar cooling is indeed a robust and reliable technology that is particularly suited for cooling in the most remote areas of the world where there are no access to electricity. The uptake of this concept by more and more manufacturers confirms that the idea of directly driven cooling is viable within the medical healthcare market, where reliability is essential. The WHO PQS web-site contains 40 different products of DD vaccine coolers, whereof 36 products are using natural refrigerant (R600a).

For other markets there are still some way to go, mainly because there are only very few DD compressors available, and they are too small for many generic cooling applications.

The future of the DD technology depends on the will of the manufacturer to develop cost-effective and more powerful compressors as well as further optimization of the electronic controller. If they succeed in this, a new range of applications in the commercial and household sector could open up.

## **ACKNOWLEDGEMENTS**

The authors would like to thank the partners of the SolarChill Partnership.

The authors would also like to thank the Danish Energy Agency for financial support to develop this new technology.

## REFERENCES

Pedersen P. H., Katic I. Direct Drive Solar Coolers, 12th IIR International Gustav Lorentzen natural working Fluids Conference, Edinburgh, 2016.

SolarChill Partnership: [www.solarchill.org](http://www.solarchill.org).

WHO PQS website: [http://apps.who.int/immunization\\_standards/vaccine\\_quality/pqs\\_catalogue/categorypage.aspx?id\\_cat=17](http://apps.who.int/immunization_standards/vaccine_quality/pqs_catalogue/categorypage.aspx?id_cat=17)

Pedersen P. H. , Maté J. “SolarChill Vaccine Cooler and Refrigerator: A Breakthrough Technology”, Industria Informatione, special international issue on refrigeration and air conditioning, UNEP, ATF and Centro Studi Galileo, 2007.

Pedersen P.H., Maté J. SolarChill technology, Solar powered direct drive refrigerators with hydrocarbon refrigerants. 9<sup>th</sup> IIR Gustav Lorentzen Natural Working Fluids Conference, Sydney, 2010.

Jensen, J.K., Moeller H., Katic I., Pedersen P.H., Markussen W.B. Comparison of compressor control strategies for solar direct drive refrigerators. The 25<sup>th</sup> IIR International Congress of refrigeration, August 2019, Montreal, Canada.

## 8.6 Appendix F: Paper: Comparison of compressor control strategies for solar DD refrigerators

Manuscript ID: 1086

DOI: 10.18462/iir.icr.2019.1086

### Comparison of compressor control strategies for solar direct drive refrigerators

**Jonas K. JENSEN<sup>(a)</sup>, Hendrik MOELLER<sup>(c)</sup>, Ivan KATIC<sup>(b)</sup>,  
Per Henrik PEDERSEN<sup>(b)</sup>, Wiebke B. MARKUSSEN<sup>(b)</sup>**

<sup>(a)</sup> Department of Mechanical Engineering, Technical University of Denmark  
Kgs Lyngby, 2800

<sup>(b)</sup> Danish Technological Institute,  
Gregersensvej 2, DK-2630 Taastrup

<sup>(c)</sup> Nidec Global Appliance Germany GmbH,  
Flensburg, 24939, Germany, europe@mail.nidec.com

#### ABSTRACT

The influence of the applied compressor control strategy on the performance of a solar direct drive refrigeration system was investigated using numerical modelling and simulations. Two compressor types and three compressor control strategies were investigated. Further, four configurations were included: a 360 W and a 180 W PV panel both with and without compressor start power delivered from the PV panel. Results showed that both the choice of compressor and the applied control strategy affected the systems ability to utilize the available power from the PV panel, especially under lower irradiance conditions and when the PV panel was downsized. However, results show that if the need for compressor start power delivered by the PV panel was alleviated the size of the PV panel can be halved without significant reductions in performance.

Keywords: Solar Direct Drive, PV Panel, Control Strategy, Compressor Speed Control, Ice Bank Storage.

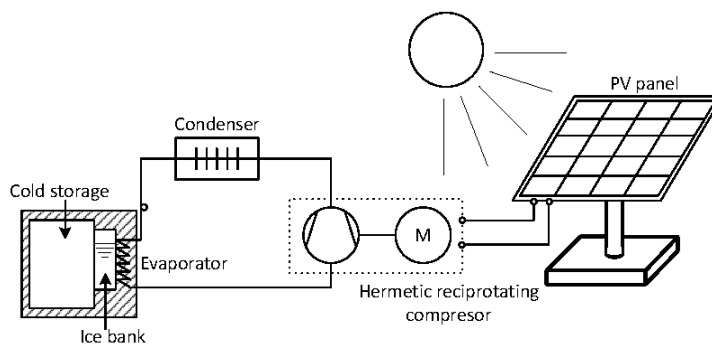
#### INTRODUCTION

People in rural areas of many developing countries have non or unreliable access to electricity (IEA, 2012). In such areas correct storage of temperature sensitive products such as food or more importantly medical equipment such vaccines is a significant challenge. This may affect as many as 1.3 billion people worldwide (IEA, 2012), wherefore finding good solutions for off-grid refrigerators is an important task.

Different types of absorption refrigeration systems driven by combustibles such as kerosene or gas have been developed but have been found to be unreliable and require high maintenance (McCarney et al., 2013). Alternatively solar driven systems have been developed since the 1980s first utilizing batteries to store electricity to power the system during night time. Later battery free systems or solar direct drive system have been developed as presented by Pedersen et al. (2019). McCarney et al. (2013) state that battery free solar direct drive systems are the most promising solution for off-grid vaccine storage.

Myers et al. (2017) investigate the potential for harvesting excess energy from solar direct drive refrigerators applied as medical cold chain equipment and found that significant amounts of energy could be utilized to power secondary equipment without compromising the temperature of the stored





goods. This is investigated with a traditional on/off compressor control. The potential to harvest ex-

cess energy may though be reduced if more advanced compressor control strategies are applied. The present work focused on analysing the operation of a direct drive solar powered refrigeration system with an ice bank storage under different compressor control strategies. A principle sketch of such a system may be seen in Fig. 1. As seen the refrigeration system consists of a hermetic reciprocating compressor, a finned tube condenser, a capillary tube and an evaporator placed in direct contact with an ice bank storage.

## METHODS

In a configuration such as the one seen in Fig. 1 it is the control of the compressor speed that will ensure optimal utilization of the available power from the PV panel. Here it is important to realize that the operation of a PV panel is characterized by the voltage - current curves seen in Fig. 2 (right). Here the solid black lines represent the voltage - current relation for a given solar irradiance. As seen for a given solar irradiance the current first shows a small decrease with increased voltage up to, in this case 25 V, where after it will experience a rapid decrease to a current of 0 A. Further, the greater the solar irradiance the higher the current will be for the same voltage.

Realizing that the power extracted from the PV panel is the product of the voltage and current results in the dashed blue lines. These naturally assume values of 0 W when either the voltage or current are 0. Further, it may be seen that for each solar irradiance there is a peak power point and that this point occurs at approximately the same voltage. Finally, it is seen that the higher the solar irradiance the higher the peak power.

If the system driven by the PV panel, in this case the compressor, tries to draw more power from the panel than the peak power at the given irradiance, the PV panel will experience what is called a collapse. A collapse results in no power being delivered and consequently that the system is turned off. If the compressor is run too fast there is thus a risk that it will collapse the PV panel and force a shut down of the system. However, if the compressor is run too slow, the refrigeration system will not be utilizing as much of the available power.

Therefore, it is relevant to find compressor control strategies that can ensure that the system will operate as close to the peak power point as possible at the varying solar irradiance the system will experience during a day or a year. In the present work it was assumed that the PV panel was south facing and located on the northern hemisphere somewhere close to the equator. On a location such as this the duration of which sunlight will reach the PV panel is roughly 8 hours per day with the peak irradiance in the middle of this period and a symmetrical increase and decrease around the peak.

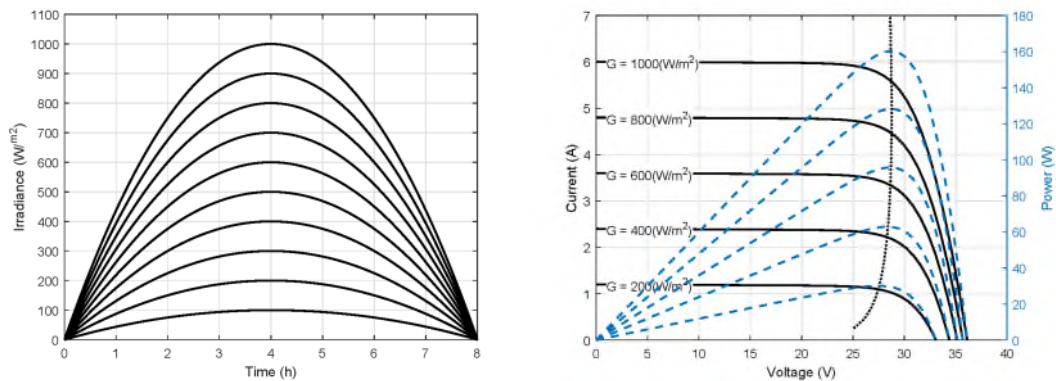


Figure 2: Daily solar profile and principle sketch of the operating characteristics of a PV panel.

A sketch of the daily solar profile may be seen in Fig. 2 (left). As seen here the profile is sketched for peak irradiances from 100  $\text{Wm}^{-1}$  to 1000  $\text{Wm}^{-1}$ . These peak irradiance variations may resemble both seasonal variation but also cloud covers of different intensity. The present work will be limited to the smooth profiles seen in Fig. 2 and will thus not include spotted cloud covers and the rapid transients involved in these. The different compressors and compressor control strategies will be evaluated at the different range of solar profiles seen in Fig. 2. This, as it was relevant to investigate both the minimum peak irradiance needed for the system to deliver a cooling load but also the peak irradiance at which the available power from the solar panel cannot be fully utilized due to speed restriction of the compressor.

To perform this investigation numerical models were developed for both the PV panel and the refrigeration system. Further, the different control strategies were implemented in these models.

### Photovoltaic Modelling

The behavior of the PV-panel was modelled using a "one diode" model as described in Duffie and Beckmann (2013). The one diode model uses an equivalent circuit to describe the operation of a single solar cell. Assuming all cells to operate identically the one diode cell model can be used to model a complete PV panel.

The values for the shunt and series resistances as well as the diode quality factor were determined based on standard test conditions (STC) data for a given 60 cell PV panel. The STC data may be seen in Table 1 where the assumed cell operating temperature is also stated.

As seen in Table 1 each PV panel has a STC max power output of 90 W. In order to supply sufficient power to the refrigeration systems several PV panels in parallel were applied. The present work investigated the application of both 2 and 4 PV panels in parallel, these two solutions will in the following be referred to as the 180 W and 360 W PV panels, respectively, in reference to the resulting STC maximum power output of the total installation. It should be noted that the actual maximum power of the PV panels, may be reduced as the assumed cell operating temperature of 35 °C was higher than the STC cell operating temperature.

### Refrigeration System and Compressor

The modelled refrigeration system may be seen in Fig 1. Assuming a constant ambient temperature in the room where the refrigeration system was located and that the ice bank storage was kept at a constant temperature of 0 °C, it was assumed that the evaporation and condensation temperatures as well as the level of super-heating and sub-cooling would not change significantly during the operation of the system. Therefore, these values were assumed constant at the values stated in Table 1.

**Table 4. Input data for the PV panel model of a single 60 cell array, operating conditions for the refrigeration system and data for the investigated compressors**

PV panel			Refrigeration system			Compressor			
Number of cells	60	-	$T_{evap}$	-10	°C		BD35K	BDS5.0K	
Temp. Coeff.	0.03	K <sup>-1</sup>	$T_{cond}$	50	°C	Disp. Vol.	3	5	cm <sup>3</sup>
STC Max Power	90	W	$\Delta T_{SH}$	10	K	Min. Speed	2000	1000	RPM
STC Max Power Voltage	32	V	$\Delta T_{SC}$	5	K	Max. Speed	3500	3000	RPM
STC Open Circuit Voltage	39.5	V							
STC Short Circuit Current	3	A							
Cell operating temp.	35	°C							

Two different compressors were investigated for the application in the refrigeration system, both compressors are built for R600a. The first was the BD35K which is a DC compressor produced by Nidec, the second compressor was the BDS5.0K, also produced by Nidec. The displacement volumes and speed ranges of the two compressors are stated in Table 2. As seen the BD35K has a lower displacement volume compared to the BDS5.0K and further the dynamic range of the BD35K is also significantly lower than that of the BDS5.0K.

The operational characteristics of the two compressors, i.e. isentropic and volumetric efficiencies, were modelled using speed specific compressor polynomials supplied by the manufacturer. The polynomials were supplied at four values of compressor speed ranging from the minimum to the maximum speed. For operation at speeds in between the supplied polynomials the efficiencies were interpolated between the values of the nearest polynomials.

A part from the work derived from the application of the compressor polynomials, the initial start-up of the compressor requires additional power. This will in the following be referred to as the compressor start power. The compressor start power is associated with the initial positioning of the rotor. The start power for both compressors has been assumed to be 60 W. However, soft start procedures or the application of super capacitors may alleviate the need for the PV panel to supply the start power. Consequently, results were derived both with and without the 60 W compressor start power.

### Compressor Speed Control Strategies

As the compressor in the suggested system was driven directly by the PV panel, the only manner by which sufficient utilization of the available power can be ensured was to impose a suitable compressor speed control strategy. In the present work three different speed control strategies have been investigated and compared based on their ability to utilize as much of the available power during a complete day.

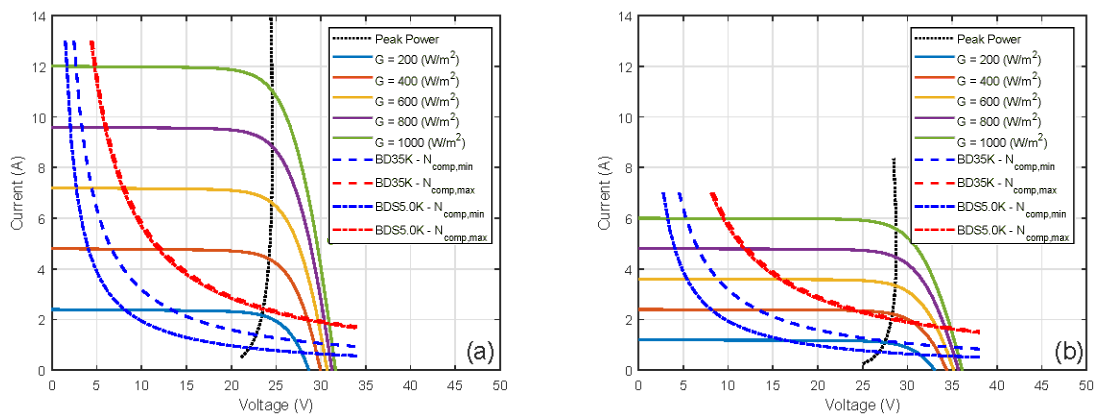
To quantify to which extent the compressors utilize the available power a Utilization Factor was defined. The Utilization Factor was defined as the ratio of the integrated compressor work from sunrise to sundown over the integrated peak power over the same duration. The Utilization Factor thus indicates how well the compressor control strategy was at adapting the speed during the increasing and decreasing irradiance experienced during a day.

A part from the utilization factor the Accumulated Daily Cooling Load was also determined as the integrated cooling load delivered over the full day.

The first control strategy investigated was the PPT control. This control strategy requires the application of an external peak power tracker. The peak power tracker required the measurement of both solar irradiance and cell operating temperature which the peak power tracker then used to calculate the peak power point. This was then applied as a set point for the compressor speed regulation. Consequently, the PPT control ensured that when the compressor was on it ran at a speed at which

the needed compressor power was equal to the PV panels peak power. However, the ability to run at the requested speed was limited by the minimum and maximum speeds of the compressors. An alternative to the PPT control is CVC. As seen in Fig 2 the peak power points for increasing irradiance coincide at a close to constant voltage. Hence, it is possible to approximate the peak power point by measuring only the voltage over the PV panel. Supplying the speed control of the compressor with a set point for the PV panel voltage would thus allow the compressor to adjust the speed in order to attain a constant voltage and thus operate close to the peak power point. This control strategy alleviates the need for solar irradiance and cell temperature measurements and may thus be simpler to implement. The set point for the CVC was set to 22 V.

The final investigated control strategy was AEO. The AEO control strategy requires no additional measurements and was therefore implemented directly in the compressor, it may therefore be the most simple to implement. The principle of the AEO strategy was to continuously ramp up the compressor speed until the compressor would collapse the PV panel thus shutting the compressor off. The speed at which the collapse occurred was then stored in the controller. The compressor was



then kept off for a short duration to allow pressure equalization between the condenser and evaporator in order to reduce the power consumption during start-up. It was assumed that three minutes would allow sufficient pressure equalization. After the short off-period the compressor was then turned on at a speed lower than the one at which the collapse occurred.

Two inputs are thus needed in order to run the AEO strategy, the compressor speed ramp-rate and the speed reduction when restarting the compressor. These were assumed to be constants during the operation of the system. The choice of these two constants both influence the utilization factor of the PV panel. It was found that a ramp rate of 2000 RPM h<sup>-1</sup> and a speed reduction of 400 RPM was a good trade-off for all investigated combinations of PV panels size and compressor types.

## RESULTS

Fig. 3 shows the voltage - current curves for the 360 W (a) and 180 W (b) PV panels, respectively. Further, the voltage - current curves for the two compressors are presented under the operating conditions shown in Table 1 and their respective minimum and maximum compressor speeds. The compressor voltage - current curves are thus iso-power lines corresponding to the compressor power at minimum and maximum speeds. For a given solar irradiance the compressor must thus run between the intersections of the minimum and maximum compressor curve and the voltage - current curve at the given irradiance. If the curves do not intersect the compressor will collapse the PV panel at the minimum compressor speed and will thus not be able to run. If the PV panel voltage - current curve only intersects with the minimum speed compressor curve the compressor will be able to run at the peak power point for that irradiance and will thus be able to utilize all the available power. If the PV panel voltage - current curve intersects with both the minimum and maximum compressor

speeds the compressor will not be able to run at the peak power point and will thus not be able to utilize all the available power.

This figure thus gives an indication of how well the compressor can utilize the available power from the PV panel. It may be seen that the maximum speed curves for the two compressors occurred at more or less the same point. However, the BDS5.0K could run at a lower power as the BDS5.0K had a lower minimum speed. The BDS5.0K would thus be able to run at lower levels of irradiance. Further, it may be seen that for the 360 W PV panel both compressors would not be able to run at the peak power point at irradiances much higher than  $200 \text{ Wm}^{-2}$  for the 180 W this was possible up to  $400 \text{ Wm}^{-2}$ . However, the 180 W PV panel would require a higher irradiance before the compressor could run.

It should be noted that the compressor start power was not included in the curves shown in Fig. 3. The need for compressor start power would shift the minimum speed curves upwards thus reducing the gap between the minimum and maximum curves.

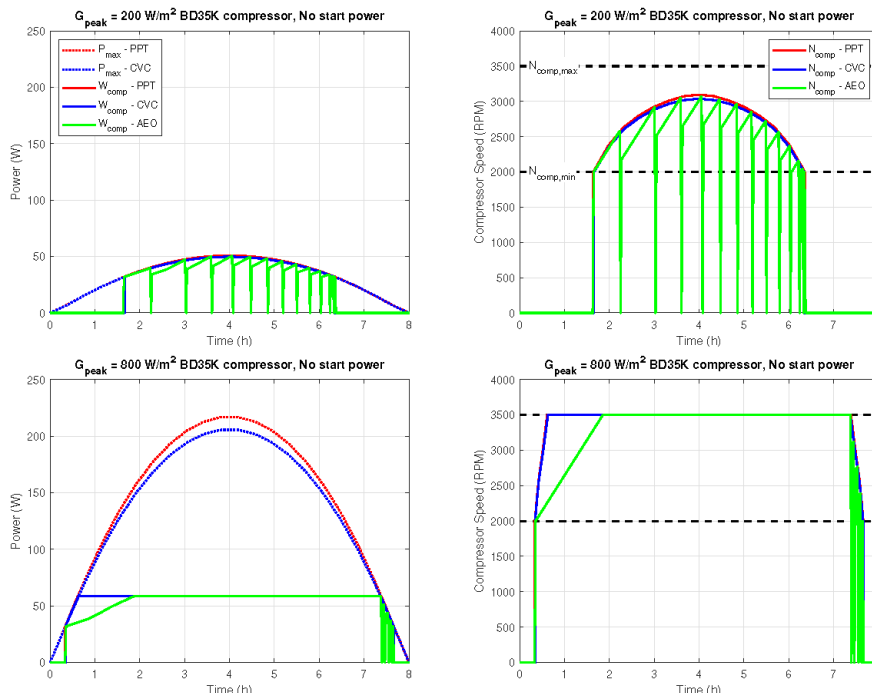


Figure 4: Compressor power and compressor speed for the PPT, CVC and AEO control strategies under two different irradiance profiles with  $200 \text{ Wm}^{-2}$  and  $800 \text{ Wm}^{-2}$  peak irradiance, respectively. Results are shown for the BD35K compressor without start power.

Fig. 4 shows an example of how the different control strategies perform under two different daily profiles, with  $200 \text{ Wm}^{-2}$  and  $800 \text{ Wm}^{-2}$  peak irradiance, respectively. This was exemplified with the BD35K compressor without the inclusion of compressor start power and the 360 W PV panel. Fig. 4 presents both the available and utilized power and the compressor speed. As seen for both the low and the high peak irradiance profiles the three different control strategies turned the compressors on and off at more or less the same time. It may further be seen that for the  $200 \text{ Wm}^{-2}$  profile both the PPT and CVC ran at their respective maximum values while the compressors were on, further it should be noted that the difference between the PPT and CVC maximum power was insignificant. For the  $200 \text{ Wm}^{-2}$  profile the

AEO control resulted in 13 on/off cycles, however it may also be seen that the AEO actually kept the power consumption close to the power consumption of the PPT and CVC control. For the  $800 \text{ Wm}^{-2}$  profile all three compressor control strategies ran the compressors at maximum speed after 1.8 hours of sunlight, the PPT and CVC already after 0.4 hours. The compressors then ran at maximum speed until approximately 0.5 hour before sunset. The PPT and CVC subsequently reduced their speeds to the minimum before turning off 0.25 hours before sunset. In the same duration the AEO

control ran 5 on/off cycles. It is clear that under the 800 Wm<sup>-2</sup> peak irradiance profile non of the three control strategies would be able to utilize close the total available power.

Figs. 5 and 6 show the Utilization Factor and the Accumulated Daily Cooling Load as a function of the daily peak irradiance. This was presented for both compressors under the three compressor control strategies. Further, this was presented under four different system configuration: the 360 W PV panel and the 180 W PV panel, both with and without compressor start power.

As seen for the 360 W PV panel with 60 W of compressor start power, Figs. 5 (a) & 6 (a) the BDS5.0K compressor can deliver a cooling load as soon as the daily peak irradiance exceeds 300 Wm<sup>-2</sup>, it may further be seen that the CVC control will require a slightly higher peak irradiance to run. For the BD35K the daily peak irradiance must exceed 350 Wm<sup>-2</sup> to deliver a cooling load for the PPT or AEO, while the CVC again required a higher peak irradiance of about 360 Wm<sup>-2</sup>.

As seen in Fig. 5 (a) the Utilization Factor increases rapidly after the minimum peak irradiance was attained and peaks shortly hereafter. Here the BDS5.0K attained the highest Utilization Factor with the PPT or CVC with a value of approximately 55 %. Here only 45 % was attained for the AEO. The

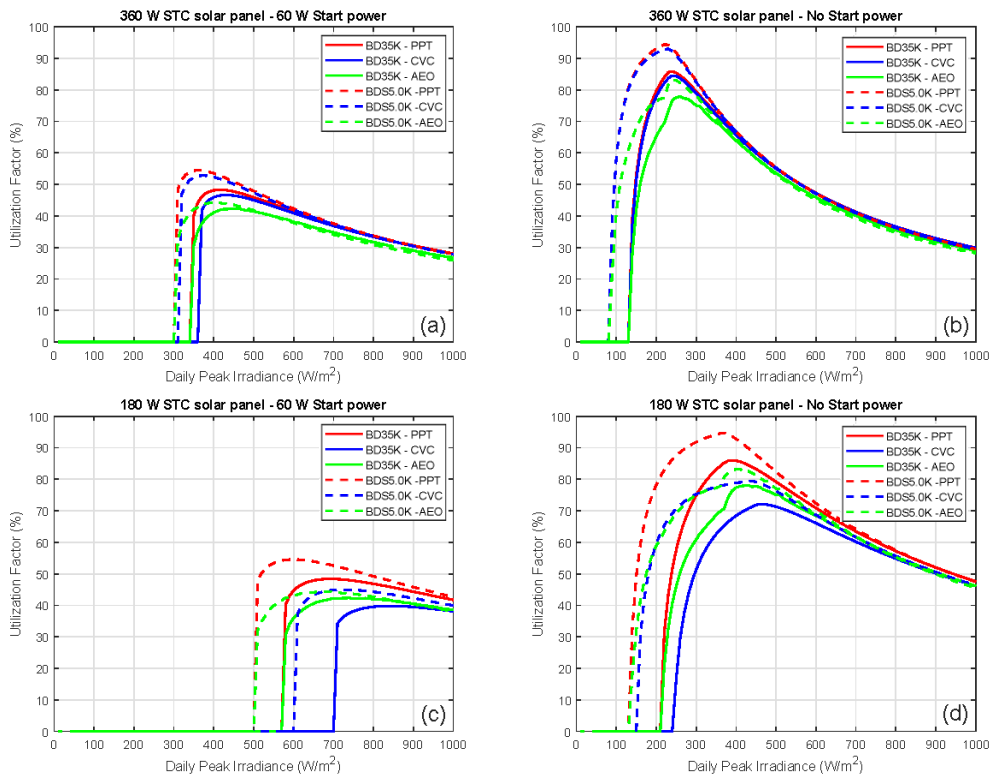


Figure 5 Compressor power and compressor speed for the PPT, CVC and AEO control strategies under two different irradiance profiles with 200 Wm<sup>-2</sup> and 800 Wm<sup>-2</sup> peak irradiance, respectively. Results are shown for the BD35K compressor without start power.

BD35K utilized less of the available power, peaking at around 48 % for the PPT and CVC and around 42 % for the AEO. As the daily peak irradiance increases the differences between the Utilization Factor of the two compressors and the different control strategies diminished and at a daily peak irradiance of a 1000 Wm<sup>-2</sup> the Utilization Factor was approximately 28 % for all six options.

As seen in Fig. 6 (a), then although there was only a minor difference between the Utilization Factor of the two compressors, the Accumulated Daily Cooling Load differs significantly. Here the BDS5.0K was capable of delivering more cooling load than the BD35K, as the BDS5.0K compressor was more efficient. Again it may be seen that the PPT and CVC attain comparable cooling loads while the AEO delivered slightly less.

Assuming that the need for compressor start power can be alleviated but keeping the PV panel size of 360 W results in the Utilization Factor and Accumulated Daily Cooling Loads seen in Figs. 5 (b) & 6 (b). As seen this allowed the compressors to run at significantly lower daily peak irradiances. Here

the all three strategies delivered a cooling load already from a daily peak irradiances of 90 W for the BDS5.0K and 120 W for the BD35K. Again the Utilization Factors show a rapid increase as soon as the minimum irradiance was attained. Here the BDS5.0K with the PPT and CVC peaks at a Utilization Factor of 94 % while the AEO reached around 83 %. The BD35K again utilized less of the available power peaking at around 84 % for the PPT and CVC and 78 % for the AEO. Again the differences between the utilization Factors of the two compressors and the three control strategies diminishes with increasing peak irradiance reaching approximately 30 % with a peak irradiance of 1000 Wm<sup>-2</sup>. As shown previously, the BDS5.0K delivers significantly more cooling load than the BD35K, see 6 (b). As was also shown earlier the AEO delivers less cooling load compared to the CVC and PPT, however when the need for start power was alleviated the AEO approaches the load delivered by the CVC and PPT.

When the PV panel size was reduced to 180 W while still supplying the 60 W of start power, the minimum peak irradiance increases significantly, see Figs. 5 (c) and 6 (c). As seen the BDS5.0K with either the PPT or AEO requires a peak irradiance in excess of 500 Wm<sup>-2</sup>, while the CVC requires 600 Wm<sup>-2</sup>. For the BD35K this was 590 Wm<sup>-2</sup> for the PPT and AEO and 700 Wm<sup>-2</sup> for the CVC. In light of these results, this configuration was deemed infeasible as it would result in the lack of cooling load for too many days.

However, if the need for compressor start power was alleviated for the 180 W panel the minimum

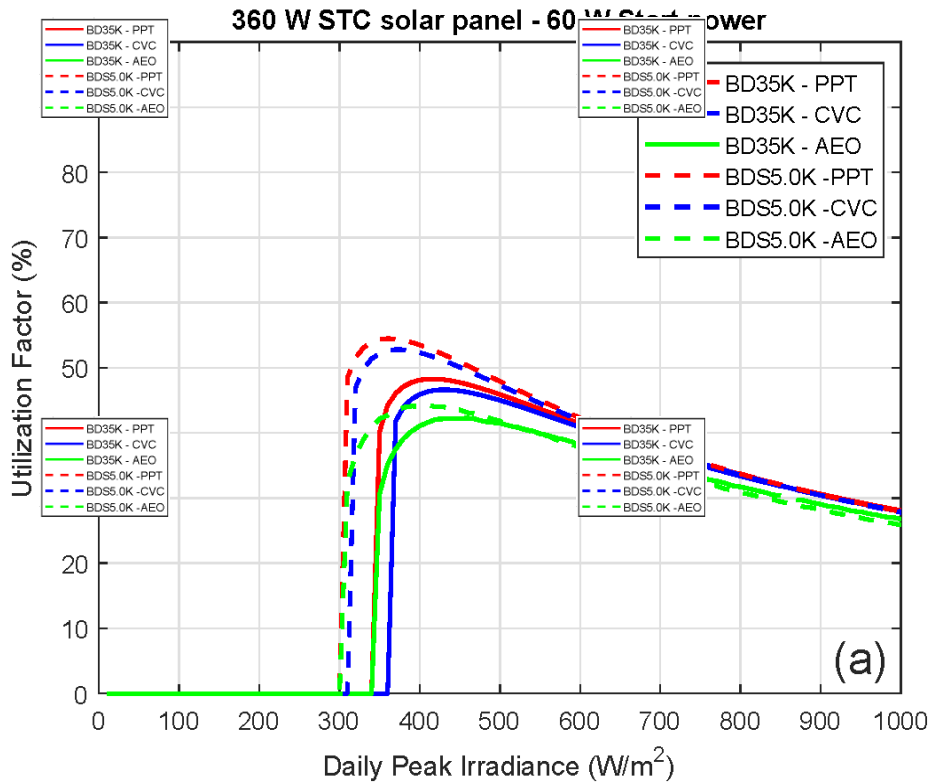


Figure 6: Daily accumulated cooling for the BD35K and BDS5.0K compressors under the PPT, CVC and AEO control strategies using both the 180 W and 360 W PV panels and with and without compressor start power delivered from the PV panel.

peak irradiance was again significantly reduced, see Figs. 5 (d) and 6 (d). Here the BDS5.0K will be able to deliver a cooling load from around 120 Wm<sup>-2</sup> while the BD35K would require slightly more than 200 Wm<sup>-2</sup>. Generally, it may be seen that the Utilization Factor for this configuration was higher than the remaining configurations. Even at 1000 Wm<sup>-2</sup> almost 50 % of the available power was utilized. As seen the Accumulated Daily Cooling Load was actually comparable to that of the 360 W with 60 W start power when both are running. As such it can be concluded that if the compressor start power can be alleviated the PV panel size can be halved without reducing the delivered cooling load, actually the cooling load can be delivered at lower irradiances with half the PV panels if start

power was avoided. Finally, it may be seen that for this configuration there was slightly higher difference between the applied control strategy.

## CONCLUSIONS

The influence of compressor type and compressor control strategy on the performance of a solar direct drive refrigeration system was investigated using numerical modelling and simulations. The Utilization Factor and Accumulated Daily Cooling Load were determined for a full day under varying daily peak irradiances. Two compressor types, the BDS5.0K and BD35K and three compressor control strategies, PPT, CVC and AEO were investigated. Further, four configurations were included: a 360 W and a 180 W PV panel both with and without compressor start power delivered from the PV panel. Results showed that both the choice of compressor and the applied control strategy affected the system's ability to utilize the available power from the PV panel, especially under lower irradiance conditions and when the PV panel was downsized. Generally, the PPT strategy delivered the highest Utilization Factor and thus the highest cooling load. The CVC was comparable to the PPT for the 360 W PV panel, while performing worse than the PPT for the 180 W configurations. The AEO generally had a lower performance than the PPT and CVC. However, compared to the simplicity of this control strategy the AEO actually performed well compared to the more challenging PPT and CVC controls. The BDS5.0K performed better than the BD35K due to both the increased efficiency and the increased speed range. Finally, results show that if the need for compressor start power delivered by the PV panel was alleviated the size of the PV panel can be halved without a significant reduction in performance.

## ACKNOWLEDGEMENTS

This research project is financially funded by EUDP (Energy Technology Development and Demonstration). Project title: "Second Generation Solar Direct Drive Refrigerators", project number: 64017-0556

## REFERENCES

- Duffie, J.A., Beckmann, W.A., 2013. *Solar Engineering of Thermal Processes*. John Wiley and Sons, New Jersey.
- IEA, 2012. *Measuring progress towards energy for all: power to the people? World energy outlook*, Organisation for Economic Co-operation and Development, Paris, France.
- McCarney, S., Robertson, J., Arnaud, J., Lorenson, K., Lloyd, J., 2013. Using solar-powered refrigeration for vaccine storage where other sources of reliable electricity are inadequate or costly. *Vaccine* 31, 6050–6057. doi:10.1016/j.vaccine.2013.07.076.
- Myers, D., Diesburg, S., Lennon, P., McCarney, S., 2017. Energy harvesting controls for solar direct drive medical cold chain equipment. *Ghtc 2017 - IEEE Global Humanitarian Technology Conference, Proceedings 2017-*, 1–9. doi:10.1109/GHTC.2017.8239228.
- Pedersen, P.H., Katic, I., Markussen, W.B., Jensen, J.K., Cording, C., Moeller, H., 2019. Direct drive solar coolers. *The 25th IIR International Congress of Refrigeration*, August 24-30, Montreal, Canada doi:10.18462/iir.icr.2019.



## 8.7 Appendix G: Paper: Extending the autonomy time of an icelined solar powered vaccine cooler

Manuscript ID: 1006  
DOI: 10.18462/iir.icr.2019.1006

### Extending the autonomy time of an icelined solar powered vaccine cooler

Jonas K. JENSEN<sup>(a)</sup>, Christoffer BUSK<sup>(a)</sup>, Claus CORDING<sup>(c)</sup>, Per Henrik PEDERSEN<sup>(b)</sup>, Wiebke B. MARKUSSEN<sup>(a)</sup>

<sup>(a)</sup> Department of Mechanical Engineering, Technical University of Denmark  
Kgs. Lyngby, 2800, Denmark, [jkjje@me.dtu.dk](mailto:jkjje@me.dtu.dk)

<sup>(b)</sup> Danish Technological Institute

Taastrup, 2630, Denmark, [prp@mek.dtu.dk](mailto:prp@mek.dtu.dk)

<sup>(c)</sup> Vestfrost Solutions A/S

Esbjerg, 6705, Denmark, [info@vestfrostolutions.com](mailto:info@vestfrostolutions.com)

#### ABSTRACT

The autonomy time of an icelined solar powered vaccine cooler expresses the amount of hours the cooler is able to keep vaccines within an acceptable temperature range during low solar radiation conditions, i.e. when the compressor of the cooling system is idle. This study investigates how different parameters related to the cooler cabinet and ice storage affect the autonomy time. A dynamic model of the vaccine cooler cabinet including the ice storage was used for the investigation. The model was calibrated using measurements from three different experimental setups, and the calibrated model showed a good agreement with the measurements. The results show that the mass of ice in the storage was the most promising parameter to consider for prolonging the autonomy time. Furthermore, it was shown that reduction of the thermal bridges in the cabinet also is of great importance.

Keywords: Icelined Refrigerator, Autonomy Time, Solar Powered Refrigeration, Vaccine Cooler, WHO.

#### INTRODUCTION

In many developing countries, the electrical grid is either unreliable or not existing, especially in the rural regions and small villages. A study by Adair-Rohani (2013) showed that 25 % of health facilities in Sub-Saharan Africa did not have access to any kind of electricity. Furthermore, 1/3 of hospitals in the area experienced unreliable grid connections. This leads to limited use of electrical applications, such as cooling systems for of medical supplies and products.

Medical supplies such as vaccines are critical in the developing countries. According to the World Health Organization (WHO), the global immunization coverage, i.e. the amount of people with effective vaccines in their blood, has stalled at around 85 % (WHO, 2018) and only very limited progress was attained over the last years. It is stated that 1.5 million lives could be saved if the global immunization coverage improves.

One reason for the fading progress is that vaccines need to be stored cold, in order to avoid spoilage and loss of potency. According to WHO (2015) vaccines should be kept at a storage temperature between 2 °C and 8 °C at all times from manufacturing to administration, in order to ensure the quality of the vaccines. Keeping vaccines cold in rural regions of developing countries is complicated, due to the lack of reliable electricity, as well as challenging ambient conditions in terms of both temperature and humidity.

To solve this issue several commercial coolers exist, which are able to operate without a grid connection. These coolers typically use photovoltaic (PV) modules for power supply and either a battery or an ice bank for energy storage.

## Literature Review

Fatemulla (2011), investigated a refrigeration system using PV modules and a battery for energy storage. The study focused on comparing the costs of using PV, rather than conventional grid electricity. They found that a payback period of around 7 years was expected from the PV modules. Since this was shorter than the expected lifetime, the authors deemed PV a viable investment.

Several studies have investigated the use of thermoelectric coolers for off-grid cooling purposes (Hans et al., 2016, Wang et al. 2011). Hans et al. (2016) investigated a thermoelectric cooler driven by a PV and with a battery for storage. Through experimental testing, they found that the cooler was able to keep the cold room temperature within the defined boundaries of 10-15 °C, while operating with a coefficient of performance (COP) of 0.34.

Aktacir (2011) also considers a refrigerator powered by a PV / battery combination. The system performance on a daily, as well as a seasonal level was investigated for one of the warmest regions of Turkey. It is found that the PV solution was able to deliver the required amount of energy needed to operate the refrigerator at desired conditions.

As stated in Pedersen et al. (2019) experience has shown that the use of batteries in vaccine coolers often is related to increased costs, since the life-time of the batteries is suffering from the high ambient temperatures and the frequent deep discharging. This encouraged the development of direct drive solar powered vaccine coolers with ice storage. Since PV modules generate direct current (DC), it is often advantageous to use a DC compressor for the refrigeration system. In this way the compressor may be connected directly to the PV panels, as a so-called direct drive compressor.

In a study by Ekren (2013), such a DC compressor was investigated, to see if the energy usage could be reduced by use of a variable speed controller, rather than an on/off controller. It was found that the use of variable speed control leads to an increase in COP as well as exergetic efficiency, particularly at high rotation speeds.

In Jensen et al. (2019) three different compressor control strategies were investigated for two different direct drive compressors. Through numerical modelling it was found that by selecting an appropriate compressor control strategy the amount of PV panels needed to operate a vaccine cooler could be halved if the compressor start power could be supplied by e.g. a capacitor or a smart start algorithm.

Pilatte (1984) investigated a refrigerator powered by PV cells, which had the ability to produce ice and use this for energy storage. The cooler was relatively large, with a vaccine storage chamber of 70 litres, and an additional storage room of 70 litres, with a temperature of about 10 °C. The ice-storage of 14 litres was able to produce 2 kg of ice within 24 hours. Performing several tests revealed that the cooler was able to deliver the requirements set by the WHO for vaccine coolers in tropical regions. During operation, the cooler had an average energy consumption of 370 Wh within 24 hours and by using a high level of thermal insulation COPs as high as 1.6 were measured.

Walker (2007) investigated how to design a low-cost vaccine cooler, focusing on a heat transfer regulating device, whose purpose is to control the temperature within the vaccine storage chamber. This cooler also utilized an ice storage. Through modelling of the system, the temperature response of the vaccine chamber due to openings of the cooler lid was investigated. It was found that even though only one vial is present, and the entire cooler is filled with air at 45 °C, the single vial still remained within the boundary of the acceptable temperature range.

## Scope

Autonomy time of a vaccine cooler, as defined by WHO, is the number of hours the vaccine cooler can keep the vaccines within the acceptable temperature range during low solar radiation conditions, i.e. lower than what is required for the compressor to run, but low-consumption equipment such as fans or electronics might be operating. A measurement of the autonomy time starts when the compressors shuts off and ends once a single temperature measurement of the vaccines reaches a

temperature of 8 °C. In the present study we focus on extending the autonomy time of vaccine coolers using ice storage. By use of numerical analysis, we investigate how different parameters of the ice storage and cabinet affect the autonomy time of the vaccine cooler.

### METHODS

In order to investigate the autonomy time of a vaccine cooler a dynamic model of the cabinet including the ice storage was created. The model was implemented in Engineering Equation Solver (Klein, 2018).

#### Cabinet Model

Fig. 1 (left) shows a sketch of the considered vaccine cooler layout. The sketch is a cut through the middle of the vaccine cooler and it should be noted that the ice-storage surrounds the four side walls of the vaccine compartment. Furthermore, the evaporator is a spiral-shaped pipe, wrapped around the ice-storage. The condenser is also a long pipe, but placed on one side of the unit, similarly to a household refrigerator. The ice-storage itself is placed in the top part of the side wall and separated of the vaccine chamber by the frame with a thin layer of plastic material between the frame and the ice-storage. All walls are insulated with PU foam as well as a vacuum insulation panel on the outside of the insulation. The vaccine cooler also contains a lid, which is insulated by PU foam.

For the modelling the condenser and evaporator tubes were disregarded, since the refrigeration system is idle during autonomy time. The vaccine cooler was divided into eight control volumes as seen in Figure 1 (right). The arrows indicate how a given control volume interacts with the neighbouring control volumes. Red arrows indicate heat transfer by convection, calculated by multiplying a convective heat transfer coefficient with the heat transferring area and the temperature difference between the surface and the ambient or cabinet inside air temperature.

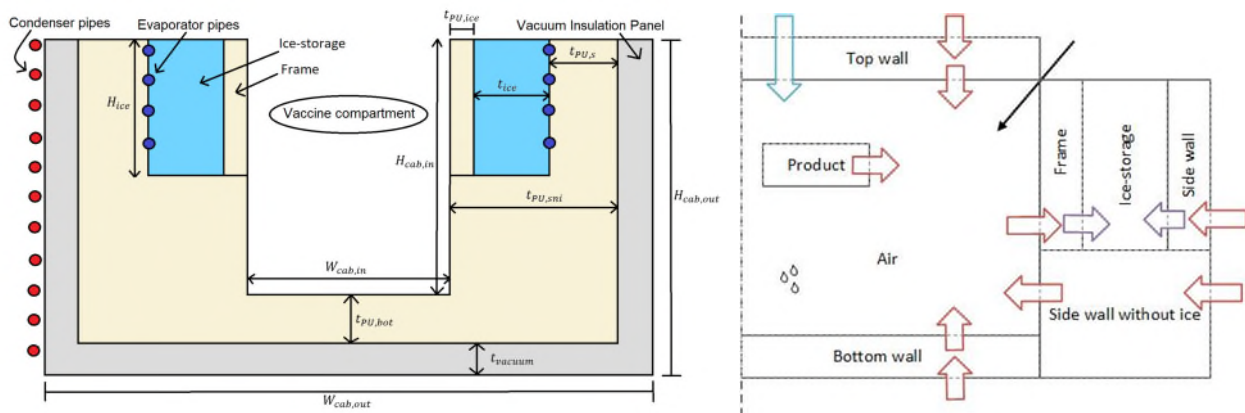


Figure 1: (Left) Sketch of the vaccine cooler cabinet with ice storage. (Right) Sketch of the modelled control volumes and their interactions.

The two purple arrows indicate heat transfer by conduction. The blue arrow indicates heat transfer through thermal bridges. This was modelled by fixing a UA-value for the thermal bridges and multiplying this with the temperature difference between the ambient air and the air inside the vaccine compartment. Air infiltration, indicated by the solid black arrow in Figure 1, was taken into account in the energy balance of the air control volume as well as possible condensation of moist air, as indicated by the water droplets in the figure.

Dynamic mass and energy balances were formulated for all control volumes. For the air, product and ice-storage control volumes a lumped capacitance approach was chosen, while transient conduction through a composite wall was applied for the wall and frame insulation control volumes. The walls consisted of an outer layer of steel, a vacuum insulation panel, a layer of insulation material (PU-foam) and another layer of steel on the inside. The walls were discretised such that a calculation

node was placed at each material interface and additionally 10 nodes were placed inside the layer of PU foam.

The frame consisted of an aluminium layer, a thin layer of insulation material and another aluminium layer. Since the insulation material only a thin layer only 3 nodes were added in this layer. Furthermore, a contact resistance of  $500 \text{ W m}^{-2}\text{K}^{-1}$  between the ice and the aluminium layer was defined.

The product consisted of a number of vials. Each vial was assumed to have a cylindrical shape. The density and heat capacity of the vials was assumed to be similar to liquid water.

### Ice Bank Storage

The ice bank storage was able to interact with the frame and the side wall. The model was built such that both freezing and thawing of the ice could be simulated. Since the water is placed in a closed

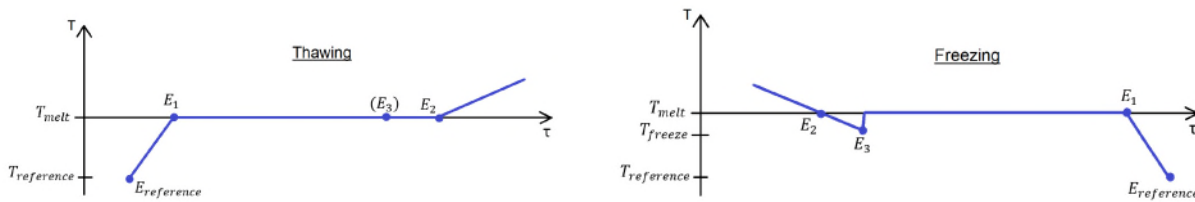


Figure 2: Temperatures and energy levels in the ice-storage during freezing and thawing.

and stable container some degree of subcooling of the liquid is experienced prior to freezing and the water will be at a metastable state until it reaches the freezing point. For the simulations the freezing point temperature was a user input, based on experiences from experimental tests. The properties of the subcooled water were considered similar to non-sub-cooled liquid water. When reaching the freezing point temperature, part of the ice would freeze rapidly and the temperature would instantly increase to  $0 \text{ }^\circ\text{C}$ . Figure 2 sketches the assumed temperature course during freezing and thawing. A reference temperature was defined at  $-15 \text{ }^\circ\text{C}$ . This reference temperature was used for calculating reference levels of internal energy of the ice:

$$E_{\text{reference}} = M_{\text{ice}} \cdot u(T_{\text{reference}}, p) \quad \text{Eq. (1)}$$

$$E_1 = E_{\text{reference}} + M_{\text{ice}} \cdot c_{\text{ice}} \cdot (T_{\text{melt}} - T_{\text{reference}}) \quad \text{Eq. (2)}$$

$$E_2 = E_1 + M_{\text{ice}} \cdot \Delta h_{fs} \quad \text{Eq. (3)}$$

$$E_3 = E_2 - M_{\text{ice}} \cdot c_{\text{water}} \cdot (T_{\text{melt}} - T_{\text{freeze}}) \quad \text{Eq. (4)}$$

By comparing the changes in internal energy of the ice calculated from the dynamic energy balance to the energy levels,  $E_1$ ,  $E_2$  and  $E_3$  the current temperature and ice fraction was calculated. The melting point temperature,  $T_{\text{melt}}$ , was set to  $0 \text{ }^\circ\text{C}$ , while the freezing point temperature,  $T_{\text{freeze}}$ , was set to  $-6 \text{ }^\circ\text{C}$ .

### Calibration

As a first step a calibration of the model was carried out. The parameters fixed in the calibration were:

- The UA-value representing the losses through thermal bridges in the cabinet
- The convective heat transfer coefficient on the inside of and outside of the cabinet

It was assumed that the heat transfer coefficient on the outside of the cabinet was equal to the heat transfer coefficient on the inside of the cabinet, and also the heat transfer coefficient between the product and the air was assumed equal to the heat transfer coefficient between the inside wall and the air. For the calibration the simulated results were compared to test results from autonomy time measurements of three different test setups using the considered vaccine cooler cabinet. Apart from the autonomy time also the steady state temperature was used as a target parameter. The steady

state temperature denotes the temperature of the air, when the entire system is in a steady state condition during phase change in the ice-storage.

One of the tests was carried out according to the WHO performance quality and safety (PQS) standard at hot zone conditions, i.e. an ambient temperature,  $T_{amb} = 43\text{ °C}$  (WHO, 2010). According to the test standard, 1/5 of the nominal cabinet volume should be filled with water packages, each package containing 0.4 kg of water, which corresponded to 4.4 kg for the considered cabinet. For the simulations a single volume of water was assumed. The second test was carried out by the Danish Technological Institute (DTI), at temperate zone conditions i.e.  $T_{amb} = 32\text{ °C}$ . In this test the hold-over time was measured instead of the autonomy time. This meant that the measurement was carried out until the vaccines reached a temperature of 12 °C in stead of 8 °C, which was the case for the two other tests. The product inside the cooler cabinet was one test package Tylose gel of 0.5 kg. The last test was carried out at DTU. In this test the ambient conditions were not controlled, and the average ambient temperature in the lab during measurements was 22.1 °C. In this test the cabinet was empty during measurements and the time was stopped when the air inside the cabinet reached 8 °C.

### Simulated Cases

A baseline model was established using geometrical data from the considered vaccine cooler cabinet and values of the convective heat transfer coefficient and UA-value representing the thermal bridges obtained from the calibration procedure. Taking this baseline model as a reference, the following parameters were varied in order to investigate their impact on the autonomy time and steady state temperature:

- The height of the ice bank. In this case the mass of ice was kept constant, while the thickness of the ice bank was changed as a function of the height.
- The mass of the ice. The thickness of the ice storage was held constant while the height was changed to give room for extra mass.
- The thickness of the PU insulation. For this case the inner dimensions of the cabinet were held constant while extra insulation was added on all walls.
- The UA-value of the thermal bridges.

## RESULTS

### Model Calibration

By running the model with different combinations of the convective heat transfer coefficient and the overall heat transfer coefficient representing the thermal bridges, the best combination of parameter values was found using the values stated in Table 1.

**Table 5. Values of calibrated parameters**

Convective heat transfer coefficient, $\text{W m}^{-2} \text{K}^{-1}$	7
UA-value of thermal bridges, $\text{W K}^{-1}$	0.26

Using the baseline model including the values presented in Table 1 and input parameters for ambient conditions corresponding to the three different measurement environments, simulated autonomy times were found as seen in Table 2. The simulated autonomy times corresponded well with the measurements, showing discrepancies of less than 3 %. Apart from the autonomy time also the steady state temperatures are shown in Table 2. As seen the steady state temperature during simulations corresponded very well with the measured temperatures.

**Table 6. Comparison of autonomy time and steady state temperature of the air for measurements and simulations with the calibrated model**

	Measured h	Simulated h	Deviation h	Deviation %
WHO	72.4	74.5	2.1	2.9
DTI	111.3	111.6	0.3	0.3
DTU	156.4	154.3	2.7	1.7
	Measured °C	Simulated °C	Deviation °C	
WHO	5.8	5.8	0.0	n/a
DTI	4.3	4.2	0.1	n/a
DTU	3.0	2.9	0.1	n/a

### Extending Autonomy Time

In Fig. 3 (left) the autonomy time and steady state temperature of the air inside the cabinet is shown as a function of the ice bank height for two different ambient temperatures. The mass of ice was kept constant in this case, which meant that the ice bank thickness was decreasing with added height. As seen the autonomy time decreases slightly with increasing height for both 32 °C and 43 °C ambient temperature. At the same time the steady state temperature was found to decrease. By increasing the ice bank height also the area between air and frame is increased, which results in an increased convective heat transfer from this surface, and the air temperature thus decreases. The lower air temperature inside the cabinet then results in larger heat losses through the outer walls which causes the decrease in autonomy time. At an ambient temperature of 32 °C the steady state temperature of the air got below the lower limit 2 °C when increasing the ice bank height by 18 cm. Fig. 3 (right) shows the autonomy time and steady state temperature as a function of the ice bank mass. In this case the height of the ice bank was also increased while the thickness was kept constant. In this

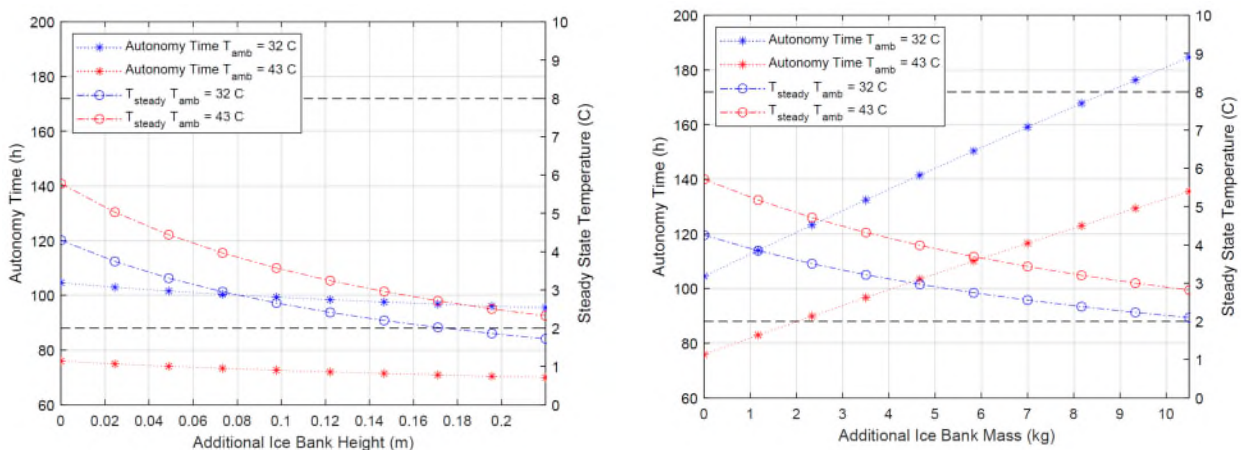


Figure 3: Autonomy time and steady state temperature as a function of additional ice bank height (left) and additional ice bank mass (right) compared to the baseline model.

case the autonomy time increases significantly with added mass of the ice. This trend was expected as added mass in the ice bank means a larger storage capacity. Adding 10 kg of ice to the storage of the reference model resulted in around 80 % increase in autonomy time for both ambient temperatures. The steady state temperatures show a similar decrease as for the case where height is increased with constant the ice bank mass, however, staying within the limits, above 2 °C.

Fig. 4 (left) shows the autonomy time and steady state temperature as a function of added PU-insulation in all outer cabinet walls. As seen the autonomy time increases slightly with increasing

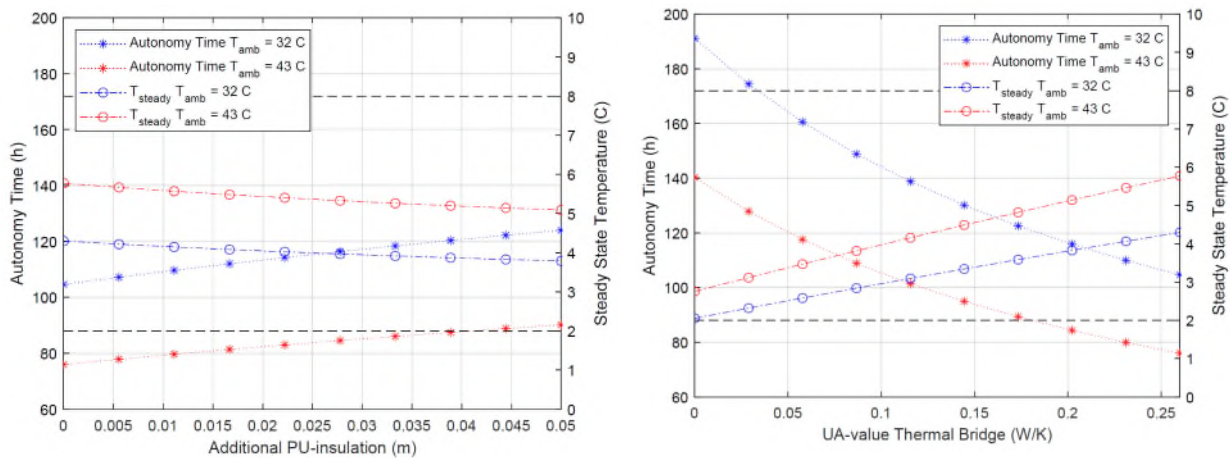


Figure 4: Autonomy time and steady state temperature as a function of additional PU- insulation in the cabinet walls (left) compared to the baseline model and as a function of the UA-value of the thermal bridges (right).

insulation thickness. Increasing the insulation thickness of the outer walls reduces the convective heat loss through the walls, which leads to the increase in autonomy time. Adding extra 5 cm to the insulation of the outer walls increases the autonomy time by 10 to 20 % depending on the ambient temperature. The steady state temperature is mainly governed by the insulation thickness between the ice storage and the vaccine chamber, and therefore only changing less than 1 °C, when adding 5 cm to the insulation thickness of the outer walls.

In Fig. 4 (right) the UA-value of the thermal bridges was varied between 0 WK<sup>-1</sup>, meaning no losses due to thermal bridges, up to 0.26 WK<sup>-1</sup>, which was the value found from the calibration of the baseline model. For a cabinet without thermal bridges autonomy times of 190 h and 140 h were obtained for ambient temperatures of 32 °C and 43 °C, respectively. Removing all thermal bridges thus has almost the same impact on the autonomy time as adding 10 kg of ice to the ice storage. Also the steady state temperatures are significantly influenced by the thermal bridges. At an ambient temperature of 43 °C the steady state temperature decreases from 5.8 °C to 2.9 °C when removing the thermal bridges, and at an ambient temperature of 32 °C the steady state temperature decreases from 4.2 °C to 2.0 °C, which is at the limit of the acceptable air temperature inside the cabinet.

For the solar powered vaccine cooler a longer autonomy time means a less vulnerable system in periods with low solar radiation. For extending the autonomy time, the results presented in Figure 3 and Fig. 4 suggest that focus is put on increasing the mass of the ice storage and reducing the thermal bridges of the cabinet.

## DISCUSSION

The model showed good agreement with measured values of the autonomy time, when using the calibrated values of the heat transfer coefficient and UA-value of the thermal bridges. Considering the UA-value of the thermal bridges the results showed that both the autonomy time and the steady state temperature were quite sensitive to the chosen value. A more thorough analysis of the thermal bridges therefore seems relevant for future work. Considering the convective heat transfer coefficient, the same value was used for calculating the heat transfer on the inside wall, the outside wall and between the product and the air. Due to different geometries, air flow conditions and different temperature levels it is expected that the heat transfer coefficients would not be equal in reality. A refinement of the convective heat transfer coefficients could possibly lead to a more realistic model, however this would also increase the number of parameters to be calibrated.

For the air, ice and product control volumes it was assumed that the lumped capacitance method could be applied. In reality temperature gradients are expected in all three control volumes. A sensi-

tivity analysis calculating the Biot number for different combinations of convective heat transfer coefficients and ice storage thicknesses relevant in this study, showed that the Biot numbers were close to 0.1, which is usually seen the limit of the validity of the lumped capacitance method. Furthermore, as soon as the ice starts to melt and the ice storage is filled with an increasing amount of liquid water natural convection will occur inside the ice storage, which is not accounted for in the current model. Natural convection on the water side will decrease the resistance and might thus decrease the expected autonomy time.

## CONCLUSIONS

A dynamic model of an ice-lined vaccine cooler cabinet was used to investigate the autonomy time and the steady state temperature of the air during phase change of the ice. A baseline model representing an existing cabinet was calibrated against experimental results from three different measurement setups. The calibrated baseline model showed a good agreement with the measurements. It was investigated how different parameters related to the cooler cabinet and ice storage affected the autonomy time, while making sure that the steady state temperature stayed in an the acceptable range between 2 °C and 8°C. The results showed that the mass of ice in the storage was the most promising parameter to consider for prolonging the autonomy time. Furthermore, it was shown that a reduction of the thermal bridges in the cabinet also is of great importance.

## ACKNOWLEDGEMENTS

This research project is financially funded by EUDP (Energy Technology Development and Demonstration). Project title: "Second Generation Solar Direct Drive Refrigerators", project number: 64017-0556

## NOMENCLATURE

$c$	Specific heat ( $\text{J kg}^{-1} \text{K}^{-1}$ )	$p$	pressure (kPa)
$E$	Internal energy level (J)	$T$	temperature (K)
$M$	mass (kg)	$u$	Specific internal energy (J/kg)

## REFERENCES

- Adair-Rohani, H., Zukor, K., Bonjour, S., Wilburn, S., Kuesel, A.C., Hebert, R., Fletcher, E.R., 2013. Limited electricity access in health facilities of sub-Saharan Africa: a systematic review of data on electricity access, sources, and reliability. *Global Health: Science and Practice* 1 (2) 249-261.
- Aktacir, M.A., 2011. Experimental study of a multi-purpose PV-refrigerator system. *International Journal of Physical Sciences* 6(4):746-757.
- Ekren, O., Celik, S., Noble, B., Krauss, R., 2013. Performance evaluation of a variable speed dc compressor. *International Journal of Refrigeration* 36(3),745-757.
- Fatehmulla, A., Al-Shammari, A.S., Al-Dhafiri, A.M., and Al-Bassam A.A., 2011. Design of energy efficient low power PV refrigeration system. In *Electronics, Communications and Photonics Conference (SIECPC), 2011 Saudi International*, pages 1-5. IEEE.
- Hans R., Kaushik S.C., Manikandan, S., 2016. Experimental study and analysis on novel thermoelectric cooler driven by solar photovoltaic system. *Applied Solar Energy* 52 (3) ,205-210.



- Jensen, J.K., Moeller, H., Katic, I., Pedersen, P.H., Markussen, W.B., 2019. Comparison of compressor control strategies for solar direct drive refrigerators. In Proceedings of the 25th IIR International Congress of Refrigeration, August 24-30, Montreal, Canada
- Klein, S.A., 2018. Engineering equation solver academic professional v10.478.
- Pedersen, P.H., Katic, I., Markussen, W.B., Jensen, J.K., Cording, C., Moeller, H., 2019. Direct drive solar coolers. In Proceedings of the 25th IIR International Congress of Refrigeration, August 24-30, Montreal, Canada
- Pilatte, A., 1984. A photovoltaic refrigerator for storage of vaccines and icemaking. In Energy for Rural and Island Communities. In Proceedings of the Third International Conference Held at Inverness, Scotland, pages 229-237. Elsevier.
- Walker, C.D., 2007. Design and manufacture of low cost vaccine cooler. PhD thesis, Massachusetts Institute of Technology, 2007.
- Wang F.J., Chang J.C., Lin K.C., Yau, Y.H., 2011. Performance testing of a thermoelectric cooler for medical application. In Advanced Materials Research 255, 1537-1540.
- WHO, 2010, Refrigerator or combined refrigerator and water-pack freezer: compression-cycle. Solar direct drive without battery storage, PQS Independent type-testing protocol, E003/RF05-VP.2
- World Health Organization, 2015. Immunization in practice: a practical guide for health staff, 2015 update. World Health Organization. <http://www.who.int/iris/handle/10665/193412>
- World Health Organization, 2018. Immunization coverage. <http://www.who.int/mediacentre/factsheets/fs378/en/>, last visited January 31, 2019.

## 8.8 Appendix H: Data sheet for the new compressor

**SECO**

### BDN50K Direct Current Compressor R600a 12/24V DC



**General**

Code number (without electronic unit)	109Z0420
Electronic unit - Variable Speed	101N2740, xx pcs: TBD
Compressors on pallet	200

**Approvals**

CB
----

TBD= To be defined



**Application**

Application	LBP/MBP
Evaporating temperature °C	-30 to 5
Voltage range VDC	9.6 - 17 / 19 - 34
Max. condensing temperature continuous (short) °C	60 (70)
Max. winding temperature continuous (short) °C	125 (135)



Approvals and warning label

**Cooling requirements**

Application	LBP	MBP	HBP
32°C	S	S	-
38°C	S	S	-
43°C	S	S	-

- S = Static cooling normally sufficient
- O = Oil cooling
- F<sub>1</sub> = Fan cooling 1.5 m/s (compressor compartment temperature equal to ambient temperature)
- F<sub>2</sub> = Fan cooling 3.0 m/s necessary
- SG = Suction gas cooling normally sufficient
- = not applicable in this area

Remarks on application:

**Motor**

Motor type	permanent magnet, brushless DC
Speed rpm	variable speed
Resistance, all 3 windings (25°C) Ω	3

**Design**

Displacement cm <sup>3</sup>	2.60
Oil quantity (type) cm <sup>3</sup>	53 (polyolester)
Maximum refrigerant charge g	70
Free gas volume in compressor cm <sup>3</sup>	472
Weight - Compressor/Electronic unit kg	1.35 / 0.14

**Standard battery protection settings**

Voltage (0.1 steps)		Default	Min. value	Max. value
12V ± 0.3V DC, all values	Cut out level VDC	10.4	8.5	17
24V ± 0.3V DC, all values	Cut out level VDC	21.3	19	32
Battery cut-in difference VDC		1.3	0.5	10

**Dimensions**

Height mm	A	89.0
	B	81.9
	B1	79.8
	B2	43.4
Suction connector location/I.D. mm   angle	C	6.2   2°
material   comment	Copper   Rubber plug	
Process connector location/I.D. mm   angle	D	6.2   45°
material   comment	Copper   Rubber plug	
Discharge connector location/I.D. mm   angle	E	5.0   90°
material   comment	Copper   Rubber plug	
Connector tolerance I.D. mm	±0.09, on 5.0 +0.12/+0.20	

